

10-14-2010

# The Biocomplexity of Benthic Communities Associated with a Shallow-water Hydrothermal System in Papua New Guinea

David J. Karlen  
*University of South Florida*

Follow this and additional works at: <http://scholarcommons.usf.edu/etd>

 Part of the [American Studies Commons](#)

---

## Scholar Commons Citation

Karlen, David J., "The Biocomplexity of Benthic Communities Associated with a Shallow-water Hydrothermal System in Papua New Guinea" (2010). *Graduate Theses and Dissertations*.  
<http://scholarcommons.usf.edu/etd/3652>

This Dissertation is brought to you for free and open access by the Graduate School at Scholar Commons. It has been accepted for inclusion in Graduate Theses and Dissertations by an authorized administrator of Scholar Commons. For more information, please contact [scholarcommons@usf.edu](mailto:scholarcommons@usf.edu).

The Biocomplexity of Benthic Communities Associated with  
a Shallow-water Hydrothermal System in Papua New Guinea

by

David J. Karlen

A dissertation submitted in partial fulfillment  
of the requirements for the degree of  
Doctor of Philosophy  
Department of Cell Biology, Microbiology and Molecular Biology  
College of Arts and Sciences  
University of South Florida

Major Professor: James R. Garey, Ph.D.  
Susan S. Bell, Ph.D.  
Pamela Hallock-Muller, Ph.D.  
Kathleen M. Scott, Ph.D.

Date of Approval:  
October 14, 2010

Keywords: biocomplexity, shallow-water hydrothermal vents, environmental gradients,  
benthic infaunal communities, eukaryotic diversity

© Copyright 2010, David J. Karlen

## **Dedication**

In memory of my father, Rev. Marloe H. Karlen.

September 30, 1933 – April 25, 2008

## Acknowledgments

There are so many people to whom I owe my gratitude for their help and support during my time working on this dissertation. First I would like to thank Dr. James R. Garey for his guidance and encouragement these past nine years as my major professor, and for providing me with the opportunity to work on this project. I would also like to thank my committee members, Dr. Susan Bell, Dr. Pamela Hallock-Muller, and Dr. Katie Scott for all of their help and advice. I wish to also thank Dr. Richard Turner for agreeing to serve as chairman for my defense.

This dissertation was part of a National Science Foundation Biocomplexity grant (BE: CBC# 0221834) awarded to Dr. Thomas Pichler, and I am grateful to him for having had the opportunity to participate in this project and to travel to Papua New Guinea. I also would like to thank my other fellow researchers on the grant, Roy Price, Pamela Hallock-Muller, Brian McCloskey, Jan Amend, and Darcy Meyer-Dombard for their field assistance in collecting samples, sharing data and for their friendship. Thanks also goes to the crew of the M/V *Star Dancer* for two wonderful trips in Papua New Guinea and for their help in the field and to Dr. Steve Sanders for hosting our stay in PNG and serving as our tour guide in Rabaul.

This research project was a very large undertaking, and I could have never finished without the help of many people. I owe a lot to Terry Campbell, Stefi Depovic and Tiehang Wu from the Garey lab for their assistance with the 18S rDNA molecular work that was part of this research. I would still be trying to get my PCR to work if not

for their help. Haydn Rubelmann in the Garey Lab provided the bacterial 16S rRNA data for the bacterial community analysis. Sarah Mike sorted macrofauna samples and Stacie Villanueva spent many hours sorting meiofauna samples and making slide mounts of specimens for me. Dr. Ping Wang and Dr. John Lawrence allowed me to use their lab facilities for sediment analysis and Roy Price provided sediment and pore water analysis for arsenic.

I would also like to thank my bosses and fellow workers at the Environmental Protection Commission of Hillsborough County for their support, encouragement and understanding while I pursued my research. I am also greatly indebted to my employer for allowing me the use of our lab facilities to conduct my research and supporting me in my academic endeavors.

And finally I owe a lifetime of gratitude to my parents for the love and support they have always given me.

## Table of Contents

List of Tables.....	iii
List of Figures .....	vi
Abstract.....	xi
Chapter One. Introduction .....	1
1.1 Background .....	1
1.2 Dissertation outline .....	2
1.3 Ambitle Island hydrothermal vent system.....	3
1.4 Other shallow-water hydrothermal vent systems.....	4
1.5 Arsenic in the marine environment .....	6
1.6 The effects of pH.....	7
1.7 Animal-sediment relationships and biogeochemistry .....	9
1.8 The concept of biocomplexity .....	10
Chapter Two. Site Description and Physical Characteristics.....	12
2.1 Introduction.....	12
2.2 Material and methods.....	12
2.2.1 Sampling design and field collection.....	12
2.2.2 Sediment analysis .....	16
2.3 Results .....	17
2.4 Discussion.....	32
2.5 Summary and conclusions .....	36
Chapter Three. Changes in Benthic Macrofauna associated with a Shallow-water Hydrothermal Vent Gradient in Papua New Guinea .....	38
3.1 Introduction.....	38
3.2 Material and methods .....	41
3.3 Results .....	46
3.4 Discussion.....	57
Chapter Four. Macrofaunal communities associated with the shallow water hydrothermal vent system at Ambitle Island, Papua New Guinea .....	61
4.1 Introduction.....	61
4.2 Material and methods .....	62
4.2.1 Sampling design and field collection.....	62
4.2.2 Sample processing and identification .....	62

4.2.3 Data analysis.....	63
4.3 Results .....	64
4.4 Discussion.....	81
4.5 Summary and conclusions .....	85
Chapter Five. Meiofaunal communities associated with the shallow water hydrothermal vent system at Ambitle Island, Papua New Guinea .....	
5.1 Introduction.....	87
5.2 Material and methods .....	90
5.2.1 Sampling design and field collection.....	90
5.2.2 Sample processing and identification .....	91
5.2.3 Data analysis.....	92
5.3 Results .....	92
5.4 Discussion.....	116
5.5 Summary and conclusions .....	118
Chapter Six. Molecular diversity of eukaryotic and bacterial communities associated with the shallow water hydrothermal vent at Ambitle Island, Papua New Guinea.....	
6.1 Introduction.....	119
6.2 Material and methods .....	120
6.2.1 Sampling design and field collection.....	120
6.2.2 DNA extraction and amplification.....	121
6.3 Results .....	125
6.4 Discussion.....	161
6.5 Summary and conclusions .....	164
Chapter Seven. Biocomplexity of the communities associated with the shallow- water hydrothermal system at Tutum Bay, Ambitle Island, Papua New Guinea. ....	
7.1 Comparison of different biological communities and physical parameters.....	166
7.2 Summary of findings and conclusions: the biocomplexity of the Tutum Bay hydrothermal system: .....	171
7.2.1 The Vent Community (0 m) .....	171
7.2.2 Diffuse Venting Zone Community (30 m – 140 m). ....	172
7.2.3 The Low-hydrothermal Activity Zone Community (180 m – 300 m) .....	174
7.2.4 Danlum Bay Reference Site .....	176
7.3 Conclusions.....	177
Literature Cited .....	182
About the Author.....	End Page

## List of Tables

Table 2.1 Site depths and median, minimum and maximum values for pore water variables by site (n = 5 measurements per site).....	19
Table 2.2 Median, minimum and maximum dry weight percentage of sediment by Wentworth size class..	24
Table 2.3 Median, minimum and maximum measurements for sediment parameters. ....	25
Table 2.4 Principal component eigenvalues and percent variation.....	29
Table 2.5 Principal component eigenvectors. ....	29
Table 2.6 Spearman correlation coefficients between pore water and sediment characteristics..	31
Table 3.1 Summary of pore water characteristics at Tutum Bay, Ambitle Island, Papua New Guinea November 2003.....	47
Table 3.2 Sediment grain size class percentages, percent organic carbon and carbonates (mean $\pm$ 1 standard deviation); arsenic concentrations from Price and Pichler (2005).....	48
Table 3.3 Benthic community index values cumulated for all five replicate samples at each site.....	49
Table 3.4 SIMPER analysis results by distance (Bray-Curtis Similarity among five replicate samples) and percent contribution of top five taxa. ....	53
Table 3.5 BIO-ENV results for single and multiple parameters.....	56
Table 4.1 Median, minimum and maximum values for macrofaunal community indices by site .....	65
Table 4.2 Top ranked taxa comprising >50% of the relative abundance at each site.....	70
Table 4.3 SIMPER results from macrofaunal community groups defined by Bray-Curtis similarity groupings.....	79



Table 4.4a BIO-ENV correlations between the benthic macrofaunal community structure and physical parameters.....	80
Table 4.4b BIO-ENV correlations between the benthic macrofaunal community structure and physical parameters; reference site omitted.....	80
Table 5.1 Meiofaunal total taxonomic richness (S), abundance (N) and relative abundance (%) by site.....	99
Table 5.2 Median, minimum and maximum meiofaunal community index values for taxonomic richness, raw abundance counts, Shannon diversity index (base e), and evenness by site.....	103
Table 5.3 Relative abundance of dominant taxa representing >50% relative abundance at the 0 m site (excluding crustacean larvae).....	103
Table 5.4 Median, minimum and maximum values for nematode and copepod abundances and the nematode:copepod ratio at each site.....	107
Table 5.5. SIMPER results for meiofaunal community groupings.....	114
Table 5.6a BIO-ENV Spearman correlations and best fit of physical parameters with the meiofaunal community structure.....	115
Table 5.6b BIO-ENV Spearman correlations and best fit of physical parameters with the meiofaunal community structure; reference site omitted.....	115
Table 6.1 Ranked OTUs representing 50% of the 2,987 total sequences. OTUs ranked by percent abundance and then by number of sites at which they occur.....	134
Table 6.2 Relative abundance the top five ranked OTUs (including ties) at each site.....	135
Table 6.3a BIO-ENV correlations between eukaryotic community structure and physical parameters.....	141
Table 6.3b BIO-ENV correlations between eukaryotic community structure and physical parameters; reference site omitted.....	141
Table 6.4 Top ten ranked metazoans comprising >50% of the 1,059 metazoan sequences.....	144

Table 6.5a BIO-ENV correlations between metazoan community structure and physical parameters. ....	152
Table 6.5b BIO-ENV correlations between metazoan community structure and physical parameters; reference site omitted.....	153
Table 6.6 Number of OTUs (S) and sequences (N) for bacterial phyla for all sites (Total) and individual sites.....	156
Table 7.1 Second Stage MDS Spearman correlations. Physical parameters, macrofauna and meiofauna relative abundance data averaged by site for comparison .....	169
Table 7.2 Second Stage MDS Spearman correlations for physical parameters, macrofauna, and meiofauna relative abundance for all replicate samples.....	169

## List of Figures

Figure 2.1 Ambitle Island, Papua New Guinea sampling locations.....	13
Figure 2.2 Focused venting at Tutum Bay.....	13
Figure 2.3 Diffuse venting (background) at Tutum Bay. ....	14
Figure 2.4 Sampling quadrat and hand corer for macrofaunal samples .....	15
Figure 2.5 Ambitle Island May/June 2005: mean pore water temperature $\pm$ 1 standard deviation. ....	20
Figure 2.6 Ambitle Island May/June 2005: mean pore water salinity $\pm$ 1 standard deviation. ....	20
Figure 2.7 Ambitle Island May/June 2005: mean pore water pH $\pm$ 1 standard deviation .....	21
Figure 2.8 Ambitle Island May/June 2005: mean pore water oxidation-reduction potential $\pm$ 1 standard deviation. ....	21
Figure 2.9 Ambitle Island May/June 2005: mean pore water arsenic concentrations $\pm$ 1 standard deviation. ....	22
Figure 2.10 Ambitle Island May/June 2005: mean median grain size $\pm$ 1 standard deviation. ....	26
Figure 2.11 Ambitle Island May/June 2005: mean sorting coefficient $\pm$ 1 standard deviation. ....	26
Figure 2.12 Ambitle Island May/June 2005: mean sediment organic carbon content $\pm$ 1 standard deviation.....	27
Figure 2.13 Ambitle Island May/June 2005: mean sediment carbonate content $\pm$ 1 standard deviation. ....	27
Figure 2.14 Ambitle Island May/June 2005: Principal components analysis of pore water and sediment characteristics.....	28

Figure 3.1 A: Map of Papua New Guinea and its geographic relation to Australia.....	42
Figure 3.1 B: Map of Ambitle Island with the study sites marked with arrows. ....	42
Figure 3.2 Photograph of focused hydrothermal vent at Tutum Bay, Ambitle Island, Papua New Guinea with surrounding diffuse venting (Photo credit: DJK).....	43
Figure 3.3A: The mean number of taxa (S) and abundance (N) of benthic macrofauna/sample at the transect and reference sites.....	50
Figure 3.3B: Mean Shannon-Wiener Diversity (H') and Pielou's Evenness (J') values at transect and reference sites.....	50
Figure 3.4 A: Mean number of taxa by major taxonomic groups at transect and reference sites. ....	52
Figure 3.4 B: Mean abundance of major taxonomic groups at transect and reference sites .....	52
Figure 3.5 Cluster analysis: Bray-Curtis Similarity based on square root transformed macrofaunal abundance data. ....	55
Figure 4.1 Ambitle Island May/June 2005: Mean number of macrofaunal taxa $\pm$ 1 standard deviation. ....	72
Figure 4.2 Ambitle Island May/June 2005: Mean macrofaunal abundance $\pm$ 1 standard deviation .....	72
Figure 4.3 Ambitle Island May/June 2005: Mean macrofaunal diversity $\pm$ 1 standard deviation .....	73
Figure 4.4 Ambitle Island May/June 2005: Mean macrofaunal evenness $\pm$ 1 standard deviation .....	74
Figure 4.5 Ambitle Island May/June 2005: Benthic macrofauna multi-dimensional scaling plot based on Bray-Curtis similarity between site replicates.....	76
Figure 4.6a Ambitle Island May/June 2005: Benthic macrofauna multi- dimensional scaling plot based on Bray-Curtis similarity averaged by site .....	76

Figure 4.6b Ambitle Island May/June 2005: Benthic macrofauna multi-dimensional scaling plot based on Bray-Curtis similarity averaged by site; reference site omitted.....	77
Figure 4.7 LINKTREE showing physical parameters characterizing site groups based on the benthic macrofauna similarity .....	81
Figure 5.1 Relative taxonomic composition of total meiofaunal abundance (N = 17346 individuals) by phylum (top graph) and subsets for Nematoda (bottom left; N = 6,935 individuals) and Arthropoda (bottom right; N = 8,019 individuals) .....	97
Figure 5.2 Meiofaunal taxonomic composition by site. ....	98
Figure 5.3 Ambitle Island May/June 2005: Mean meiofaunal taxonomic richness $\pm$ 1 standard deviation. ....	104
Figure 5.4 Ambitle Island May/June 2005: Mean meiofaunal abundance $\pm$ 1 standard deviation. ....	105
Figure 5.5 Ambitle Island May/June 2005: Mean meiofaunal Shannon diversity index $\pm$ 1 standard deviation. ....	105
Figure 5.6 Ambitle Island May/June 2005: Mean meiofaunal evenness $\pm$ 1 standard deviation. ....	106
Figure 5.7 Ambitle Island May/June 2005: Mean nematode abundance $\pm$ 1 standard deviation. ....	108
Figure 5.8 Ambitle Island May/June 2005: Mean copepod abundance $\pm$ 1 standard deviation .....	108
Figure 5.9 Ambitle Island May/June 2005: Mean nematode:copepod ratio $\pm$ 1 standard deviation .....	109
Figure 5.10 Ambitle Island May/June 2005: Meiofaunal Bray-Curtis similarity cluster analysis.....	112
Figure 5.11a Ambitle Island May/June 2005: Meiofaunal Bray-Curtis similarity cluster analysis averaged by site. ....	113
Figure 5.11b Ambitle Island May/June 2005: Meiofaunal Bray Curtis similarity cluster analysis averaged by site; reference site omitted.....	113

Figure 5.12 LINKTREE diagram of meiofaunal community site groupings and corresponding physical characteristics. ....	116
Figure 6.1 Cyclesequencing reaction for eukaryotic 18S gene amplification.....	122
Figure 6.2 Cyclesequencing reaction for bacterial 16S gene amplification.....	124
Figure 6.3 Ambitle Island May/June 2005: Number of eukaryotic sequences obtained per site. ....	126
Figure 6.4 Ambitle Island May/June 2005: Number of eukaryote operational taxonomic units (OTUs) obtained per site.....	126
Figure 6.5 Linear regression analysis of OTUs vs. number of sequences.....	127
Figure 6.6 Ambitle Island May/June 2005: Percentage of eukaryote sequences by kingdom level taxonomic category for all sites combined .....	128
Figure 6.7 Ambitle Island May/June 2005: Percentage of eukaryote sequences by kingdom level taxonomic category at each site. ....	128
Figure 6.8 Ambitle Island May/June 2005: Percentage of eukaryote OTUs by kingdom level taxonomic category for all sites combined. ....	129
Figure 6.9 Ambitle Island May/June 2005: Percentage of eukaryote sequences by kingdom level taxonomic category at each site. ....	129
Figure 6.10a Ambitle Island May/June 2005: Multi-Dimensional Scaling (MDS) of eukaryotic community structure based on Bray-Curtis similarity among sites.....	139
Figure 6.10b Ambitle Island May/June 2005: Multi-Dimensional Scaling (MDS) of eukaryotic community structure based on Bray-Curtis similarity among sites; reference site omitted.....	140
Figure 6.11 LINKTREE results showing physical characteristics between eukaryotic community site groups.....	143
Figure 6.12 Proportion of metazoan sequences by phyla. ....	145
Figure 6.13 Proportion of metazoan OTUs by phyla. ....	145
Figure 6.14 Percentage of metazoan sequences by phyla at each site and all sites combined (All).....	149

Figure 6.15 Percentage of metazoan OTUs by phyla at each site and for all sites combined (All).....	149
Figure 6.16a Non-metric Multi-Dimensional Scaling (MDS) plot of metazoan sequence Bray-Curtis similarity between sites. ....	150
Figure 6.16b Non-metric Multi-Dimensional Scaling (MDS) plot of metazoan sequence Bray-Curtis similarity between sites; reference site omitted.....	151
Figure 6.17 LINKTREE results showing physical characteristics between metazoan sequence community site groups .....	154
Figure 6.18 Percentage of total bacterial OTUs (S = 1,081) by phyla .....	158
Figure 6.19 Percentage of total bacterial sequences (N = 1,973) by phyla. ....	158
Figure 6.20 Total number of bacterial phyla represented at each transect site.....	159
Figure 6.21 Total number of bacterial OTUs represented at each transect site.....	159
Figure 6.22 Percentage of bacterial OTUs by phyla at each transect site. ....	160
Figure 6.23 Percentage of bacterial sequences by phyla at each transect site. ....	160
Figure 6.24 Cluster analysis of bacterial sequence Bray-Curtis similarity between sites .....	161
Figure 7.1 Second Stage Multi-Dimensional Scaling plot showing correlation between the different datasets.....	169
Figure 7.2 Percentage of meiofaunal abundance (top graph) and metazoan sequences (bottom graph) by phyla.....	170

## Abstract

Shallow-water hydrothermal vents occur world-wide in regions of volcanic activity. The vents located at Tutum Bay, Ambitle Island, Papua New Guinea are unique in that the vent fluids and surrounding sediments contain some of the highest concentrations of arsenic in a natural system. This study addresses the effects of the vent system on the benthic communities, focusing on the eukaryotes, macrofauna, meiofauna and bacteria.

Samples were collected in November 2003 and May/June 2005. Analysis of the 2003 macrofaunal samples indicated that pH, rather than arsenic was influencing the benthic community, and that the hydrothermal influence occurred at a greater distance than expected. Results of more intensive sampling carried out in 2005 are the primary focus of this dissertation.

The pore water and sediment characteristics revealed distinct physical habitats corresponding with distance from the vent. There was a trend of decreasing temperature and arsenic concentration and increasing salinity and pH with distance from the vent. The vent sediment was poorly sorted volcanic gravel, while sediments along the transect showed a gradient from fine, well sorted volcanic sands to coarser carbonate sands farther away.

The macrofauna showed a trend of increasing diversity with distance from the vent and similar taxa were present in both the 2003 and 2005 samples. The vent community was dominated by the polychaete *Capitella cf. capitata*. The inner transect



from 30 m to 140 m had low diversity. Dominant taxa included thalassinid shrimp and the amphipod *Platyischnopus* sp.A. The 180 m to 300 m sites had significantly higher diversity. The Danlum Bay reference site had relatively higher diversity than the nearshore transect sites and was dominated by deposit feeding polychaetes. Macrofaunal community structure was influenced by the sediment characteristics, notably by CaCO<sub>3</sub> content, sorting and median grain size.

The meiofaunal community also showed changes with distance from the vent. Chromadorid nematodes were dominant at the vent site and were a major component of the meiofauna at most sites, along with copepods. The meiofaunal community at the reference site showed greater similarity to the vent community and both sites had low abundances. Nematodes were more abundant than copepods near the vent, but copepods were more abundant farther offshore and at the reference site. Meiofaunal community structure was influenced primarily by the pore water temperature and salinity. Biological interactions with the macrofaunal community through physical disturbance and predation may also influence the meiofaunal community.

The molecular analysis of eukaryotic and bacterial diversity also revealed changes with distance from the vent. The 0 m and reference sites grouped together due to the presence of fungal sequences and the 140 m and 300 m sites grouped together due to a common molluscan sequence. Metazoans and fungi dominated the eukaryote sequences. The most abundant eukaryotic OTUs included fungi matching *Paecilomyces* sp. and *Cladosporium cladosporioides* and metazoans matching *Viscosia viscosa* (Nematoda) and *Astarte castanea* (Mollusca). The eukaryotic community structure correlated with sediment sorting, pore water arsenic and median grain size. The bacterial community was

represented by 24 phyla and was dominated by Actinobacteria and  $\gamma$ -Proteobacteria. More bacterial phyla were present near the vent, while more overall OTUs were found at the intermediate sites along the transect. The most distant site had much lower diversity dominated by Firmicutes.

The macrofaunal community had the strongest correlation with environmental variables. Comparison between the meiofauna and the metazoan sequences showed the proportion of nematodes found in both datasets were comparable, but the meiofauna analysis found a higher proportion of arthropods, while the molecular results were disproportionately high for platyhelminthes.

Overall, the vents increased the complexity of the system by creating unique habitats. The extreme environment created by the hydrothermal activity maintained the surrounding habitat at an early successional stage colonized by a few opportunistic species. There was a gradation in the benthic communities away from the vent towards a more carbonate based climax community. The low pH environment had an effect on the sediment composition, which in turn influenced the benthic community. These findings can serve as a model for studying the potential effects of ocean acidification and climate change on benthic communities and marine biocomplexity.

## **Chapter One**

### **Introduction**

#### **1.1 Background**

The shallow-water hydrothermal vent system at Ambitle Island, Papua New Guinea, is a unique marine habitat which is most notably characterized by extremely high concentrations of arsenic in the pore water and sediments. Earlier studies at this site reported arsenic concentrations which were 275 times that of normal seawater (Pichler *et al.* 1999b). The surrounding reef habitat and fauna appeared to be unaffected by the elevated concentration of arsenic (Pichler and Dix 1996). In order to further study the biodiversity and biogeochemistry of this unique system, a team of scientists and graduate students from the University of South Florida and Washington University in St. Louis were awarded a National Science Foundation Biocomplexity grant (BE: CBC# 0221834) in 2003. Two sampling trips were made to Ambitle Island, the first in November 2003 and the second in May-June 2005. The group consisted of four teams, each of which focused on different components of the hydrothermal system including the pore water and sediment chemistry, the archaeobacterial community and their biogeochemical processes, the foraminiferan community, and the sediment eubacterial, eukaryotic and metazoan communities. The results from the sediment and pore water analysis and the

foraminiferan community analysis from this project have been published in two doctoral dissertations and a master's thesis (Price 2008, McCloskey 2009, Engel 2010) and peer-reviewed papers (Price and Pichler 2005, Pichler *et al.* 2006, Price *et al.* 2007, Karlen *et al.* 2010). The primary goal of my study is to investigate the effect of a natural hydrothermal gradient on the benthic infaunal community structure. To do this, I utilized measurements by collaborators for pore water and sediment arsenic concentrations, temperature, pH, and characterized the sediment composition and benthic fauna at different distances from a shallow hydrothermal vent. This dissertation will focus on the biodiversity and community structure of the eubacteria, eukaryota and the benthic infauna around the hydrothermal vent system and will further look at the biocomplexity among these different biotic communities and the physical environment surrounding the hydrothermal vent.

## **1.2 Dissertation outline**

This dissertation is organized into seven chapters. The first chapter presents background information on the overall project and a review of other shallow-water hydrothermal vent systems around the world and of past work conducted at Ambitle Island, Papua New Guinea. Chapter two presents results from the pore water and sediment analysis and sets the environmental context for the following chapters on the biotic communities. Chapter three presents data on the macrofaunal community collected from the 2003 sampling trip and recently published in *Pacific Science* (Karlen *et al.* 2010). Chapters four and five present the results from the 2005 macrofaunal and meiofaunal community analyses respectively and their relationships to the environmental

parameters. Chapter six presents results from the molecular analysis of the eukaryotic and bacterial communities, and chapter seven summarizes the overall biocomplexity of the hydrothermal system and compares trends in the community structure at the different levels of biodiversity presented in the previous chapters (molecular, meiofaunal and macrofaunal) and relates these trends with the environmental conditions.

### **1.3 Ambitle Island hydrothermal vent system**

The shallow-water hydrothermal vent system at Ambitle Island was first reported by Pichler and Dix (1996). Two types of venting occur in this system, focused venting of hydrothermal fluid at discrete openings of 10-15 cm diameter in the seafloor and diffuse venting of gas bubbles and hydrothermal fluids through the sand and gravel sediments surrounding the focused vents (Pichler and Dix 1996). The focused vents discharge hydrothermal fluids at a rate of 300-400 L/min at temperatures of 89 - 98°C (Pichler and Dix 1996, Pichler *et al.* 1999a). The diffuse venting consists of CO<sub>2</sub> gas bubbles released through the sandy sediments as far as 150 m from the focused vent (Pichler *et al.* 1999a). Previous work carried out on Ambitle Island focused on the geochemistry of the hydrothermal fluids and surrounding sediment. Vent and pore waters are enriched in several elements, but most notably, arsenic concentrations are 275 times that of normal seawater making this site one of the highest naturally occurring sources of arsenic on record (Pichler *et al.* 1999b). Arsenic is naturally occurring in the volcanic bedrock of Ambitle Island and under heat and pressure is mobilized by ground water, which is the source of the hydrothermal fluids at these vents (Pichler *et al.* 1999b).

Despite the elevated concentration of arsenic, the surrounding reef habitat and fauna appear to be unaffected (Pichler and Dix 1996). This is likely due to the removal of arsenic from the water column via the precipitation of Fe (III) oxyhydroxides (Pichler and Veizer 1999, Pichler *et al.* 1999a) which binds the bioavailable arsenic in the sediments (Price and Pichler 2005, Price 2008).

In addition to the high arsenic concentrations, other environmental factors characteristic of the vent system are high temperatures, low salinity and low pH from the degassing of CO<sub>2</sub>. The temperature and salinity extremes are limited to the immediate area of focused venting, but the reduced pH extends farther away due to the diffuse venting of CO<sub>2</sub>. The effects of the reduced pH on the foraminiferan communities at Ambitle Island were reported by McCloskey (2009), who found low abundances of foraminiferans in the area of diffuse venting, and by Engel (2010), who documented the dissolution of foraminiferan tests near the vent site. Karlen *et al.* (2010) also noted that molluscan macrofauna were absent near the vent, which was attributed to the low pH.

#### **1.4 Other shallow-water hydrothermal vent systems**

Shallow water hydrothermal vents occur worldwide and there have been several earlier studies focused on the geochemistry and biology of such systems. Vents that have been studied in some detail include sites in the Mediterranean and Aegean Seas (Varnavas and Cronan 1988, Thiermann *et al.* 1994 and 1997, Gamenick *et al.* 1998a, Morri *et al.* 1999, Cocito *et al.* 2000, and reviews by Dando *et al.* 1999, 2000), Antarctica (Bright *et al.* 2003, Deheyn *et al.* 2005), the Kurile Islands (Tarasov *et al.* 1990, Sorokin *et al.* 2003, Kamenev *et al.* 2004), New Zealand (Kamenev *et al.* 1993), Mexico and

southern California (Melwani and Kim 2008) and Rabaul harbor, Papua New Guinea (Tarasov *et al.* 1999).

The geochemistry at vent systems varies depending on the local geology and source water of the vent fluids; elevated arsenic concentrations have been reported at other vents (Varnavas and Cronan 1988). Some vent systems, such as the one at Milos, Greece, show elevated levels of H<sub>2</sub>S and host communities of sulfide bacteria and sulfide tolerant infauna (Thiermann *et al.* 1994, 1997, 2000, Gamenick *et al.* 1998a, 1998b, Wenzhöfer *et al.* 2000). Unlike deep-sea hydrothermal vents, which host a biological community of uniquely adapted species, the biological communities around shallow-water vents tend to represent a subset of the more stress tolerant species from the surrounding biota (Giménez and Marín 1991, Thiermann *et al.* 1997, Melwani and Kim 2008). Invertebrate taxa dominant at high sulfide vents do however exhibit adaptations to these environments and may host symbiotic sulphide metabolizing microbes. Gamenick *et al.* (1998a) studied the *Capitella capitata* population associated with the hydrothermal vent system at Milos Greece originally found by Thiermann *et al.* (1997). They designated this population as “*Capitella* sp. M” and found through protein analysis and crossbreeding experiments with several other *C. capitata* sibling species populations that the Milos population represented a distinct sibling species which was characterized by a tolerance to high sulfide concentrations and anoxic conditions (Gemenick *et al.* 1998a). Bright *et al.* (2003) sampled the meiofaunal communities associated with shallow-water fumaroles at Deception Island, Antarctica. This system was also characterized by high sulfide concentrations. The dominant metazoan meiofaunal taxon was an unidentified flatworm which was tolerant of high temperatures and also had presumably symbiotic

bacteria colonizing the worm's outer surface (Bright *et al.* 2003). Similarly, a nematode found associated with bacterial mats around the shallow-water vents in the Bay of Plenty, New Zealand, was found to have symbiotic sulfur bacteria which colonized the surface of the nematode's cuticle (Tarasov 2006).

### **1.5 Arsenic in the marine environment**

Elemental arsenic is commonly found in two inorganic forms in the marine environment: the oxidized form arsenate [As (V)] and the more toxic reduced form arsenite [As (III)] (Francesconi and Kuehnelt 2002, Oremland and Stolz 2003, Watt and Le 2003). These compounds can be metabolized by several prokaryotes either through the respiration of arsenate or the oxidation of arsenite; particularly in extreme environments (Inskeep *et al.* 2002, Oremland and Stolz 2003, Oremland *et al.* 2005) including shallow-water hydrothermal vents (Handley *et al.* 2009). Additionally, eukaryotic organisms can convert inorganic arsenic into organic compounds via methylation (Andreae 1979, Kitts *et al.* 1994, Cutter *et al.* 2001). Specifically invertebrate organisms have adapted physiological mechanisms to detoxify or eliminate high concentrations of arsenic and other contaminants (Langdon *et al.* 2003). Most metabolic pathways in marine invertebrates involve the reduction of As (V) to As (III) which is then methylated through a series of organoarsenical compounds typically to arsenobetaine (AB) as the end product (Langdon *et al.* 2003, Argese *et al.* 2005, Grotti *et al.* 2010). There is some evidence that these can be transferred and accumulated among different trophic levels (Kirby and Maher 2002, Barwick and Maher 2003).



## 1.6 The effects of pH

Previous studies at the Ambitle Island vents found reduced pH levels in the vent fluids which were attributed to high levels of CO<sub>2</sub> in the fluids and gas bubbles discharging from the vents (Pichler *et al.* 1999b). Pore water pH is an important variable in geochemical processes and can influence sediment composition by the dissolution of carbonate sediments (Burdige and Zimmerman 2002). Initial field observations at the Ambitle Island study site indicated a distinctive gradation in the sediment composition in relation to the measured offshore distance from the vent. Field observations also indicated that carbonate content of sediment was lower nearer the vent, with carbonates increasing with distance from the vent. Near shore and in the vicinity of the vents the sediments were predominately fine grained volcanic sands, with some gravel sized deposits near the vent. A gradual mixture of biogenic carbonates was observed starting around 100 m from the vent, consisting of fragments of calcareous algae and coral rubble from the surrounding reef.

Low pH can also impair carbonate incorporation in shell-bearing organisms such as mollusks and foraminiferans (Green *et al.* 1993). McCloskey (2009) observed that shell-bearing foraminiferans were absent from sediments near the Ambitle Island vent, which was attributed to the acidic conditions of the pore water. A similar trend was seen in the macrofaunal mollusks (Karlen *et al.* 2010).

There has been a lot of attention recently on global climate change and the effects of increased atmospheric CO<sub>2</sub> from anthropogenic sources on lowering ocean pH, a process referred to ocean acidification or hypercapnia (Caldeira and Wickett 2003, 2005, Feely *et al.* 2004, Pelejero *et al.* 2005) and the possible effects this may have on marine

organisms. Atmospheric levels of CO<sub>2</sub> have increased by nearly 100 ppm since the beginning of the Industrial Revolution due mainly to the combustion of fossil fuels (Feely *et al.* 2004), and current models predict further increases during the 21<sup>st</sup> Century. The oceans act as a sink for around 30% of the CO<sub>2</sub> released into the atmosphere (Feely *et al.* 2004). The increased CO<sub>2</sub> dissolved in the ocean water reacts with carbonate ions and water molecules forming carbonic acid:



The formation of carbonic acid results in a reduction in the pH of the ocean water and decreased saturation of carbonate ions (Caldeira and Wickett 2003). Globally, ocean pH has decreased by 0.1 pH units over the past 200 years and climate models predict the pH could drop by another 0.4 units by the end of the 21<sup>st</sup> Century (Feely *et al.* 2004). Possible impacts of lowered pH on marine organisms include bleaching and reduced symbiotic productivity in corals, as well as reduced growth and calcification in reef building corals (Anthony *et al.* 2008); reduced calcification and dissolution in shell bearing organisms (Fabry *et al.* 2008, Dupont *et al.* 2010); physiological impacts due to acid-base imbalance which can result in metabolic suppression and affect blood oxygen binding (reviewed in Fabry *et al.* 2008) and reduced growth rates (Shirayama and Thornton 2005, Wood *et al.* 2010). Other studies, however, suggest that marine organisms are more adaptable to the projected changes in ocean pH and question the significance of long term impacts to the function of marine ecosystems (Hendriks and Duarte 2010, Hendriks *et al.* 2010, Byrne *et al.* 2010).

Because of the release of CO<sub>2</sub> from the hydrothermal fluids, shallow-water vent systems offer a unique opportunity for looking at these effects on marine organism (Hall-

Spencer *et al.* 2008). Acidification of sea water associated with release of CO<sub>2</sub> at shallow water vents has also been observed off of Italy by Hall-Spencer *et al.* (2008). In their study they reported reduced densities of calcareous algae and invertebrates at sites with reduced pH and observed signs of shell dissolution on live gastropods (Hall-Spencer *et al.* 2008). Several other recent studies have taken advantage of shallow vent systems, including Tutum Bay, to look at the impacts of low pH on calcareous organisms such as bryozoans (Rodolfo-Metalpa *et al.* 2010) and foraminiferans (Engel 2010).

### **1.7 Animal-sediment relationships and biogeochemistry**

The relationship between sediment characteristics (grain size, organic carbon content) and the benthic infaunal community have long been recognized (Sanders 1958). The interrelationships of sediment properties and benthic communities are complex (Snelgrove and Butman 1994), but in general, fine grained sediments and high organic carbon content tend to be dominated by deposit feeders while coarse sediments tend to support more suspension-feeding organisms (Mancinelli *et al.* 1998).

Bioturbation by burrowing organisms can further affect grain size and carbonate content of the sediment (Aller 1982) as well as the geomorphology and the stabilization/destabilization of sediments (Paarlberg *et al.* 2005). Burrowing organisms, furthermore, influence the biogeochemical processes in the sediments (Snelgrove *et al.* 1997, Mermillid-Blondin 2006).

## 1.8 The concept of biocomplexity

Biocomplexity is a fairly recent term that was first used in the late-1990s by the National Science Foundation as part of a new funding initiative to look at the complex interrelationships in the environment (Anand and Tucker 2003). Michener *et al.* (2001) defined biocomplexity as “...properties emerging from the interplay of behavioral, biological, chemical, physical, and social interactions that affect, sustain, or are modified by living organisms...” and further go on to discuss that biocomplexity is an interdisciplinary field that takes a “holistic” approach to studying ecological systems as opposed to traditional reductionist methods. Cadenasso *et al.* (2006) further developed the concept by presenting a framework of biocomplexity which incorporates three dimensions: spatial heterogeneity; organizational connectivity; and historical contingency. Spatial heterogeneity is presented in terms of patches or discrete areas that differ in structure, organizational connectivity refers to the interactions among the defined patches, and historical contingency refers to the development of indirect effects over time (Cadenasso *et al.* 2006).

In terms of my study of the biocomplexity of the benthic communities associated with the hydrothermal vent system in Tutum Bay, the spatial heterogeneity component will encompass evaluating the changes in the physical environmental parameters and in the different biological communities along the hydrothermal gradient. Organizational connectivity is addressed by evaluating the interrelationships among the different hierarchal levels of the biological communities (macrofauna, meiofauna, molecular eukaryota and eubacteria). The historical contingency component of biocomplexity will

only be briefly addressed in the comparison of the macrofauna results from the 2003 and 2005 sampling periods.

## **Chapter Two**

### **Site Description and Physical Characteristics**

#### **2.1 Introduction**

Benthic organisms are intimately tied to their physical environment. Factors such as pore water chemistry and the sediment characteristics determine the assemblage of species which are found in a given habitat and are thus the controlling factors structuring the biological community. The primary focus of this chapter is to establish the environmental context of the biocomplexity at Tutum Bay in terms of the pore water and sediment characteristics. To do this, sampling sites along the hydrothermal gradient and at a non-hydrothermal reference site are classified using Principal Component Analysis (PCA), grouping them into discrete habitats based on their pore water chemistry and sediment type. The established habitat groups will serve as the basis of comparison for the different levels of biological communities in Tutum Bay.

#### **2.2 Material and methods**

##### **2.2.1 Sampling design and field collection**

Samples were collected along a transect originating at the focused vent and running 300 meters offshore. Sampling sites were located at the vent (0 meters) and at 30 – 50 meter intervals along the transect for a total of nine transect sites; 0, 30, 60, 90, 120, 140, 180, 250 and 300 meters. Samples were also collected at an additional reference site (Danlum Bay, samples designated as “Ref”) located in a non-hydrothermally influenced

area 2 km south of the Tutum Bay vent site (Figure 2.1). The reference site was chosen based on the apparent similarity of the sediment type to that of the vent transect.



**Figure 2.1 Ambitle Island, Papua New Guinea sampling locations. © 2009 Google Earth; Image ©2010 Terra Metrics and Europa Technologies.**

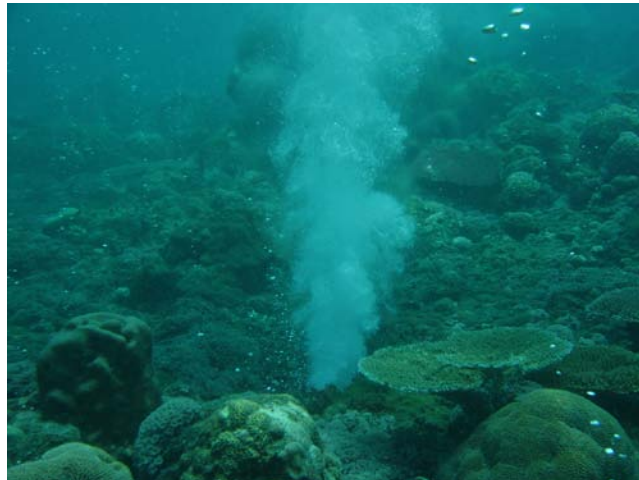


**Figure 2.2 Focused venting at Tutum Bay**



**Figure 2.3 Diffuse venting (background) at Tutum Bay.**

At each sampling site a 1m<sup>2</sup> PVC quadrat, divided into 100 10x10 cm grid cells was placed on the sediment surface (Figure 2.4). Grid cells were numbered by an x,y coordinate system and random cells were selected for sampling using a random number table (Rolf and Sokal 1981). Within selected cells, samples were collected for pore water chemistry, sediment analysis and biology. The 1 m<sup>2</sup> quadrat was repositioned an additional four times and sampling was repeated for a total of five replicate samples for each measured parameter at a given sampling site.





**Figure 2.4 Sampling quadrat and hand corer for macrofaunal samples.**

Temperature was measured *in situ* at a sediment depth of 5 cm using a Fisher Scientific Tractable digital thermometer (Price 2008). Pore water samples were collected by inserting a plastic probe attached to a 60 cc syringe to a sediment depth of 5 cm. Measurements for pH and oxidation-reduction potential (ORP) were made on board using a Myron-L pH meter. Salinity was measured using an optical refractometer. Procedures for the handling and analysis of the pore water samples for arsenic analysis are detailed in Price (2008). Laboratory analyses for total arsenic and arsenic speciation were conducted by the Center for Water and Environmental Analysis, University of South Florida Geology Department (Price 2008).

### 2.2.2 Sediment analysis

Surface sediments were collected for sediment grain size, organic carbon and carbonate content analysis using a 60 cc syringe modified as a sediment corer by cutting off the end (diameter = 3.0 cm). The sediment samples were dried at 60° C and a 50 – 60 g subsample was mixed with 50 ml of approximately 0.5% sodium hexametaphosphate then wet sieved through a 63 µm mesh screen with deionized water to separate the sand and silt+clay fractions. The sand fraction and silt+clay fractions were rinsed into pre-weighed beakers and dried at 60°C. Once dried, the two fractions were weighed and the sand fraction was sieved through a series of 29 sieves by mechanical shaking. The sieve series ranged from 8 mm (-3Φ) down to 0.062 mm (4Φ), decreasing in 0.25Φ increments. The retained sediment in each sieve was weighed and divided by the total dry weight to derive the dry weight percentage. The weight of any residual sediment falling into the bottom pan (<0.0625mm) was added to the silt+clay fraction for the final dry weight percentage. The percent error was calculated as a quality control check from the difference of the initial dry weight prior to sieving minus the total recovered dry weight/initial dry weight.

The weight percentages were farther grouped into the seven Wentworth size classes (Percival and Lindsay, 1997): Gravel (> 2mm; -1Φ), Very Coarse Sand (>1mm; 0Φ), Coarse Sand (> 0.5mm; 1Φ), Medium Sand (>0.25mm; 2Φ), Fine Sand (> 0.125mm; 3Φ), Very Fine Sand (>0.0625mm; 4Φ) and Silt + Clay (< 0.0625mm; <4Φ). The median grain size was calculated by plotting the cumulative frequency distribution against Φ size and finding the “best fit” equation using TableCurve 2.0 (Systat Software,

San Jose, CA). The “best fit” equation was selected from a ranked list of possible curves based on a combination of the  $r^2$  value and on the visual inspection of the curves’ fit to the plotted data points. The median grain size was then calculated by substituting 0.5 for “y” in the equation to generate the corresponding  $\Phi$  value. The resulting  $\Phi$  value was converted to millimeters using the formula:

$$mm = 2^{-\Phi}$$

The sorting coefficient was calculated using the Inclusive Graphic Standard Deviation method (Gray and Elliot 2009):

$$[(\Phi_{84} - \Phi_{16})/4] + [(\Phi_{95} - \Phi_5)/6.6]$$

The required  $\Phi$  values for the sorting coefficient calculation were derived from the “best fit” equation in TableCurve 2.0 (Systat Software, San Jose, CA). Sorting classification is as defined in Gray and Elliot (2009).

The organic content of the sediment was determined by loss on ignition (LOI) from 2 g of sample at 550°C for 4 hours and sediment carbonate content were calculated after additional LOI at 950°C for 2 hours following Heiri *et al.* (2001).

## 2.3 Results

Median, minimum and maximum readings for the pore water variables are shown in Table 2.1. Temperatures were highest at the vent with a median value near 70°C (Table 2.1). The pore water temperature dropped rapidly away from the vent to near ambient seawater (approximately 30°C; but were variable among replicate samples from each site between 0 m and 140 m (Table 2.1; Figure 2.5).

Pore water salinities were significantly lower at the vent relative to the other sites, but highly variable ranging from 3 – 25 psu (Table 2.1, Figure 2.6). The salinity increased to near 30 psu at 30 m but was widely variable as far as 140 m along the transect, with minimum readings as low as 25.5 psu (Table 2.1, Figure 2.6). Salinities at the 180 m, 250 m, and 300 m sites showed less variability than the other transect sites and had median salinity values around 34 psu (Table 2.1). The median salinity at the reference site was slightly lower than at the farthest transect sites.

The pore water pH values fell within three general groups along the transect: 0 – 60 m, 90 – 140 m, and 180 – 300 m with the reference site. The pH values at the 0 – 60 m sites were low and highly variable (Table 2.1; Figure 2.7). Several individual measurements at the 90 – 140 m sites were also in the acidic range, with the lowest overall reading (5.81) at the 120 m site (Table 2.1). The pH approached normal seawater levels (near 8.0) farther away from the vent and were less variable among replicate samples, however the reference site exhibited a slightly lower pH than the farthest transect locations.

The oxidization-reduction potential (ORP) was highly variable along the transect, but significantly lower at the vent site (Table 2.1; Figure 2.8). With the exception of a few measurements at the vent, all of the transect sites had ORP readings within the oxidizing (i.e., positive) range. The ORP was significantly lower at the reference site relative to all of the transect sites. All of the ORP readings at the reference site were in the negative mV range indicating a reducing sediment environment.

The pore water total arsenic concentration was highest at the vent site and decreased by two orders of magnitude along the transect (Table 2.1; Figure 2.9). Median

arsenic concentrations ranged from close to 600 µg/L at the vent to below 4 µg/L at the 300 m site, and individual measurements ranged widely at each site. The pore water arsenic concentration was also slightly elevated at the reference site relative to the farthest transect sites (Table 2.1; Figure 2.9).

**Table 2.1 Site depths and median, minimum and maximum values for pore water variables by site (n = 5 measurements per site).**

Site	n	Depth meters	Temperature °C		Salinity psu		pH		ORP mV		Pore water [As] µg/L	
0 m	5	8.84	69.8		5.5		6.26		1.00		595.44	
			51.3	81.9	3.0	25.0	6.11	6.99	-32.00	32.00	128.09	868.85
30 m	5	10.06	31.6		30.0		6.34		126.00		49.65	
			31.4	33.6	29.0	30.5	6.05	7.23	96.00	136.00	21.95	151.93
60 m	5	11.58	34.6		31.5		6.40		108.00		38.61	
			31.7	35.6	30.0	33.0	6.03	6.69	66.00	112.00	17.63	76.02
90 m	5	12.50	31.1		34.0		7.68		155.00		20.94	
			30.9	31.3	33.5	35.0	6.65	7.81	148.50	165.00	10.08	33.84
120 m	5	13.11	31.1		33.5		6.13		112.00		34.24	
			29.8	34.2	25.5	34.0	5.81	7.41	83.00	130.00	11.18	114.37
140 m	5	14.63	30.4		33.0		7.34		42.00		19.72	
			29.8	35.4	26.5	33.0	5.96	7.57	32.00	87.00	13.20	57.98
180 m	5	17.68	30.7		33.5		7.81		72.00		9.90	
			30.7	30.7	33.0	33.5	7.73	7.98	69.00	89.00	4.88	17.39
250 m	5	23.77	29.6		34.0		7.80		79.00		3.98	
			29.6	29.7	33.5	34.5	7.64	7.94	22.00	144.00	3.03	7.72
300 m	5	28.35	29.6		34.0		7.78		78.00		3.77	
			29.6	29.7	33.5	34.0	7.61	7.83	75.00	132.00	2.38	9.58
Ref	5	12.50	30.0		32.5		7.46		-54.00		12.75	
			29.9	30.0	32.5	33.5	7.32	7.65	-530*	-41.00	5.88	15.38

\* Outlying value excluded from statistical analysis

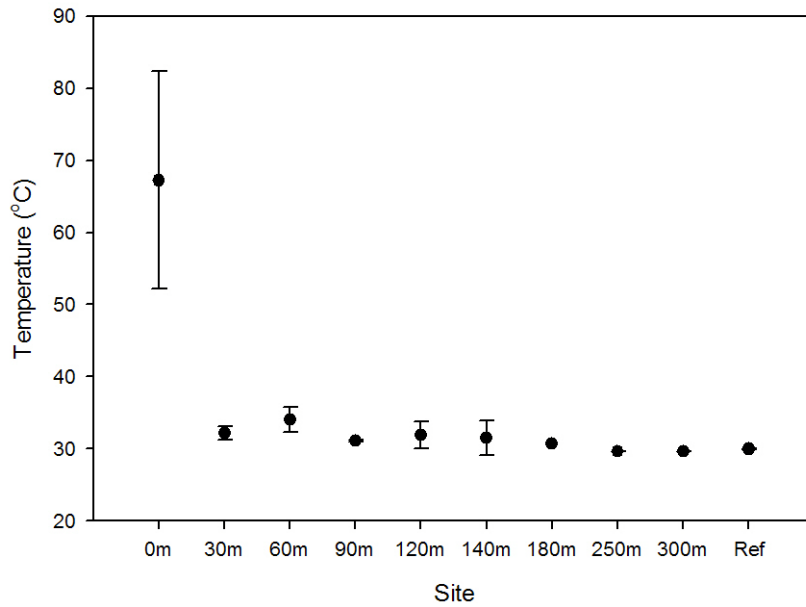


**Figure 2.5 Ambitle Island May/June 2005: mean pore water temperature  $\pm 1$  standard deviation.**

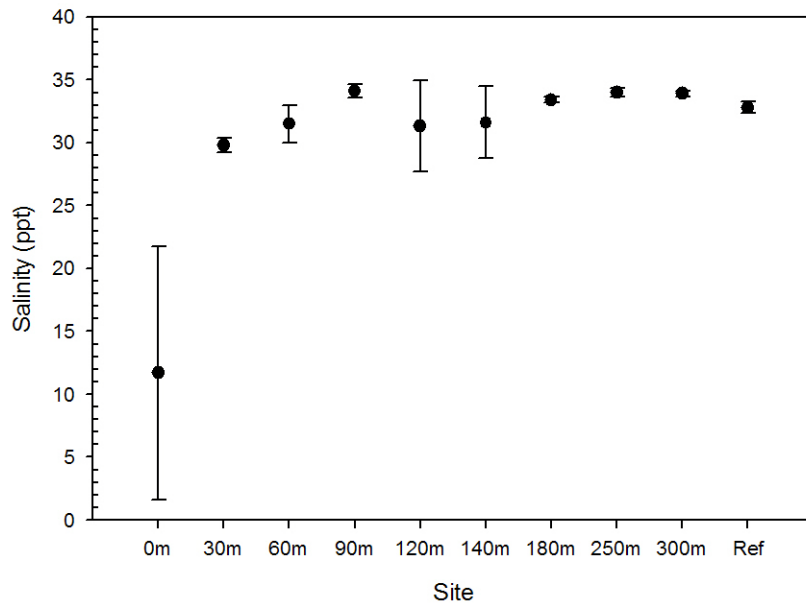


**Figure 2.6 Ambitle Island May/June 2005: mean pore water salinity  $\pm 1$  standard deviation.**

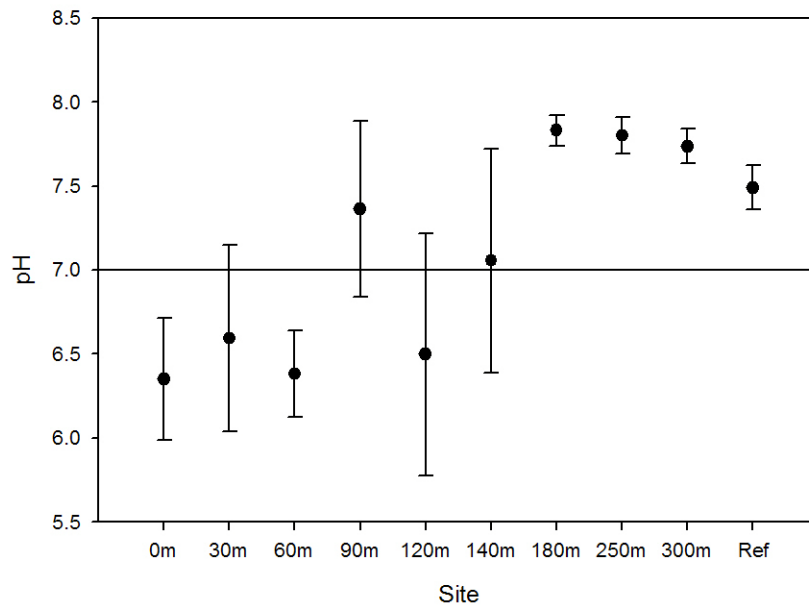


**Figure 2.7 Ambitle Island May/June 2005: mean pore water pH  $\pm$  1 standard deviation.**

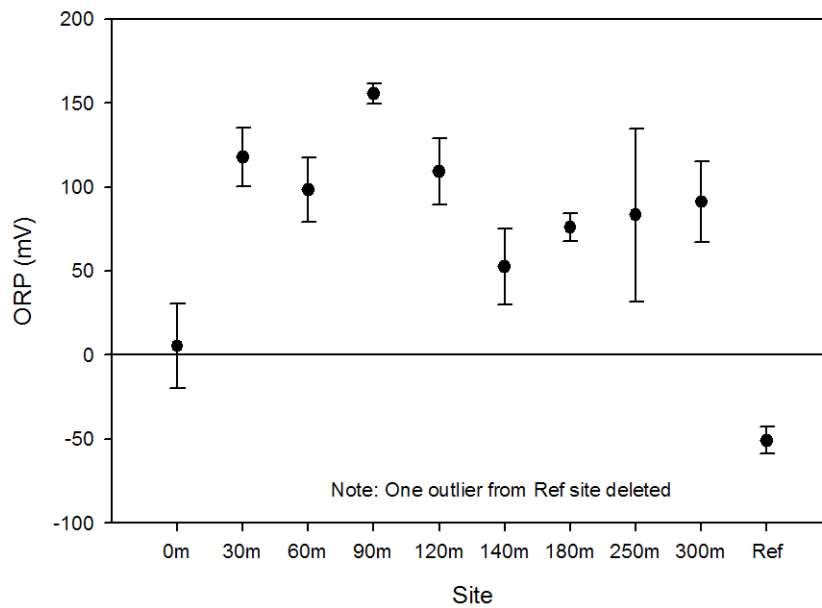


**Figure 2.8 Ambitle Island May/June 2005: mean pore water oxidation-reduction potential  $\pm$  1 standard deviation.**

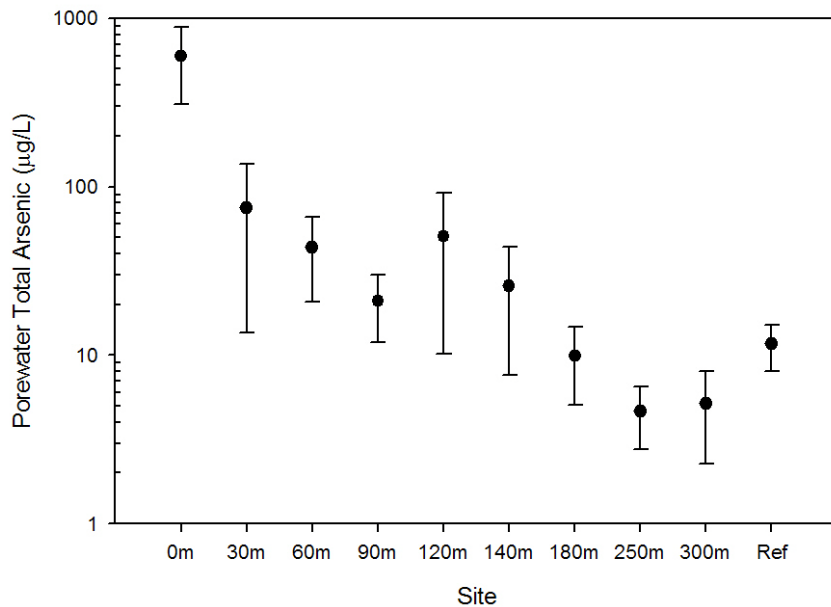


**Figure 2.9 Ambitle Island May/June 2005: mean pore water arsenic concentrations  $\pm 1$  standard deviation.**

The sediment characteristics at each site are summarized in Tables 2.2 and 2.3. Sediments at the vent site were composed primarily of gravel sized fragments, and the median grain size was significantly larger than at the other sites (Tables 2.2 & 2.3; Figure 2.10). Fine sands composed the largest fraction of the sediments from 30 -140 meters along the transect and there was a steady, curvilinear increase in the median grain size moving out towards the 300 m site (Table 2.2 & 2.3; Figure 2.10). Fine sands were less prevalent at the 180 – 300 m sites as median grain sizes increased towards the medium to coarse sands range (Figure 2.10). The gravel size fraction also increased starting at the 180 m site and comprised over 25% of the sediments at the 250 and 300 m sites (Table 2.2). The reference site sediments were composed of fine sands with a median grain size similar to the 90 meter site (Tables 2.2 & 2.3; Figure 2.10).



The sediment sorting coefficient at the vent site was significantly higher than at the other sites and indicated the sediments were very poorly sorted (Table 2.3; Figure 2.11). The sediment sorting coefficients exhibited an increasing trend along the transect with values falling within the “well sorted” to the “moderately well sorted” range out to the 140 m site and increasing to the “poorly sorted” range at the 180 – 300 m sites (Figure 2.11). The sediments at the reference site were “moderately” to “poorly” sorted with a median sorting coefficient value falling right at the border between these two sorting classifications (Table 2.3; Figure 2.11).

The percent organic carbon in the sediments generally increased with distance from the vent and was highest at the reference site (Table 2.3; Figure 2.12). The percentage of carbonates in the sediments was low at the vent site and at the transect sites out to the 140 m site (Table 2.3; Figure 2.13). Carbonates increased significantly at the 180 m site and were highest at the 250 m and 300 m sites. There was no significant difference in the percent sediment carbonate between the reference site and the 180 m site, both of which were significantly lower than the 250 m and 300 m sites, but significantly higher than the 0 m – 140 m sites (Figure 2.13).

**Table 2.2 Median, minimum and maximum dry weight percentage of sediment by Wentworth size class.**

Site	n	Gravel %		Very Coarse Sand %		Coarse Sand %		Medium Sand %		Fine Sand %		Very Fine Sand %		Silt + Clay %	
0 m	5	65.18		6.30		3.93		6.34		11.44		2.88		3.63	
		60.12	70.40	6.00	7.31	3.59	5.57	5.71	8.11	9.39	14.14	1.75	3.50	1.86	4.41
30 m	5	0.00		0.38		0.30		2.71		61.10		33.29		2.10	
		0.00	0.05	0.22	0.73	0.26	0.33	1.42	2.83	56.82	63.87	30.25	38.87	2.04	2.81
60 m	5	0.00		0.07		0.11		2.91		68.06		26.86		1.57	
		0.00	0.06	0.04	0.69	0.00	0.28	2.02	11.75	66.99	76.53	9.97	28.98	1.50	1.64
90 m	5	0.07		1.78		0.77		7.93		76.14		11.86		1.02	
		0.04	0.47	0.71	3.46	0.39	1.23	6.39	9.56	73.37	77.74	10.55	13.68	0.97	1.67
120 m	5	0.00		1.05		1.16		16.83		74.45		4.23		1.17	
		0.00	0.15	0.48	2.56	0.69	1.86	14.10	19.67	72.92	77.14	3.62	5.86	1.03	1.26
140 m	5	0.04		2.75		5.70		27.28		60.33		2.22		1.27	
		0.00	0.22	1.70	4.42	4.01	6.67	23.26	37.53	51.76	64.64	1.00	3.32	1.00	1.45
180 m	5	13.25		8.82		11.35		27.61		34.51		3.45		0.88	
		8.11	19.99	8.65	10.67	9.63	14.80	23.41	30.72	27.14	36.28	1.67	5.11	0.84	2.18
250 m	5	26.52		13.23		14.05		20.79		22.73		4.06		1.15	
		9.20	27.54	10.89	14.25	12.55	17.25	18.94	26.51	20.66	25.76	3.70	5.61	1.05	1.63
300 m	5	28.74		15.94		14.93		17.72		16.32		2.84		0.99	
		22.94	33.15	14.01	20.46	13.69	18.09	15.42	19.69	13.08	18.67	2.07	3.90	0.89	1.45
Ref	5	0.42		2.16		8.56		16.09		43.41		25.21		4.42	
		0.18	0.90	1.41	2.77	6.87	9.59	15.24	19.75	41.45	45.81	21.39	26.16	4.40	4.73

**Table 2.3 Median, minimum and maximum measurements for sediment parameters.**

Site	n	Median Grain Size mm		Sorting Coefficient Φ		Organics %		CaCO <sub>3</sub> %	
0 m	5	4.33		2.34		2.24		0.73	
		3.49	5.35	2.12	2.45	1.93	2.45	0.48	0.96
30 m	5	0.14		0.45		1.81		0.32	
		0.13	0.15	0.44	0.46	1.44	2.06	0.25	0.46
60 m	5	0.15		0.42		1.55		0.39	
		0.14	0.17	0.41	0.43	1.41	1.82	0.31	0.47
90 m	5	0.17		0.44		1.48		0.52	
		0.17	0.18	0.42	0.58	1.39	1.57	0.39	0.70
120 m	5	0.20		0.41		1.46		0.39	
		0.19	0.20	0.38	0.47	1.42	1.51	0.33	0.60
140 m	5	0.22		0.60		1.60		0.42	
		0.22	0.24	0.54	0.69	1.52	1.70	0.36	1.18
180 m	5	0.29		1.59		3.91		6.71	
		0.28	0.34	1.33	1.86	3.41	4.30	6.34	9.71
250 m	5	0.51		1.85		5.79		28.38	
		0.36	0.60	1.46	1.97	5.49	7.48	24.55	33.48
300 m	5	0.79		1.80		7.11		30.77	
		0.68	1.12	1.66	1.92	6.28	8.22	28.52	37.04
Ref	5	0.17		1.00		9.18		6.37	
		0.16	0.18	0.91	1.07	7.52	9.40	5.85	7.40

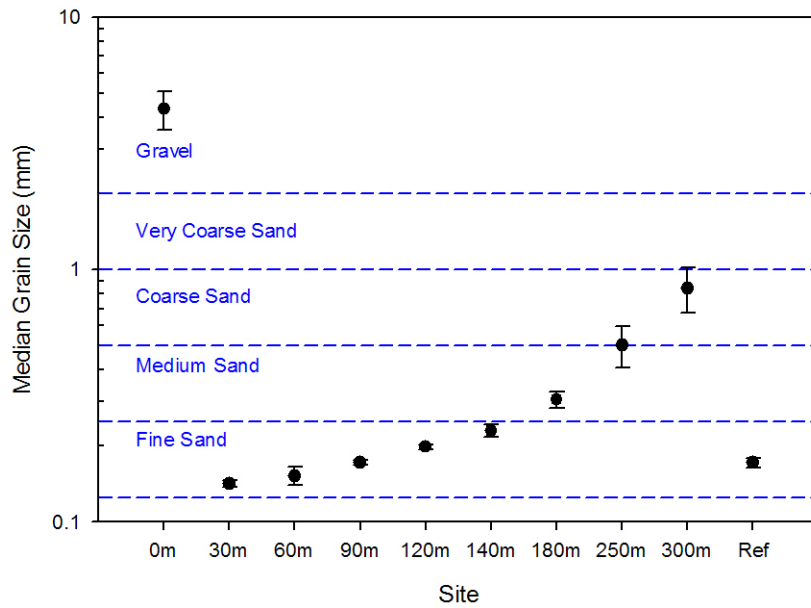


**Figure 2.10 Ambitle Island May/June 2005: mean median grain size  $\pm$  1 standard deviation.**

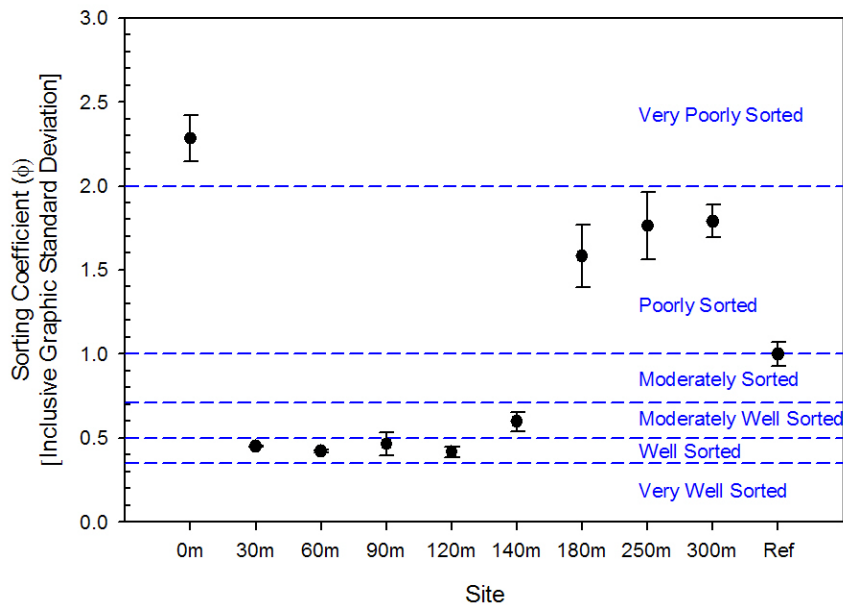


**Figure 2.11 Ambitle Island May/June 2005: mean sorting coefficient  $\pm$  1 standard deviation.**

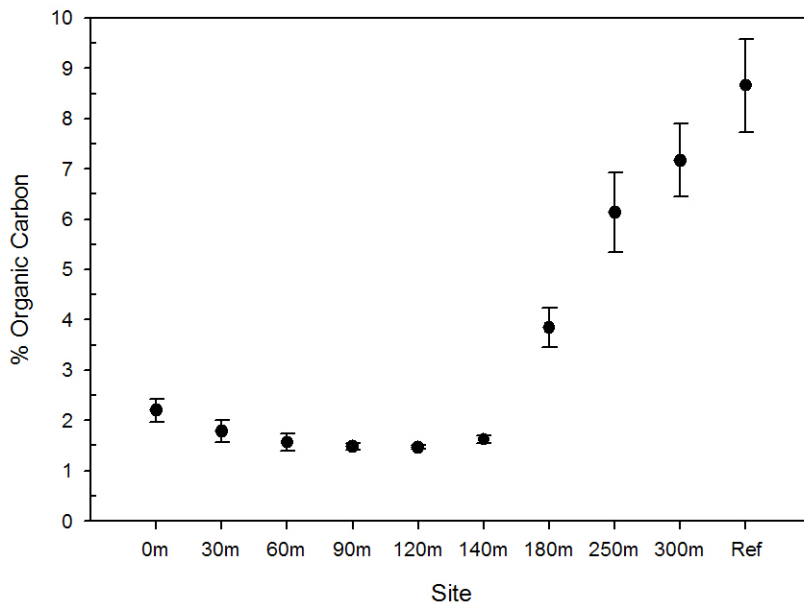


**Figure 2.12 Ambitle Island May/June 2005: mean sediment organic carbon content  $\pm 1$  standard deviation.**

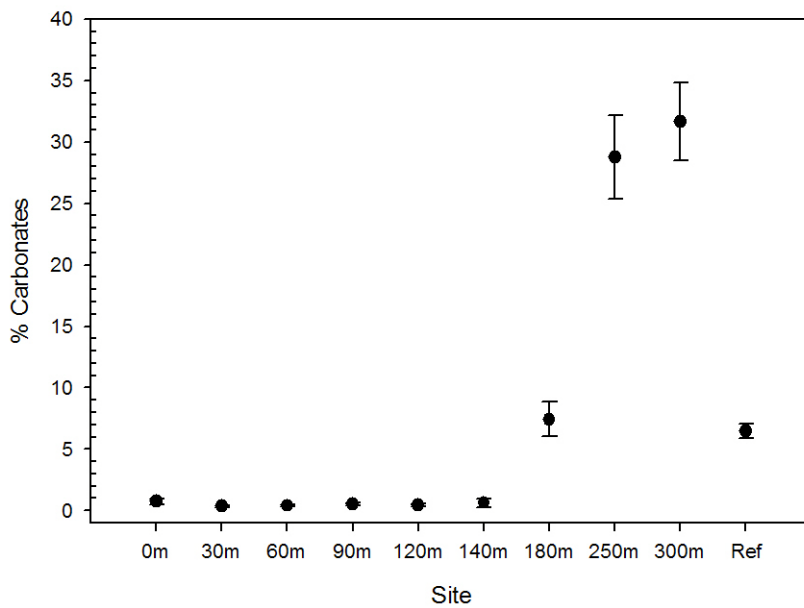


**Figure 2.13 Ambitle Island May/June 2005: mean sediment carbonate content  $\pm 1$  standard deviation.**

Principal component analysis (PCA) of the sediment and pore water variables (Figure 2.14) shows four general groupings of the sampling sites based on their environmental attributes. The five 0 m replicates separate out from the rest of the samples along the first principal component axis (PC1). The wide distance between the five 0 m data points reflects the high variability in the physical parameters measured at that site. The remaining samples generally group together according to their distance along the transect. Three distinct groupings are seen: the 30 m – 140 m samples; the 180 m + the reference site samples, and the 250 m + 300 m samples (Figure 2.14).

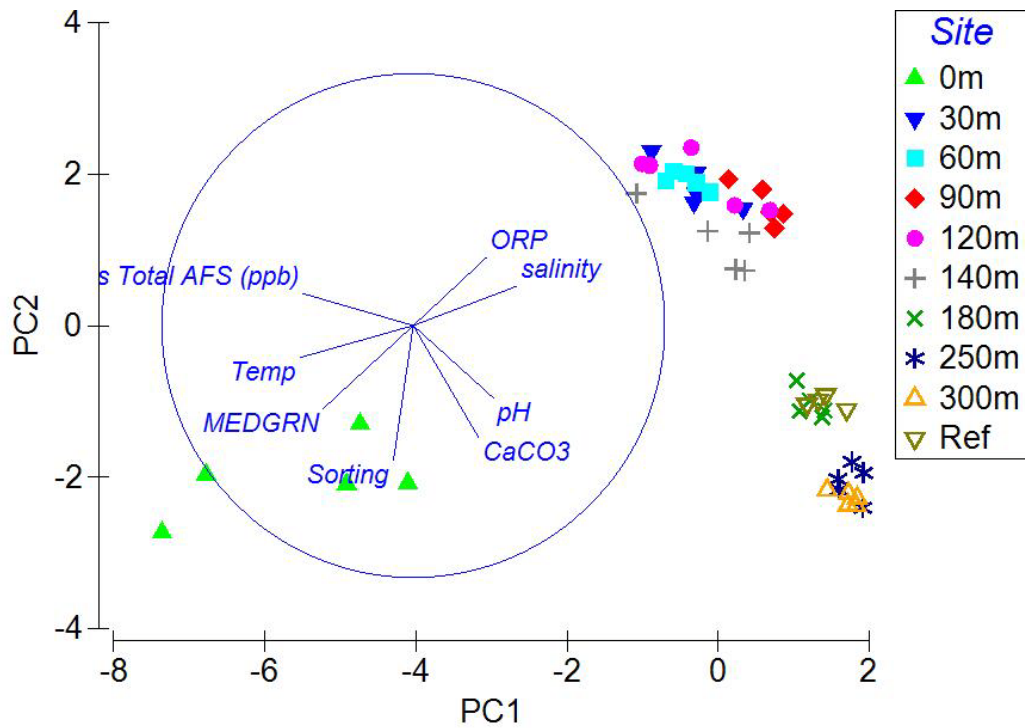


**Figure 2.14 Ambitle Island May/June 2005: Principal components analysis of pore water and sediment characteristics.**

The first two principal component axes account for 85% of the variation in the data (Table 2.4). The first principal component (PC1) accounted for nearly half of the variation (Table 2.4) and was weighted primarily by the pore water temperature, salinity and total arsenic concentration (Table 2.5). The second principal component (PC2) accounted for 35% of the variation in the data (Table 2.4) and was weighted largely by the sediment parameters, particularly the sorting coefficient, and percent carbonates and organics (Table 2.5).

**Table 2.4 Principal component eigenvalues and percent variation.**

Principal Component	Eigenvalues	% Variation	Cum.% Variation
1	4.48	49.7	49.7
2	3.18	35.3	85.0
3	0.49	5.4	90.5
4	0.382	4.2	94.7
5	0.219	2.4	97.2

**Table 2.5 Principal component eigenvectors.**

Variable	PC1	PC2	PC3	PC4	PC5
Temperature	-0.450	-0.127	0.071	0.014	-0.059
pH	0.319	-0.287	0.141	-0.823	0.177
ORP	0.290	0.270	0.873	0.195	-0.063
Salinity	0.410	0.155	-0.355	0.113	-0.577
Total pore water [As]	-0.438	0.127	0.101	0.049	0.158
% Organic	0.221	-0.442	-0.092	0.431	0.565
% CaCO <sub>3</sub>	0.260	-0.445	0.096	0.283	-0.128
Median grain size	-0.360	-0.331	0.197	-0.055	-0.327
Sorting	-0.079	-0.534	0.143	0.023	-0.402

Table 2.6 presents the Spearman correlations between the measured pore water and sediment variables. For the pore water variables, there were strong negative correlations ( $\rho \geq |0.70|$ ) between temperature and pH and between temperature and salinity, while salinity and pH showed a strong positive correlation. The pore water pH was also negatively correlated with total pore water arsenic and positively with the sediment carbonates.

The ORP exhibited negative correlations with the sediment organic content and the sorting coefficient. The total arsenic concentration was negatively correlated with salinity and sediment carbonates. The sediment organics, carbonates and sorting coefficient were positively correlated with each other.



**Table 2.6 Spearman correlation coefficients between pore water and sediment characteristics. Significance (p) in parenthesis.**

	pH	ORP	Salinity	Total [As]	% Organic	% CaCO <sub>3</sub>	Median Grain Size	Sorting
Temp	-0.78 (0.000)	0.09 (0.549)	-0.76 (0.000)	0.88 (0.000)	-0.56 (0.000)	-0.67 (0.000)	-0.25 (0.076)	-0.29 (0.044)
pH		-0.11 (0.451)	0.74 (0.000)	-0.81 (0.000)	0.53 (0.000)	0.74 (0.000)	0.31 (0.028)	0.44 (0.001)
ORP			0.35 (0.013)	0.06 (0.674)	-0.57 (0.000)	-0.35 (0.013)	-0.35 (0.012)	-0.50 (0.000)
Salinity				-0.75 (0.000)	0.13 (0.355)	0.49 (0.000)	0.14 (0.334)	0.06 (0.671)
Total [As]					-0.58 (0.000)	-0.71 (0.000)	-0.25 (0.077)	-0.30 (0.034)
% Organic						0.79 (0.000)	0.43 (0.002)	0.72 (0.000)
% CaCO <sub>3</sub>							0.63 (0.000)	0.73 (0.000)
Median Grain Size								0.80 (0.000)

## 2.4 Discussion

The pore water and sediment variables show a strong environmental gradient with distance from the vent which can influence the structure of the surrounding sediment community. High temperatures associated with tectonic activity are the defining characteristic of hydrothermal systems. Temperatures of the hydrothermal fluids at the Tutum Bay vent are near 100°C when they emerge from the focused vent opening (Pichler and Dix 1996, Pichler *et al.* 1999b) and the temperatures of the interstitial pore waters near the vent were as high as 82°C (Table 2.1). The variability in temperatures at several sites along the transect was due to the sporadic diffuse venting that occurred as far away as 150 m from the focused vent. This was most evident at the 60 m, 120 m and 140 m sites. McCloskey (2009) deployed temperature data loggers at selected sites along the transect during the 2005 field sampling trip to Ambitle Island. The data loggers were buried approximately 1cm in the sediment and recorded temperature readings every minute over a seven day period. These loggers revealed localized temperature spikes of 10 - 15°C extending as far as 150 m from the vent (McCloskey 2009), further showing the influence of diffuse venting along this section of the transect.

The reduced salinity observed at the vent is attributed to the source water of the hydrothermal fluids, which is ultimately from meteoric (i.e. rain) derived groundwater from Ambitle Island (Pichler and Dix 1996, Pichler *et al.* 1999b). The high variability in the salinity measurements at the 0 m site may possibly be due to the entrainment of the ambient seawater during sampling, or could reflect the actual patchiness of the vent fluid percolating through the sediments surrounding the vent opening. The coarse sediments at

the 0 m site readily allowed mixing of the interstitial waters with the ambient seawater. The median salinity value of 5.5 psu and minimum reading of 3.0 psu however, agree with the salinities reported from earlier studies at Tutum Bay (Pichler *et al.* 1999b). The variable salinity measurements observed along the transect at the 120 m and 140 m sites are due to the diffuse venting of hydrothermal fluids and correspond to the spikes in temperature observed at these two sites.

With high temperature and low salinity, the hydrothermal fluid is less dense than the surrounding seawater and quickly rises to mix with the surface waters (Pichler *et al.* 1999b). Pichler *et al.* (1999b) used the concentration of silica in the vent fluid as a tracer to model the dissipation of the vent water as it mixes with the surrounding seawater and found that the surface water over the vents showed a 10x higher concentration of vent fluid constituents relative to the bottom water at the vent opening. Those findings suggest that harmful constituents, such as arsenic, are rapidly transported away from the benthic habitat surrounding the vent, mitigating potential harmful effects on the benthic fauna.

The pH values at all of the sites were lower than expected for normal marine systems, which are typically above 8.0 pH units. The pH measures had an overall range of 2.17 pH units, with the lowest reading of 5.81 and highest measurement of 7.98 pH units. By comparison, pH measured on the Great Barrier Reef by Gagliano *et al.* (2010) only ranged 0.39 pH units across all habitats with the lowest value being 7.98 from water extracted from a goby burrow. The lowest pH observation was at the 120 m site, with low measurements also at 140 m, which reflects the influence of diffuse venting at these sites.

The persistence of reduced pH out to even the 300 m site illustrates the extent of influence the hydrothermal venting has on the environment at Tutum Bay.

Studies at other shallow water vent systems have also reported low pH values comparable to Tutum Bay. For example, Melwani and Kim (2008) reported mean pH values of 6.5 at their Bahía Concepción vent site and 7.2 at their White Point site. At both sites their “outside zone” pH values were 7.8 and 7.4 respectively (Melwani and Kim 2008), although they did not specify the distance from the vent area these samples were taken. Hall-Spencer *et al.* (2008) reported pH as low as 6.57 at a shallow volcanic vent in Italy. That study focused specifically on the effects of reduced pH on calcareous organisms, using the vent system as a natural laboratory to study the potential ecosystem impacts of ocean acidification due to the projected increase of atmospheric CO<sub>2</sub> over the next century (Hall-Spencer *et al.* 2008).

The pH values observed at Tutum Bay, even at the farthest site from the focused venting in predominately carbonate sediments, were still at or below the lowest values expected in a natural coral system (Gagliano *et al.* 2010) and less than end-of-century values predicted by current climate models.

The ORP measurements indicated that all of the sites had oxidizing sediment environments at 5cm with the exception of the Danlum Bay reference site. The low ORP values seen at the reference site were due to the high organic content of these sediments. The Danlum Bay reference site was near shore and close to a small stream flowing from the island. This resulted in the input of a significant amount of terrestrial detritus. The ORP values were also low, but oxidizing, at the 0 m site, with one of the replicate samples recording a negative (reducing) value. Pichler *et al.* (1999b) found that the vent

fluids are reduced and the lower ORP values at the 0 m site are a result of mixing of the vent fluids with the ambient seawater.

Past studies at the Tutum Bay vents discovered that the vent fluids and surrounding sediment deposits had the highest naturally occurring concentrations of arsenic recorded in a marine environment (Pichler and Dix 1996, Pichler and Veizer 1999, Pichler *et al.* 1999a&b). Results presented here show nearly two orders of magnitude difference in the pore water arsenic concentrations along the transect. Arsenic concentrations of seawater near the 300 m site were still higher than normal ( $\sim 2 \mu\text{g/L}$ ). The variability seen at several of the transect sites was most likely due to the influence of diffuse venting. The slightly elevated arsenic concentrations measured at the reference site may reflect the transport of volcanic sediments from Ambitle Island.

The sediment characteristics also define specific habitat types along the transect. At the 0 m site, the sediment was composed of coarse, very poorly sorted volcanic gravel. The deposition of coarse sediments is indicative of a high energy environment and may be due to the constant resuspension and transport of finer-grained sediments offshore (Gray and Elliot 2009). This is likely caused by active focused venting and the influence of wave action at the shallower depths. The transect sites from 30 m out to 140 m were characterized by fine, well-sorted volcanic sand that exhibited a steady increase in the median grain size with distance from the vent. This sediment type indicates a relatively lower energy, stable environment which allows for the deposition of finer grained sediments (Gray and Elliot 2009). The transect was surrounded by higher relief areas of coral reef, particularly towards the shoreline and the area of focused venting. This may have sheltered the inshore part of the transect from the effects of waves and currents.

Diffuse venting occurred mostly in this inshore portion of the transect, resulting in low pore water pH which likely caused the dissolution of larger grained biogenic carbonate sediments. The sediments appeared to be extensively reworked by burrowing shrimp (*Thalassinidea* spp.) at this site which may have influenced the sediment distribution and geochemistry. This will be discussed further in the chapters on the macrofaunal communities. The 180 m site represented a mixing zone of the finer-grained volcanic sands and biogenic carbonate sediments. The 250 m and 300 m were characterized by coarse-grained carbonate sediments comprised of fragments of shells, calcareous algae and coral rubble. The larger sediment grain size at these sites reflects the increased influence of offshore currents, which were noticeable especially at the 300 m site. The Danlum Bay reference site also represented a transitional sediment zone between the nearshore, volcanic sands originating from Ambitle Island, and biogenic calcareous sands from the offshore reef environment. This site had similar grain size characteristics as the inner transect sites, but was more similar to the 180 m site in terms of its mixed volcanic and carbonate sediments.

## **2.5 Summary and conclusions**

The study sites consisted of four distinct habitat types, characterized by pore water and sediment types. The 0 m site represented a unique habitat characterized by high temperature and pore water arsenic concentrations, low pore water salinity and pH, and coarse, very poorly sorted volcanic gravel with low organic carbon and carbonate content. The transect sites from 30 m to 140 m formed a distinct habitat type characterized by the zone of diffuse venting. The shared attributes of these sites were

near ambient temperature and salinity, low pH, elevated arsenic concentration and very well-sorted, fine-grained volcanic sands with low organic carbon and carbonate content. The 180 m and reference site formed a third habitat type and shared similar temperature, salinity, pore water arsenic concentrations and sediment carbonate composition. These sites represented a transitional zone between the near shore volcanic sediments and the offshore carbonate sediments. The reference site stood out from all the other sites along the transect due to its high organic carbon content. The 250 m and 300 m sites represented a fourth distinct habitat type, further removed from the effects of the hydrothermal activity. These two offshore sites were characterized by near ambient temperature and salinity values, slightly elevated arsenic concentrations, higher pH and poorly sorted, coarse carbonate sediments with relatively high organic carbon.

Each of these four habitats or zones exhibit distinct environmental characteristics which in turn influence the biological community structure found there. The succeeding chapters will focus on these biological communities at the macrofaunal, meiofaunal, and molecular eukaryotic levels and the influence of the physical environment in structuring these communities.

## Chapter Three

### Changes in Benthic Macrofauna associated with a Shallow-water Hydrothermal Vent Gradient in Papua New Guinea

*(This chapter has been published in Karlen et al. 2010)*

#### 3.1 Introduction

Shallow-water hydrothermal vents occur worldwide, but relatively few studies have been carried out on the benthic community structure of these systems (Thiermann *et al.* 1997). Several such systems that have been studied in some detail include sites in the Mediterranean and Aegean Seas (Thiermann *et al.* 1997, Gamenick *et al.* 1998a, Morri *et al.* 1999, Cocito *et al.* 2000), the Kurile Islands (Tarasov *et al.* 1990, Sorokin *et al.* 2003, Kamenev *et al.* 2004), New Zealand (Kamenev *et al.* 1993), the Gulf of California and southern California (Melwani and Kim 2008) and several sites in Papua New Guinea including Rabaul harbor (Tarasov *et al.* 1999), and Ambitle Island (Pichler and Dix 1996, Pichler and Veizer 1999, Pichler *et al.* 1999a,b). The last site was the focus of the current study.

Previous work carried out on Ambitle Island focused on the geochemistry of the hydrothermal fluids and surrounding sediment. Vent and pore waters were enriched in several elements, but most notably, arsenic concentrations were 275 times that of normal seawater (Pichler *et al.* 1999b). Despite the elevated concentration of arsenic, the surrounding reef habitat and fauna appear to be unaffected (Pichler and Dix 1996). This



is likely due to the removal of arsenic from the water column via the precipitation of Fe (III) oxyhydroxides (Pichler and Veizer 1999, Pichler *et al.* 1999a). Because of this previous work, we focused this study on the influence of arsenic, along with other vent related factors such as temperature, pH and sediment characteristics, on the benthic macrofauna near the Ambitle Island vent.

Arsenic is naturally occurring in Ambitle Island ground water, which is the source of the hydrothermal fluids at these vents (Pichler *et al.* 1999b). Elemental arsenic is commonly found in two inorganic forms: arsenate [As (V)] and arsenite [As (III)] (Francesconi and Kuehnelt 2002, Oremland and Stolz 2003, Watt and Le 2003). These compounds can be metabolized by several prokaryotes either through the respiration of arsenate or the oxidation of arsenite, particularly in extreme environments (Inskeep *et al.* 2002, Oremland and Stolz 2003, Oremland *et al.* 2005). Additionally, eukaryotic organisms can convert inorganic arsenic into organic compounds via methylation (Andreae 1979, Kitts *et al.* 1994, Cutter *et al.* 2001) and there is some evidence that these can be transferred among different trophic levels (Barwick and Maher 2003).

Pore water pH is an important variable in geochemical processes. Previous studies at the Ambitle Island vents found reduced pH levels in the vent fluids which were attributed to high levels of CO<sub>2</sub> in the fluids and gas bubbles discharging from the vents (Pichler *et al.* 1999b). Additionally, low pH can influence sediment composition by the dissolution of carbonate sediments (Burdige and Zimmerman 2002) and impair carbonate incorporation in shell bearing organisms (Green *et al.* 1993). Acidification of sea water associated with release of CO<sub>2</sub> at shallow water vents has been observed off of Italy by Hall-Spencer *et al.* (2008). In their study they reported reduced densities of calcareous

algae and invertebrates at sites with reduced pH and observed signs of shell dissolution on gastropods (Hall-Spencer *et al.* 2008).

Initial field observations at the study site indicated a distinctive gradation in the sediment composition in relation to the measured offshore distance from the vent. The relationship between sediment characteristics (grain size, organic carbon content) and the benthic infaunal community have long been recognized (Sanders 1958). The interrelationships of sediment properties and benthic communities are complex (Snelgrove and Butman 1994), but in general, fine grained sediments and high organic carbon content tend to be dominated by deposit feeders while coarse sediments tend to support more suspension-feeding organisms.

Field observations also indicated that carbonate content of sediment was lower nearer the vent, with the carbonate fraction increasing with distance from the vent. Near shore and in the vicinity of the vents the sediments were predominately fine grained volcanic sands, with some gravel sized deposits near the vents. A gradual mixture of biogenic carbonates was observed starting around 100 m from the vent, consisting of fragments of calcareous algae and coral rubble from the surrounding reef. Bioturbation by burrowing organisms can farther affect grain size and carbonate content of the sediment (Aller 1982).

The primary goal of this study is to investigate the effect of a natural hydrothermal gradient on the benthic macrofauna. To do this, we measured pore water and sediment arsenic concentrations, temperature, pH, and sediment composition, and characterized the benthic fauna at different distances from a shallow hydrothermal vent. It was expected that elevated arsenic concentrations would be a significant factor in

structuring the benthic community. Studies of similar systems focused on depth rather than distance from the shallow vents (Tarasov *et al.* 1999), sampled at only select sites (Kamenev *et al.* 1993) or short transects of 5 m (Thiermann *et al.* 1997). This study is unique in that sampling was carried out over a 150 m transect and significant effects were found even at that distance.

### **3.2 Material and methods**

The study site was located in Tutum Bay, Ambitle Island, Papua New Guinea (4° 05'S Latitude, 153° 40' W Longitude) (Figure 3.1). The island is an active volcano, with several large hot springs on shore in addition to the submarine hydrothermal vents. The hydrothermal vents in this study were located at a water depth of 10 m and were surrounded by an extensive coral reef system with intermittent patches of sand. The main vent had a focused discharge of 300-400 L/min hydrothermal fluids through a narrow, 15 cm diameter opening in the sea floor (Pichler *et al.* 1999b). In the sandy areas immediately surrounding the vent, a diffuse discharge of hydrothermal fluids and gases was observed as a steady stream of bubbles rising from the sediment. This diffuse venting was strongest near the main vent, but appeared sporadically as far as 60 m away (Figure 3.2).

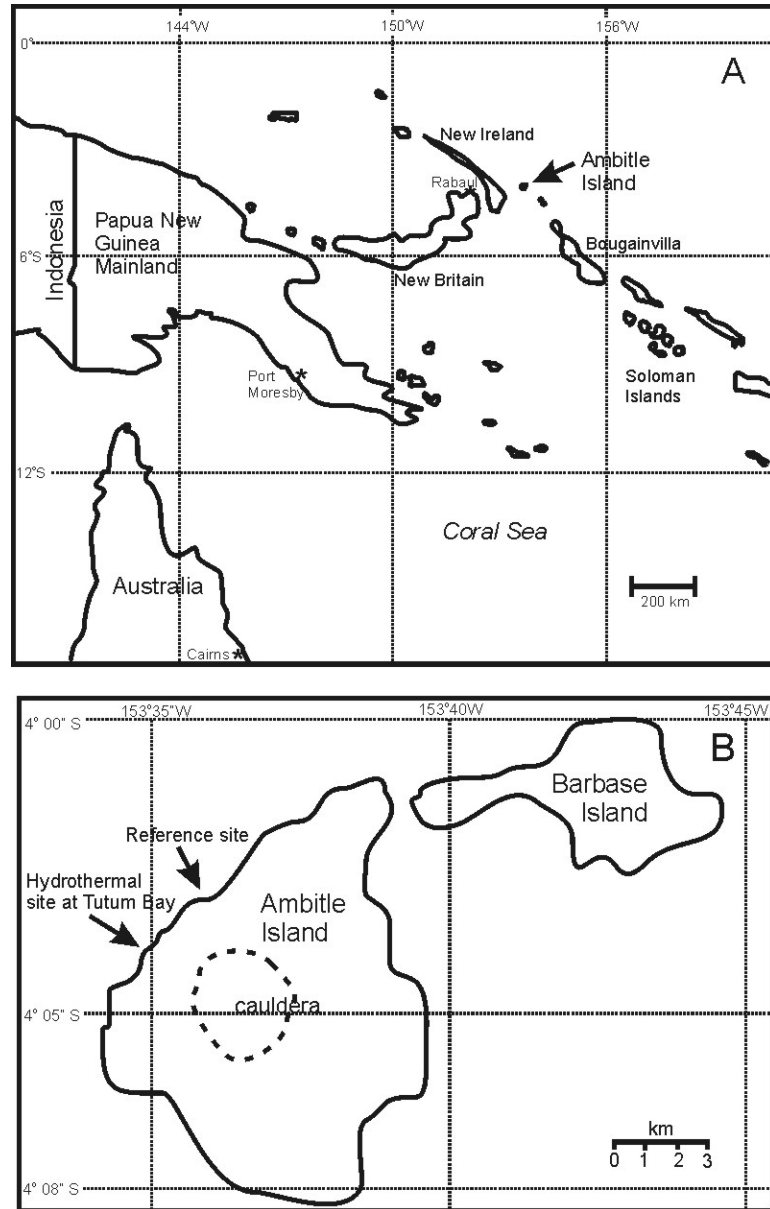


**Figure 3.1 A: Map of Papua New Guinea and its geographic relation to Australia. Ambitle Island is marked with an arrow and is located east of New Ireland. Latitude and longitude are marked in degrees. B: Map of Ambitle Island with the study sites marked with arrows. Latitude and longitude are indicated in degrees and minutes.**

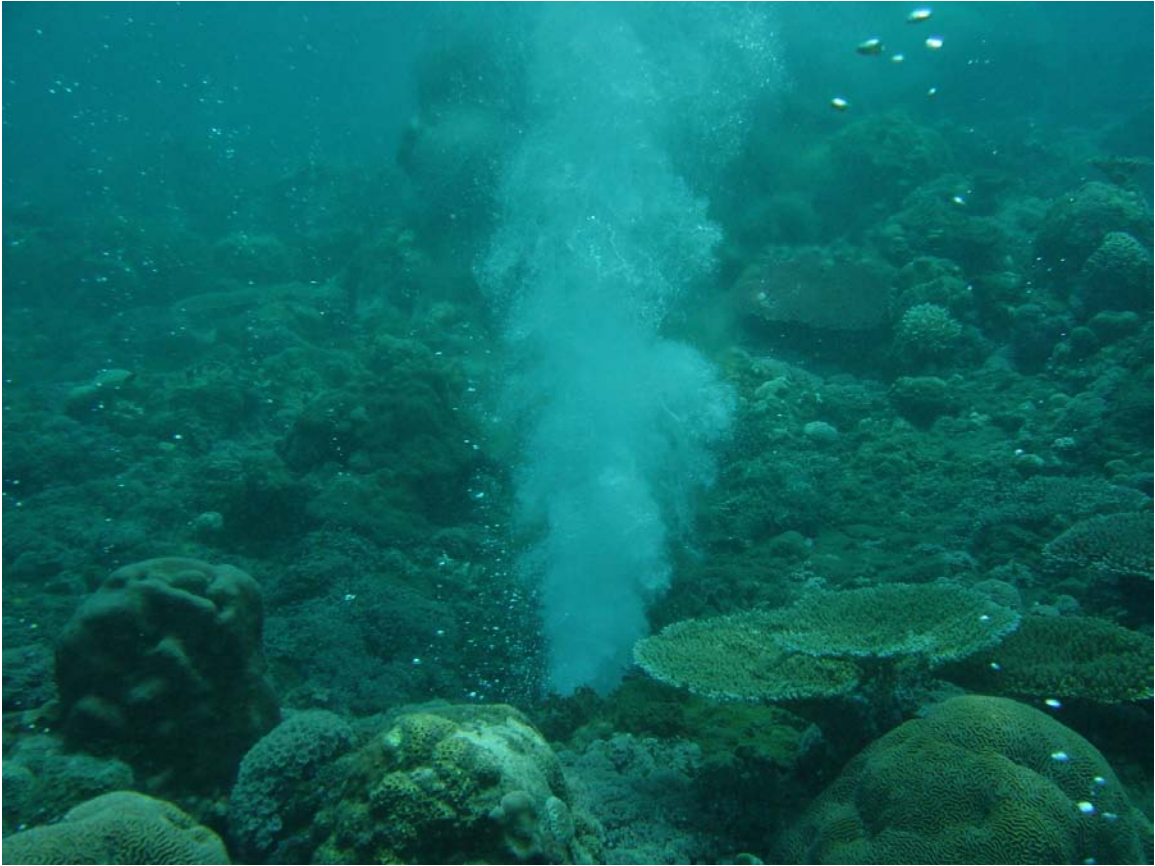


**Figure 3.2 Photograph of focused hydrothermal vent at Tutum Bay, Ambitle Island, Papua New Guinea with surrounding diffuse venting (Photo credit: DJK).**

Benthic macrofauna samples were collected at three sites along a transect running from a focused hydrothermal discharge. The transect ran southwest from the vent along a sandy bottom for 30 m, and then continued offshore to the west to avoid the reef. The maximum depth along the transect was 15 m. Sample sites were at 7.5, 60 and 150 m along the transect line, representing a subset of sites chosen for geochemical analysis. These sites were selected based on sediment temperature profiles conducted along the transect, which indicated that each site would represent a decreasing trend in the hydrothermal influence with distance from the vent, with the 150 m site presumably outside the hydrothermal zone. Additional samples were collected at a single reference

site located approximately 1.6 km north of Tutum Bay in an area not affected by hydrothermal activity and at a similar depth as the transect sites. Sampling was limited by logistical problems encountered in shipping supplies to the site and in shipping samples back to the laboratory in the U.S. At each site along the transect a 1 m<sup>2</sup> grid was placed next to the transect line. A single grid was sampled at the reference site. The grid was subdivided into 100 10x10 cm cells and five cells were selected for sampling using a random number table (Rolf and Sokal 1981). Five core samples (diameter = 7.62 cm; area = 45.6 cm<sup>2</sup>) were taken from random grid cells within the 1 m<sup>2</sup> quadrat to a depth of 15 cm. The core samples were sieved through a 500 µm mesh sieve and the retained animals were fixed in 10% formalin with Rose Bengal stain for a minimum of 72 hours, then transferred into 70% methanol for preservation. Organisms were sorted from the sediment under a dissecting microscope, identified to the lowest practical taxonomic level and enumerated.

Three smaller cores (diameter = 3.0 cm) were taken at randomly selected grid cells for sediment grain size, organic carbon and carbonate content analysis at each site. The sediment samples (50 g) were dry sieved through a stacked series of sieves and divided into six Wentworth Size Classes (Percival and Lindsay, 1997): Gravel (> 2000 µm), Coarse Sand (> 500 µm), Medium Sand (>250 µm), Fine Sand (> 125 µm), Very Fine Sand (> 63 µm), Silt + Clay (< 63 µm). The organic content of the sediment was determined by loss on ignition (LOI) from 2 g of sample at 550°C for 4 hours and sediment carbonate content was calculated after additional LOI at 950°C for 2 hours following Heiri *et al.* (2001). Methods used for the field measurements of temperature and pH, and the collection and analysis of pore water and sediment chemistry samples,

are described in Price and Pichler (2005). Pore water measurements were taken at a depth of 10 cm except where noted in Table 3.1. Sediment arsenic content indicated in Table 3.2 is from surface sediment samples.

Parametric statistical analysis was conducted using SigmaStat 3.5 (Systat Software, Richmond CA). One-Way Analysis of Variance (ANOVA) with a Holm-Sidak multiple comparison procedure test was used to test for between site differences in sediment characteristics and benthic community metrics (Species Richness, Abundance, Diversity). A nonparametric Kruskal Wallis ANOVA on ranks was used to test for the presence of between site differences in the Pielou's evenness index because index values failed normality testing. All other metrics passed for normality without data transformations. Sediment grain size, organic carbon and carbonate content data were arcsine transformed for normality prior to analysis. Between site statistical testing for the pore water temperature, pH and sediment/pore water arsenic concentrations were not performed since only one measurement or sample was collected per site. Basic community indices (Species Richness, Abundance, Shannon-Wiener Diversity and Pielou's Evenness) and multivariate analysis was done using PRIMER v.6 (Clarke and Gorley 2006). The Bray-Curtis similarity index was calculated on square root transformed abundance data to measure the similarity of the benthic species composition among replicates within a site and between sites. Analysis of Similarity (ANOSIM) was used to test for differences in the species composition between sites and The Similarity Percentage (SIMPER) procedure was used to determine which taxa contributed to the within site similarity or between site differences. The BIO-ENV analysis procedure in PRIMER v.6 was used to calculate Spearman ranked correlations between the

physical/sediment measurements and the benthic macrofauna composition. All physical and sediment data were log transformed and normalized prior to analysis.

The BIO-ENV procedure compares the underlying similarity/distance matrices for the biological and physical data to find the combination of physical variables that best explains the ordination pattern among the samples based on their species similarity (Clarke and Ainsworth 1993). This method has several advantages in that it incorporates the full range of biotic and physical data collected and is not dependent on a normal distribution of the data because it utilizes rank-based correlations.

### **3.3 Results**

There were observed differences between sites for all physical parameters (Table 3.1). Temperature showed the highest value at 7.5 m, but decreased to near ambient levels at 60 m. The pH was lowest at 7.5 m and increased with distance from the vent. Pore water arsenic was highest near the vent, decreased substantially at 60 m and increased again at 150 m. All three transect sites had greatly elevated arsenic concentrations relative to the reference site.



**Table 3.1 Summary of pore water characteristics at Tutum Bay, Ambitle Island, Papua New Guinea November 2003. All pore water measurements are from Price and Pichler (2005) and represent values measured at a depth of 10cm except \* = 0 cm.**

Distance (meters)	Temp. (° C)	pH	[As] (µg/L)
7.5	45.5	6.2	81*
60.0	33.3	6.8	16
150.0	31.0	7.2	63
REF	30.2*	7.6	3.3

Sediment characteristics also exhibited differences between sites along the transect and relative to the reference site (Table 3.2). The sediment at 7.5 m was predominantly gravel and very fine sands with low organic carbon and carbonates. The 60 m site was dominated by very fine sands low in organic carbon and carbonate. The 150 m site was also predominately very fine sand, but had a greater proportion of medium and fine sized sediments. The reference site had a high percentage of gravel largely composed of coral rubble, as well as a large amount of medium sands. There was a significant difference in the percent organic carbon between sites ( $F_{3,8} = 95.5$ ;  $P < 0.001$ ), with the 150 m site having higher values than at the 7.5 and 60 m sites and the reference site having higher values than all three transect sites. The percent carbonates were also significantly higher at the reference site ( $F_{3,8} = 2011$ ;  $P < 0.001$ ). Total arsenic in the surface sediments exhibited a decreasing trend along the transect away from the vent but all three transect sites were higher than the reference site.

**Table 3.2 Sediment grain size class percentages, percent organic carbon and carbonates (mean  $\pm$  1 standard deviation); arsenic concentrations from Price and Pichler (2005).**

Wentworth Size Class	7.5 m	60 m	150 m	REF
Gravel	32.99 $\pm$ 10.39	0.17 $\pm$ 0.06	0.92 $\pm$ 0.22	24.83 $\pm$ 10.26
Coarse Sand	0.71 $\pm$ 0.33	0.23 $\pm$ 0.17	0.19 $\pm$ 0.02	1.32 $\pm$ 0.14
Medium Sand	4.38 $\pm$ 2.27	4.30 $\pm$ 0.32	17.87 $\pm$ 2.14	36.24 $\pm$ 0.08
Fine Sand	7.36 $\pm$ 1.53	3.50 $\pm$ 0.43	36.15 $\pm$ 1.32	12.54 $\pm$ 2.25
Very Fine Sand	53.10 $\pm$ 8.61	89.60 $\pm$ 1.15	42.58 $\pm$ 1.04	18.10 $\pm$ 5.76
Silt + Clay	1.46 $\pm$ 0.11	2.20 $\pm$ 1.18	2.30 $\pm$ 0.68	6.97 $\pm$ 2.61
% Organic Carbon	1.66 $\pm$ 0.08	1.33 $\pm$ 0.29	3.57 $\pm$ 0.43	7.59 $\pm$ 1.04
% Carbonates	0.51 $\pm$ 0.11	0.29 $\pm$ 0.18	3.75 $\pm$ 0.63	50.37 $\pm$ 0.99
[As] (ppm)	783	614	402	2.2

Both the number of taxa ( $S$ ) and overall abundance ( $N$ ) increased with distance away from the vent (Table 3.3) and all transect sites were significantly lower than the reference site for both measures (Figure 3.3A;  $F_{3,16} = 44.1$  and  $27.6$  for  $S$  and  $N$  respectively;  $P < 0.001$ ). The 150 m site also was significantly higher in both numbers of taxa and abundance than the other two transect sites; however there was no significant difference between 7.5 and 60 m for either measure. The Shannon-Wiener diversity index ( $H'$ ) also showed an increasing trend with distance from the vents (Figure 3.3B). All sites

were significantly different from each other ( $F_{3,16} = 77.7, P < 0.001$ ). There was no significant difference in evenness between sites ( $df = 3, H = 0.766 P = 0.86$ ). Most taxa were represented by a single individual resulting in high evenness values.

**Table 3.3 Benthic community index values cumulated for all five replicate samples at each site. Mean values  $\pm$  1 standard deviation are shown in parenthesis. Abundance ( $N$ ) expressed as count/sample; sample area = 0.00456m<sup>2</sup>.**

Distance (meters)	Number of Taxa ( $S$ )	Abundance ( $N$ )	Diversity ( $H'$ )	Evenness ( $J'$ )
7.5	6	14	1.48	0.82
	(2 $\pm$ 0.71)	(2.8 $\pm$ 1.3)	(0.59 $\pm$ 0.38)	(0.92 $\pm$ 0.08)
60.0	20	38	2.82	0.94
	(5.8 $\pm$ 3.03)	(7.8 $\pm$ 5.4)	(1.60 $\pm$ 0.36)	(0.98 $\pm$ 0.02)
150.0	55	111	3.71	0.92
	(17 $\pm$ 3.87)	(22.2 $\pm$ 7.69)	(2.73 $\pm$ 0.21)	(0.97 $\pm$ 0.02)
REF	116	201	4.50	0.95
	(31.6 $\pm$ 7.64)	(40.2 $\pm$ 10.92)	(3.32 $\pm$ 0.25)	(0.97 $\pm$ 0.01)

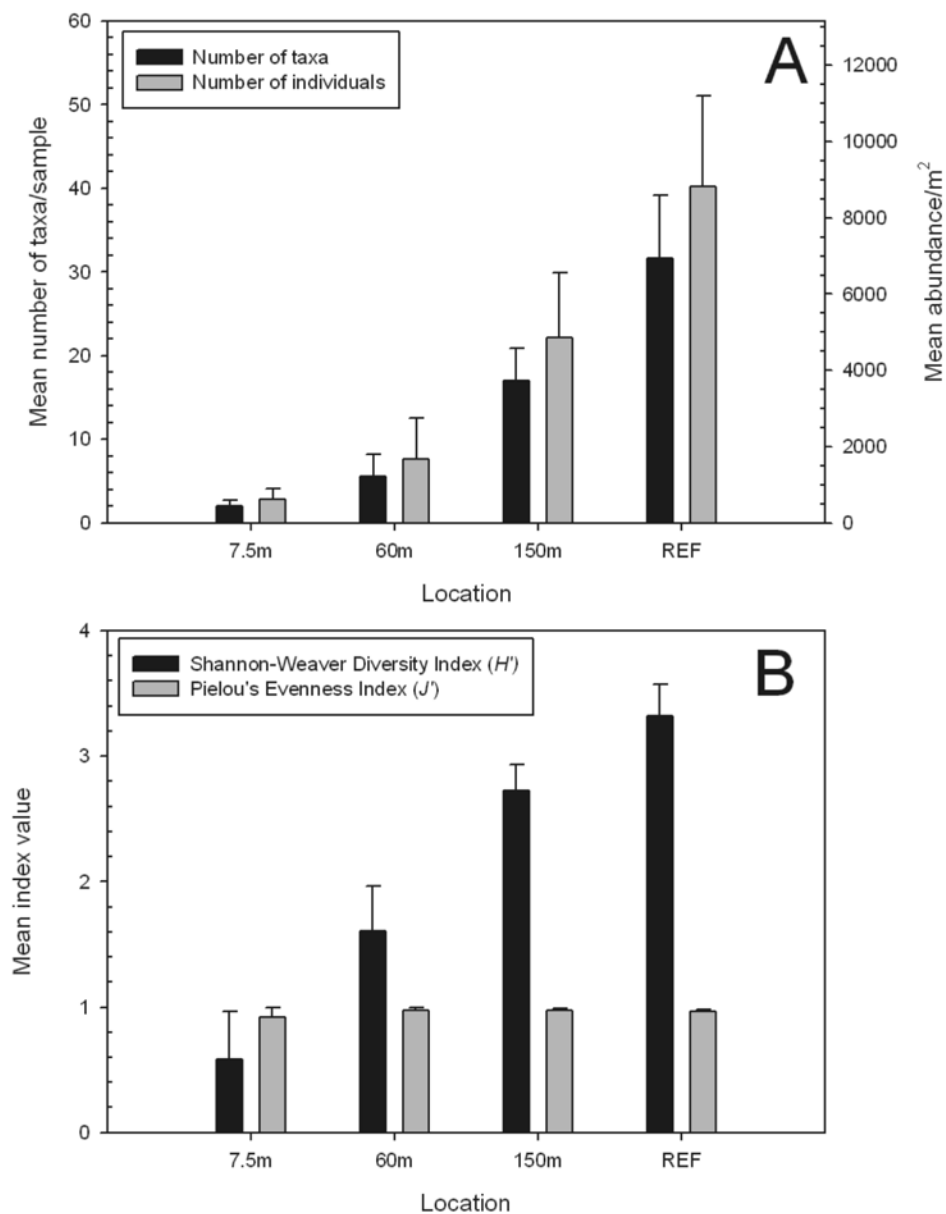


**Figure 3.3 A:** The mean number of taxa ( $S$ ) and abundance ( $N$ ) of benthic macrofauna/sample at the transect and reference sites. Error bar = 1 standard deviation, sample area = 0.00456 m<sup>2</sup>. All pairwise comparisons between the REF, 150 m and 60 m sites were significantly different for both  $S$  and  $N$ . The 60 m and 7.5 m sites were not significantly different. **B:** Mean Shannon-Wiener Diversity ( $H'$ ) and Pielou's Evenness ( $J'$ ) values at transect and reference sites. Error bar = 1 standard deviation. All pairwise comparisons between sites were significantly different for  $H'$ . There was no significant difference in  $J'$  between sites.

Annelids comprised the largest percentage of taxa at all sites, (Fig. 3.4A) and were represented by 92 taxa overall or > 50% of the taxa identified in this study. The 7.5 m site had only three annelid taxa, which represented half of the taxa found due to the low species richness at that site. The 60 m and 150 m sites had 10 and 24 annelid taxa respectively, while the reference site had 60 annelid taxa present. Annelids also were the most abundant invertebrates, comprising close to 50% of the overall abundance for all sites, followed by arthropods which represented close to 25% of the total abundance overall (Figures. 3.4A and B). Mollusks were also prevalent at 150 m and at the reference site (12 and 11 taxa respectively), but were absent at 7.5 m and were represented by only one species at 60 m (Figures.3.4A and B).

Analysis of Similarity (ANOSIM) indicated that the species composition was significantly different between sites (Global  $R = 0.764$ ,  $P = 0.001$ ). The SIMPER Analysis by distance (Table 3.4) showed that the five replicates from 7.5 m had an average similarity of 29% due to the presence of the polychaetes *Malacoceros* sp. A and *Capitella* cf. *capitata* which accounted for 52% and 48% of the similarity respectively. The 60 m replicates had an average similarity of 21% with the unidentified cumacean (designated as Cumacea sp. A) contributing 50% to the similarity. The 150 m samples had an average similarity of 26% mostly due to an unidentified sipunculan worm (sipunculan sp. B), an isopod, (Paranthuridae? sp. A) and the polychaete *Heteropodarke* sp. A. The five replicates from the reference site had an average similarity of 15.6%, with the polychaete *Typosyllis* sp. A accounting for 11% of the similarity between the samples.

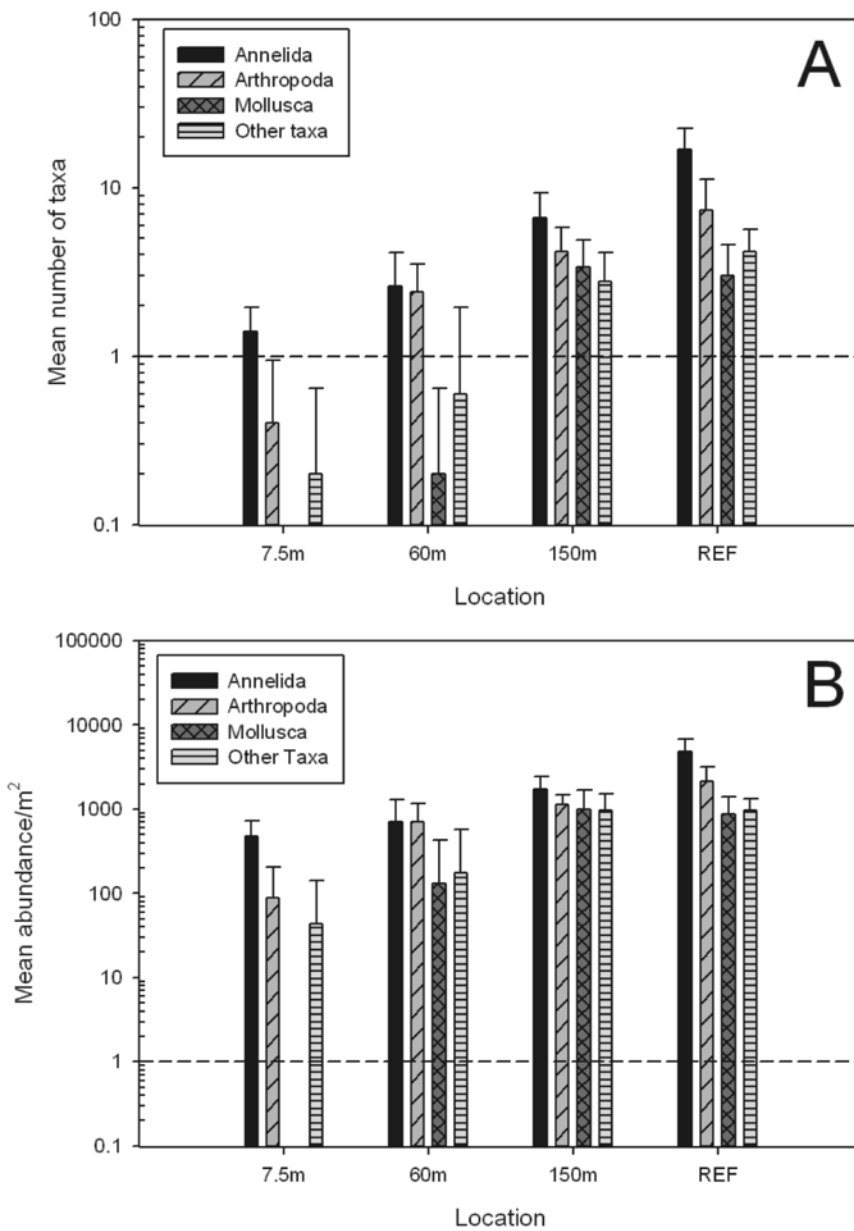


**Figure 3.4 A: Mean number of taxa by major taxonomic groups at transect and reference sites. B: Mean abundance of major taxonomic groups at transect and reference sites.**

**Table 3.4 SIMPER analysis results by distance (Bray-Curtis Similarity among five replicate samples) and percent contribution of top five taxa.**

Rank	7.5 meters Avg. Similarity = 27.40		60 meters Avg. Similarity = 21.36		150 meters Avg. Similarity = 26.48		REF Avg. Similarity = 15.59	
	Taxon	% Contribution	Taxon	% Contribution	Taxon	% Contribution	Taxon	% Contribution
1	Malacoceros sp. A	52.02	Cumacea sp. A	49.88	Paranthuridae? sp. A	20.39	Typosyllis sp. A	11.32
2	Capitella cf. capitata	47.98	Platyischopidae? sp. A	21.73	sipunculan sp. B	20.39	Lucinidae sp. A	7.52
3			Glycera sp. B	11.71	Heteropodarke sp. A	13.36	Thalassinidea? sp. A	6.10
4			Sthenelais sp. A	8.65	Cumacea sp. A	7.41	Eusamytha? pacifica?	5.90
5			Capitella cf. capitata	8.03	holothuroidean? sp. A	6.38	Ehlersia sp. A	5.81
Cumulative		100.00		100.00		67.93		36.66

The cluster analysis of abundance data showed the sites clustering in three main groups designated as A, B, and C (Figure 3.5). Group A consisted of all five replicates from 7.5 m along with two replicates from 60 m. SIMPER analysis of the cluster groups showed that the Group A sites had an average similarity of 22%, with the polychaete *Capitella cf. capitata* accounting for 64% of the similarity. Group A was divided into two subgroups: A1 and A2. The A1 subgroup consisted of three of the 7.5 m samples and had an average similarity of 48% due to the presence of the polychaete *Malacoceros* sp. A. The A2 subgroup was composed of two 7.5 m samples and two 60 m samples with an average similarity of 32% due to the polychaete *Capitella cf. capitata*. Group B was composed of the remaining three 60 m samples and all five 150 m samples and had an average similarity of 15%. The similarity among the group B samples was due to the abundance of Cumacea sp. A which accounted for 33% of the similarity. Group B was divided into two subgroups; B1 and B2. The B1 subgroup included three replicates from 60 m and had an average similarity of 25% due to the presence of Cumacea sp. A. The B2 subgroup consisted of the five 150 m replicates and had an average similarity of 26.5% due to the isopod Paranthuridae? sp. A and the sipunculan sp. B. Group C consisted of the five reference site samples and had an average similarity of 15.6% due in part to the polychaete *Typosyllis* sp. A.



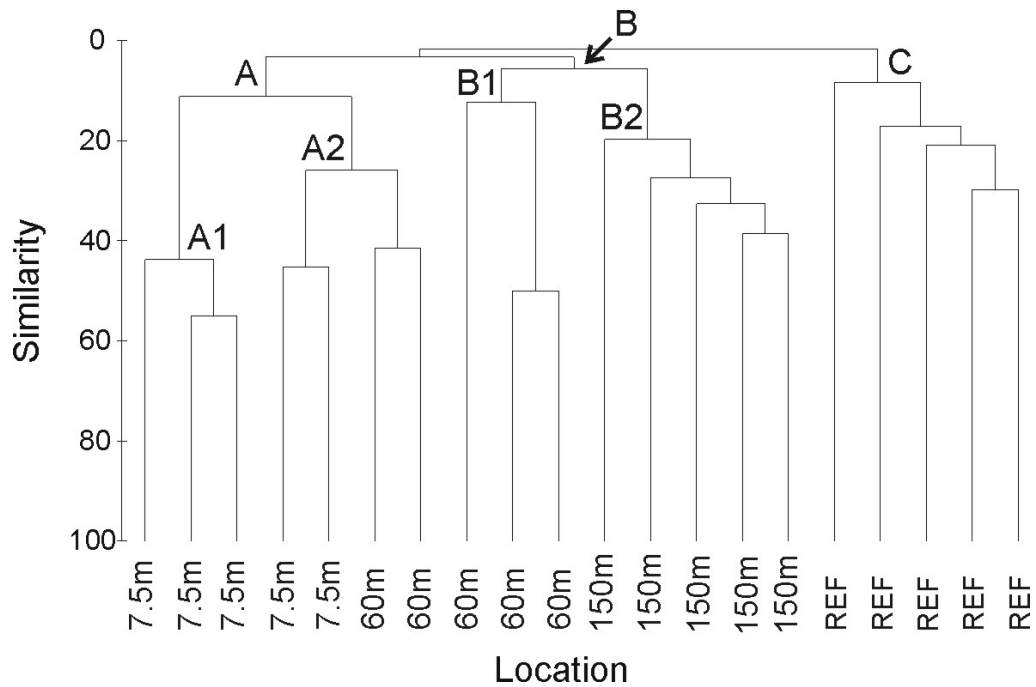


**Figure 3.5 Cluster analysis: Bray Curtis Similarity based on square root transformed macrofaunal abundance data.**

The BIO-ENV analysis indicated that for single environmental variables, pH best explained the benthic species assemblage data [Spearman correlation ( $\rho$ ) = 0.703]; followed by temperature ( $\rho$  = 0.682) (Table 3.5). The combination of pH and temperature with various sediment grain size classes resulted in a slightly higher correlation ( $\rho$  = 0.709; Table 5). Conversely, the total arsenic concentration in the sediment and pore water showed relatively weaker correlations with the benthic macrofauna assemblage (Table 5;  $\rho$  = 0.568 and 0.429 respectively).

**Table 3.5 BIO-ENV results for single and multiple parameters.**

Variable	Spearman Correlation Coefficient ( $\rho_s$ )
% CS; Temperature; pH	0.709
% G; %CS; % FS; Temperature; pH	0.709
%G; %FS; Sediment As; Temperature; pH	0.709
pH	0.703
%CO <sub>3</sub> ; Temperature; pH	0.703
%G; %FS; %CO <sub>3</sub> ; Temperature; pH	0.703
Temperature	0.682
% Silt + Clay	0.603
% Fe	0.568
Sediment As	0.568
Pore water As	0.429

%G = % Gravel; %CS = % Coarse Sand; %FS = % Fine Sand; %CO<sub>3</sub> = % Carbonates;

%Fe = % iron

### 3.4 Discussion

Despite the small sample size and limited area sampled at each site, there was a statistically significant trend of increasing species richness, abundance and diversity with distance from the vent out to 150 m. These measures were still depressed relative to the reference site, suggesting that the hydrothermal system still influenced the infaunal structure as far away as 150 m. The benthic macrofauna composition at the reference site showed little similarity to any of the transect sites as revealed by the cluster analysis (Figure 3.5). Among the three transect locations, the 7.5 and 150 m species assemblages showed little similarity to each other while the benthic community at 60 m appeared to be transitional between the other two transect sites.

Several physical variables could be responsible for the observed trends in the benthic macrofauna assemblage, including temperature, pH, arsenic content and sediment composition. Other factors such as currents, tides, wave action, and changes in the volume of vent flow could also affect the vents influence on the infaunal community but these variables were not observed in this study. There is a correlation between increasing pH and increasing presence of carbonates in the sediment. These changes in sediment composition and benthic infaunal abundance and diversity may be influenced by both geochemistry and bioturbation due to burrowing organisms (Aller 1982, Dhalgren *et al.* 1999, Widdicombe *et al.* 2000). Numerous active callianassid shrimp burrows were observed along the transect. In our core samples a single individual was found at 60 m, two at 150 m and four at the reference site. However, callianassid shrimp are likely underrepresented in our samples due to the depth of their burrows. Additionally,

observations made during a night dive along the transect revealed high densities of sea pens (Octocorallia: Pennatulacea) starting approximately 100 m out from the vent in fine grain, volcanic sand. These apparently remain in deep burrows during the day and thus were not represented in our core samples. The change in macrofaunal composition along the transect is most strongly correlated with pH although temperature and grain size were also important as shown in the BIO-ENV results (Table 3.5). Mollusks were completely absent at the 7.5 m site, a single opisthobranch gastropod (Cylichnidae - genus undetermined) was found at the 60 m site while the 150 m site contained 12 molluscan species or 22% of the species present at that site. The increased presence of shelled mollusks may be caused by the pH gradient along the transect as solid carbonates are more difficult to precipitate and maintain at low pH (Milliman 1974).

The apparent lack of molluscan fauna near the vent in this study differs from studies conducted at three other shallow hydrothermal systems (Kamenev *et al.* 1993, Thiermann *et al.* 1997, Kamenev *et al.* 2004), where mollusks were found in association with hydrothermal vents. These sites were different from Ambitle Island in that hydrogen sulfide concentrations seemed to be an important factor influencing infaunal benthic communities. Those studies did not report pH values, so the association between pH and molluscan communities was not established. One recent study (Hall-Spencer *et al.* 2008), did show that reduced pH from the release of CO<sub>2</sub> in a shallow volcanic vent caused reductions in the abundance of coralline algae and other calcareous organisms.

One species of note in this study is the capitellid polychaete *Capitella* cf. *capitata* which was found at both the 7.5 and 60 m sites. This cosmopolitan taxon has long been recognized as a complex of several morphologically similar species and historically has

been associated with degraded or disturbed habitats (Grassle and Grassle 1976). Thiermann *et al.* (1997) found a sibling species of *Capitella capitata* associated with the transition zone near a shallow-water hydrothermal vent in the Aegean Sea. This population was designated as *Capitella* sp. M and was characterized by its tolerance of high sulfide levels (Gamenick *et al.* 1998a). High sulfide concentrations have not been associated with the Ambitle Island vents (Pichler *et al.* 1999b), but the *C. capitata* specimens found in this study were associated with high temperatures and high arsenic levels as well as low pH.

Our results suggest that the infauna near the vents are represented by few taxa and low abundances and primarily consist of opportunistic taxa such as *Capitella capitata*. These taxa are most likely a subset of the surrounding benthic community rather than specialized organisms adapted to a chemosynthetic metabolism as found in deep-sea hydrothermal vents. A result similar to ours was found in shallow hydrothermal vent systems near southern California and the Gulf of California (Melwani and Kim 2008).

These results suggest that the arsenic from the vent fluids is effectively sequestered in the sediments as found in earlier studies (Pichler *et al.* 1999a) and does not significantly influence either benthic community structure or the observed surrounding reef habitat. Instead, the reduced pH appears to affect the benthic species composition around the vent which is evidenced by the absence of mollusks near the vent, the reduced molluscan fauna at 60 m and the absence of carbonate sediments at both of these sites. The influence of pH on the benthic community structure is further supported by the BIO-ENV analysis results. This finding further supports the results found at a similar site in the Mediterranean Sea (Hall-Spencer *et al.* 2008) that showed that reduced pH due to the

venting of CO<sub>2</sub> at shallow-water volcanic vents affected the abundance of calcareous organisms in the surrounding benthic community.

This study of the Ambitle Island vent system demonstrates that the effects of a small, shallow hydrothermal vent can extend much farther from the point source than previous studies have shown, presumably due to the effects of diffuse venting of CO<sub>2</sub> gas and hydrothermal fluids in the surrounding sediments. We found effects as far as 150 m from the vent, suggesting that future studies at shallow hydrothermal vents incorporate much longer transects.

## Chapter Four

### Macrofaunal communities associated with the shallow water hydrothermal vent system at Ambitle Island, Papua New Guinea

#### 4.1 Introduction

The background for this chapter can be found in Chapters 2 and 3 which report the environmental factors at the site and macrofauna findings from the 2003 sampling. Chapter three describes an increasing trend in abundance, species richness and diversity with distance away from the vent. These community measures were still reduced as far out as the 150 m transect site, which was the farthest sample collected along the transect. The 2003 results further suggested that pH, rather than the arsenic concentration, was a controlling factor in structuring the macrofaunal community (Chapter 3, Karlen *et al.* 2010). The 2003 results were based on a limited sample size due to difficulties with shipping sampling supplies to Papua New Guinea. The sampling effort was greatly expanded on the second sampling trip in May 2005. In order to confirm the preliminary results from the 2003 data, several changes were made to the sampling design. These included extending the transect to 300 m, adding six more sites, collecting samples closer to the focused vent (0 m site), and collecting replicate samples at each site over a wider spatial area instead of within a single 1 m<sup>2</sup> quadrat. A new reference site was selected (Danlum Bay) that more closely resembled the sediment characteristics found at the transect sites. These modifications to the sampling design allowed for better statistical

analysis of the benthic community trends along the hydrothermal gradient and better correlations to the pore water and sediment parameters.

## **4.2 Material and methods**

### **4.2.1 Sampling design and field collection**

Sampling and analysis methods for pore water and sediment samples collected at the transect sites and the Danlum Bay reference site are given in Chapter 2.

Sediment samples for macrofauna analysis were collected at the nine transect sites and at the Danlum Bay reference site as described in Chapter 2. At each site, macrofauna samples were collected from a random grid in each of the five quadrats at each site using a PVC corer (diameter = 7.62 cm; area = 45.6 cm<sup>2</sup>). Sediment cores were collected to a depth of 15 cm. The five cores from each site were treated as separate replicate samples. The sediment was sieved through a 500 µm mesh screen and the retained macrofaunal organisms and sediment were rinsed into HDPE sample bottles and fixed in 10% borax buffered formalin with Rose Bengal stain for a minimum of 72 hours. The samples were then transferred into 70% ETOH with Rose Bengal stain for preservation.

### **4.2.2 Sample processing and identification**

The macrofauna samples were sorted in the lab by first decanting the ETOH through a 500 µm mesh sieve, rinsing the sediment several times with tap water and decanting the water into the sieve to “float off” the more delicate organisms. The sediment was then rinsed into a stacked series of 2 - 3 sieves ranging from 4 mm to 500 µm depending on the composition of the sediment. The sediment was rinsed through the



sieve series to separate the sample into various size fractions to aid in finding and sorting the macrofaunal invertebrates. Each sediment size fraction was rinsed into a separate container and macrofauna were picked out and sorted into general taxonomic groups for identification and counting under a dissecting microscope. Macrofauna was identified to the lowest practical taxonomic level and counted. For the macrofauna analysis, “lowest practical taxonomic levels” generally was genus or species identification. In cases where more precise identifications were not possible, specimens were identified to the lowest level and assigned a letter designation based on their distinct morphological characteristics. All specimens were retained and archived for further taxonomic analysis and voucher specimens were photographed and a photographic log was kept to aid in maintaining consistency in identifications between samples.

#### **4.2.3 Data analysis**

Parametric statistical analysis was conducted using SigmaStat 3.5 (Systat Software, Richmond CA). One-Way Analysis of Variance (ANOVA) with a Holm-Sidak multiple comparison *post-hoc* test was used to test for between site differences in pore water, sediment, and benthic community metrics. Data were log (n=1) or square root transformed if it failed tests for normality and equal variances. If the transformed data failed to meet the criteria for ANOVA, a nonparametric Kruskal Wallis ANOVA on ranks was used. Biological community indices (Species Richness, Abundance, Shannon-Wiener Diversity and Pielou’s Evenness) and multivariate analysis was done using PRIMER v.6 (Clarke and Gorley 2006). The Bray-Curtis similarity index was calculated on square root transformed abundance data to measure the similarity of the benthic

species composition among replicates within a site and between sites. Results were further analyzed using cluster analysis and/or non-metric Multi-Dimensional Scaling (MDS). The Similarity Percentage (SIMPER) procedure was used to determine which taxa contributed to the within site similarity or between site differences. Principal components analysis (PCA) was used on log transformed and normalized pore water and sediment data to group sites based on their physical characteristic. The BIO-ENV analysis procedure in PRIMER v.6 was used to calculate Spearman ranked correlations between the environmental measurements and the biological community similarity and the LINKTREE procedure was used to evaluate the environmental characteristics defining the sites comprising defined biological communities.

#### **4.3 Results**

A total of 368 taxa in ten phyla were identified from all sites with a total abundance of 1,430 individuals. The annelids, predominately polychaetes, were the most speciose and abundant phylum with 185 taxa and 664 specimens, representing 50% and 46% of the species richness and abundance respectively. The arthropods were represented by 92 taxa (25%) and 560 specimens (39%), and mollusks had 48 taxa and 122 specimens (13% and 8.5% respectively). Twenty-three taxa (6%) accounted for >50% of the relative abundance while 199 taxa (54%) were represented by a single specimen. The polychaete *Capitella cf. capitata* was the most abundant species found and was dominant at the 0 m site. Other abundant taxa included the amphipod *Platyischnopus* sp. A, the burrowing shrimp *Thalassinidea* sp. A, and the amphipods *Cyrtophium?* sp. A and *Ampithoe* sp. A. No single taxon was present at all 10 sites while 253 taxa (69%) were

only present at a single site. The most widely occurring taxon was the burrowing shrimp *Thalassinidea* sp. A, which was found at 9 of the sites, and was only absent at 180 m. The amphipods *Platyischnopus* sp. A and *Ampelisca* sp. A were present at 7 sites, but both were absent at 0 m, 250 m and 300 m. The bivalve mollusk *Diplodonta* sp. A was also found at 7 sites and was absent close to the vent at the 0 m, 30 m, and 60 m sites.

The median, minimum and maximum values for the macrofauna taxonomic richness, abundance, Shannon diversity index, Pielou's evenness index and the Simpson diversity index at each site are presented in Table 4.1.

**Table 4.1 Median, minimum and maximum values for macrofaunal community indices by site.**

Site	n	Taxa Richness		Abundance		Shannon Diversity		Evenness		Simpson Index	
0 m	5	10		22		0.94		0.68		0.53	
		2	16	10	104	0.20	2.58	0.29	0.93	0.10	0.94
30 m	5	6		8		1.57		0.92		0.81	
		2	6	3	14	0.50	1.73	0.72	0.97	0.40	0.93
60 m	5	3		7		1.04		0.95		0.83	
		3	9	4	13	0.80	2.14	0.73	0.97	0.52	0.95
90 m	5	11		19		2.26		0.92		0.89	
		8	16	17	34	1.90	2.45	0.86	0.94	0.87	0.94
120 m	5	11		17		2.17		0.91		0.91	
		7	12	11	26	1.77	2.36	0.81	0.95	0.82	0.95
140 m	5	13		25		2.25		0.85		0.87	
		6	15	12	52	1.39	2.37	0.71	0.99	0.72	0.99
180 m	5	24		38		2.93		0.93		0.96	
		19	37	28	57	2.79	3.32	0.92	0.95	0.95	0.96
250 m	5	42		62		3.58		0.96		0.98	
		29	46	40	68	3.16	3.66	0.94	0.98	0.97	0.99
300 m	5	30		39		3.21		0.97		0.98	
		15	41	22	55	2.54	3.61	0.90	0.98	0.94	0.99
Ref	5	17		30		2.62		0.92		0.94	
		14	19	27	32	2.22	2.78	0.84	0.95	0.87	0.96

The 0 m site had a total of 39 taxa and 184 specimens, with a median of 10 taxa and 22 individuals per sample (Table 4.1). Twenty-four taxa (62%) were represented by a

single specimen and 27 (69%) were only found at the 0 m site. This site was strongly dominated by the polychaete *Capitella cf. capitata*, which accounted for 63% of the relative abundance at this site (Table 4.2).

The 30 m site had a total of 13 taxa and a total abundance of 40 specimens, with median values of 6 taxa and 8 individuals per sample (Table 4.1). Seven taxa (54%) were singletons and two were only present at the 30 m site. Dominant taxa at this site included *Thalassinidea sp. A* and *Platyischnopus sp. A*, which comprised 35% and 18% of the relative abundance respectively (Table 4.2).

A total of 17 taxa and 37 specimens were identified from the 60 m site, with median values of 3 taxa and 7 specimens per sample (Table 4.1). Four taxa comprised >50% of the abundance at this site and 10 taxa (59%) were singletons. Five taxa were only found at the 60 m site. *Platyischnopus sp. A* was the most abundant species, representing 27% of the relative abundance, followed by *Thalassinidea sp. A* which made up 11% of the relative abundance (Table 4.2). Other dominant taxa included the amphipod *Ampelisca sp. A*, and the polychaetes *Prionospio (Minuspio) sp. A* and *Sthenelais sp. A*, each comprising 8% of the abundance (Table 4.2).

The 90 m site had a total of 32 taxa present and 111 individual specimens, with median values of 11 taxa and 19 individuals per sample (Table 4.1). Four taxa accounted for >50% of the abundance at this site, 18 (56%) of the taxa were singletons and 9 taxa (28%) were only found at the 90 m site. The most abundant taxon was the isopod crustacean *Flabellifera sp. A*, with a relative abundance of 26% (Table 4.2). Other dominant taxa included *Platyischnopus sp. A*, *Thalassinidea sp. A*, and the mysid crustacean *Mysidacea sp. B* (Table 4.2).

The 120 m site had a total of 30 taxa and 92 individual specimens with a median of 11 taxa and 17 specimens per sample (Table 4.1). Four taxa accounted for >50% of the total abundance at this site, 18 taxa (60%) were singletons and 7 taxa (23%) were only found at the 120 m site. The amphipods *Ampelisca* sp. A and *Platyischnopus* sp. A each comprised 15% of the relative abundance (Table 4.2). The crustaceans Cumacea sp. C and Thalassinidea sp. A were also among the dominant taxa at this site.

The 140 m site had a total of 35 taxa and 135 individual specimens with median values of 13 taxa and 25 individuals per sample (Table 4.1). Four taxa comprised >50% of the abundance at this site, 18 taxa (51%) were singletons and 9 taxa (26%) were only found at the 140 m site. This site was dominated by the amphipods *Ampithoe?* sp. A and *Ampelisca* sp. A accounting for 22% and 11% of the relative abundance respectively (Table 4.2). Other abundant taxa included the polychaete *Heteropodarke* sp. A and the amphipod *Platyischnopus* sp. A.

The 180 m site had a total of 90 taxa and 206 specimens. Median taxonomic richness and abundance values were 24 taxa and 38 individuals per sample (Table 4.1). Thirteen taxa accounted for >50% of the abundance, 58 taxa (64%) were singletons, and 34 taxa (38%) were only found at the 180 m site. The dominant taxa included the amphipod *Cyrtophium?* sp. A, the polychaetes *Grubeosyllis* sp. B and *Pholoe* sp. A and the bivalve mollusk *Codakia* sp. A (Table 4.2).

The 250 m site had the highest taxonomic richness and abundance with a total of 141 taxa and 273 individual specimens. The median number of taxa and individuals per sample were 42 taxa and 62 individuals (Table 4.1). Twenty-eight taxa comprised >50% of the abundance while 91 taxa (65%) were singletons and 75 taxa (53%) were only

present at the 250 m site. The most abundant taxon was the polychaete *Grubeosyllis* sp. B, which had a relative abundance of 4.8% (Table 4.2). Other dominant taxa included the bivalve mollusk *Codakia* sp. A, the polychaetes *Amphinome* sp. A, *Typosyllis cornuta*, and *Pholoe* sp. A (Table 4.2).

The 300 m site had the second highest richness and abundance with a total of 112 taxa identified and 202 specimens. Median richness and abundances values were 30 taxa and 39 individuals per sample (Table 4.1). Twenty-three taxa accounted for >50% of the abundance at the site, 78 taxa were singletons and 62 taxa were only found at the 300 m site. The most abundant species was the amphipod *Cyrtophium* sp. A, with a relative abundance of 9.4% (Table 4.2). Other dominant taxa included the amphipod *Melita* sp. A and the polychaetes *Pholoe* sp. A, *Typosyllis cornuta*, and *Protodorvillea* sp. B.

The Danlum Bay reference site had a total of 56 taxa and 150 individual specimens. Median richness and abundance values were 17 taxa and 30 specimens per sample (Table 4.1). Seven taxa accounted for >50% of the abundance, 34 taxa (61%) were singletons and 23 taxa (41%) were only present at the reference site. The dominant taxa were primarily polychaetes *Litocorsa* sp. A, *Mediomastus* sp. A, *Heteropodarke* sp. A, and an unidentified capitellid tentatively designated as “Capitellidae w/spatulate chaetae” based on the unique morphology of its chaetae (Table 4.2). Also among the top ranked taxa was the borrowing shrimp *Thalassinidea* sp. A.

The overall trend in species richness ( $S$ ) showed an increase with distance from the vent site (Figure 4.1), with significant differences between sites (One-way ANOVA  $F=22.796$ ,  $df=9,40$ ,  $p<0.001$  – analysis on non-transformed mean values,  $n= 5$ ). There were no pair-wise significant differences in richness between the 0 m, 30 m, 60 m 90 m,

120 m and 140 m sites, or between the 0 m and the Danlum Bay reference site. Richness was significantly higher at the 180 m, 250 m and 300 m sites relative to the other sites, while the 250 m site had higher species richness than the 180 m site, but was not significantly higher than at 300 m. The 180 m and 300 m sites were also not significantly different from each other. The species richness at the Danlum Bay reference site was higher relative to the 30 m and 60 m sites and lower than at the 250 m and 300 m sites.

The macrofaunal abundance was above the overall mean value at the vent site but was highly variable (Figure 4.2). There was an increasing trend in abundance from the 30 m site out to the 250 m site, with abundance values generally below the overall mean from 30 m – 140 m and above the mean value at the 180 m – 300 m sites. The mean abundance at the reference site was nearly equal to the overall mean (Figure 4.2). Abundances were significantly different among sites [one-way ANOVA,  $df = 9, 40$ ;  $F = 11.041$ ;  $p < 0.001$ ; analysis on  $\log(n+1)$  transformed abundance data]. Most pair wise comparisons between sites were not significantly different. The 30 m and 60 m sites did have significantly lower abundances than all of the other sites except for 120 m. The 120 m site was also significantly lower than the 250 m site.

**Table 4.2 Top ranked taxa comprising >50% of the relative abundance at each site.**

0 m S = 39 N = 184		30 m S = 13 N = 40		60 m S = 17 N = 37		90 m S = 32 N = 111		120 m S = 30 N = 92	
Taxa	Rel. Abund.	Taxa	Rel. Abund.	Taxa	Rel. Abund.	Taxa	Rel. Abund.	Taxa	Rel. Abund.
Capitella cf. capitata	62.5%	Thalassinidea sp. A	35.0%	Platyischnopus? sp. A	27.0%	Flabellifera (nr. Aegidae) sp. A	26.1%	Ampelisca sp. A	15.2%
		Platyischnopus? sp. A	17.5%	Thalassinidea sp. A	10.8%	Platyischnopus? sp. A	14.4%	Platyischnopus? sp. A	15.2%
				Prionospio (Minuspio) sp. A	8.1%	Thalassinidea sp. A	9.0%	Cumacea sp. C	13.0%
				Sthenelais sp. A	8.1%	Mysidacea sp. B	9.0%	Thalassinidea sp. A	9.8%
				Ampelisca sp. A	8.1%				
Cumulative:	62.5%	Cumulative:	52.5%	Cumulative:	62.2%	Cumulative:	58.6%	Cumulative:	53.3%



**Table 4.2 Continued.**

140 m S = 35 N = 135		180 m S = 90 N = 206		250 m S = 141 N = 273		300 m S = 112 N = 202		REF S = 56 N = 150	
Taxa	Rel. Abund.	Taxa	Rel. Abund.	Taxa	Rel. Abund.	Taxa	Rel. Abund.	Taxa	Rel. Abund.
Ampithoe? sp. A	24.4%	Cyrtophium? sp. A	10.2%	Grubeosyllis sp. B	4.8%	Cyrtophium? sp. A	9.4%	Litocorsa sp. A	12.7%
Ampelisca sp. A	11.1%	Grubeosyllis sp. B	9.2%	Amphinome? sp. A	3.7%	Pholoe sp. A	4.5%	Mediomastus sp. A	12.0%
Heteropodarke? sp. A	11.1%	Pholoe sp. A	3.9%	Codakia? sp. A	3.7%	Melita? sp. A	4.5%	Heteropodarke? sp. A	6.7%
Platyschnopus? sp. A	8.9%	Codakia? sp. A	3.9%	Typosyllis cornuta	3.3%	Typosyllis cornuta	4.0%	Capitellidae w/ spatulate chaetae	6.0%
		Typosyllis cornuta	3.4%	Pholoe sp. A	2.9%	Protodorvillea sp. B	3.0%	Thalassinidea sp. A	5.3%
		Melita? sp. A	3.4%	Tanaidacea sp. C	2.6%	Mediomastus sp. A	2.5%	Diasterope? sp. A	5.3%
		Semelina? sp. A	3.4%	Aspidosiphon sp. A	2.2%	Nephasoma? sp. A	2.0%	Sigambra cf. parva	4.0%
		Exogone cf. lourei	2.9%						
		Amphipoda sp. K	2.9%						
Cumulative:	55.6%	Cumulative:	43.2%	Cumulative:	23.1%	Cumulative:	29.7%	Cumulative:	52.0%

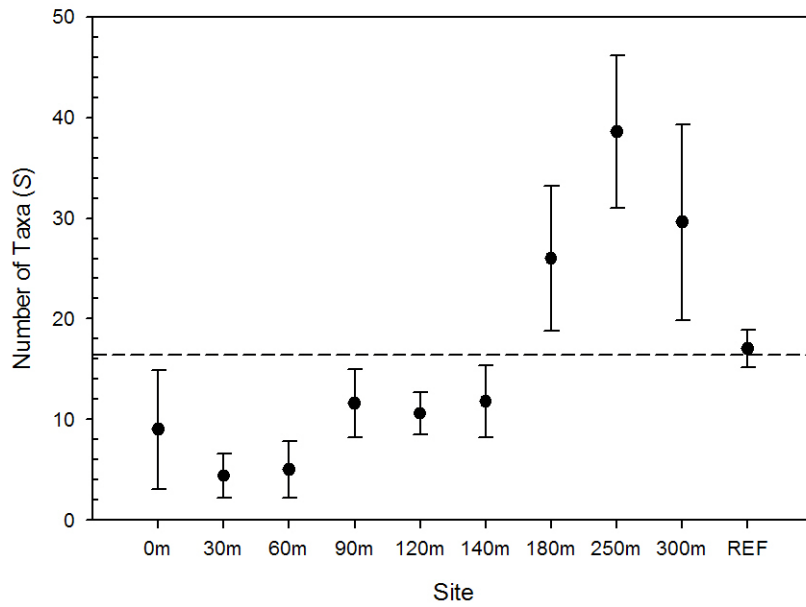


**Figure 4.1 Ambitle Island May/June 2005: Mean number of macrofaunal taxa  $\pm$  1 standard deviation.**

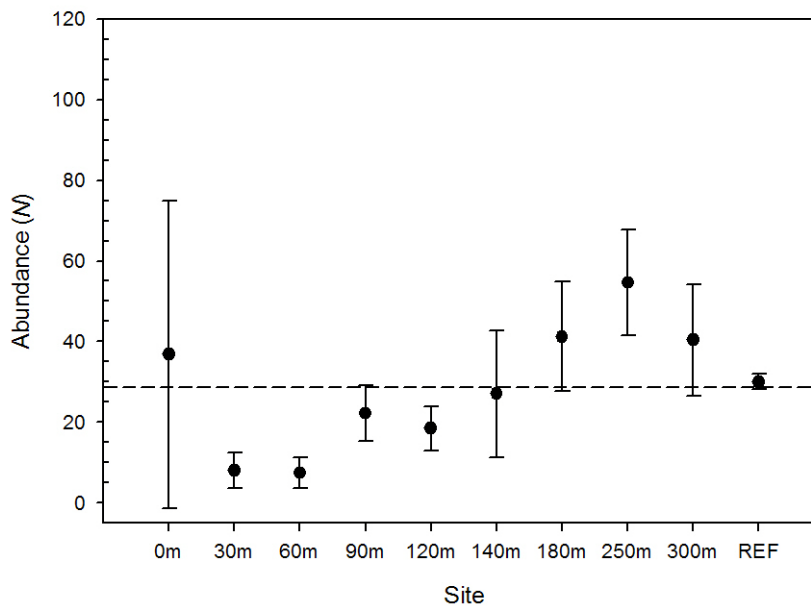


**Figure 4.2 Ambitle Island May/June 2005: Mean macrofaunal abundance  $\pm$  1 standard deviation. Abundance presented as individuals/sample.**

The Shannon-Wiener diversity index also showed an increasing trend with distance from the vent with the lowest mean value at the 30 m site and the highest value at the 250 m site (Fig 4.3). There were no significant pair-wise differences among the 0 m – 140 m sites along the transect. The 180 m and the reference sites were more diverse than the 0 m, 30 m and 60 m sites but were not significantly different from the other sites. The diversity at the 250 m and 300 m sites was significantly higher than the inner transect locations from 0 m to 140 m.

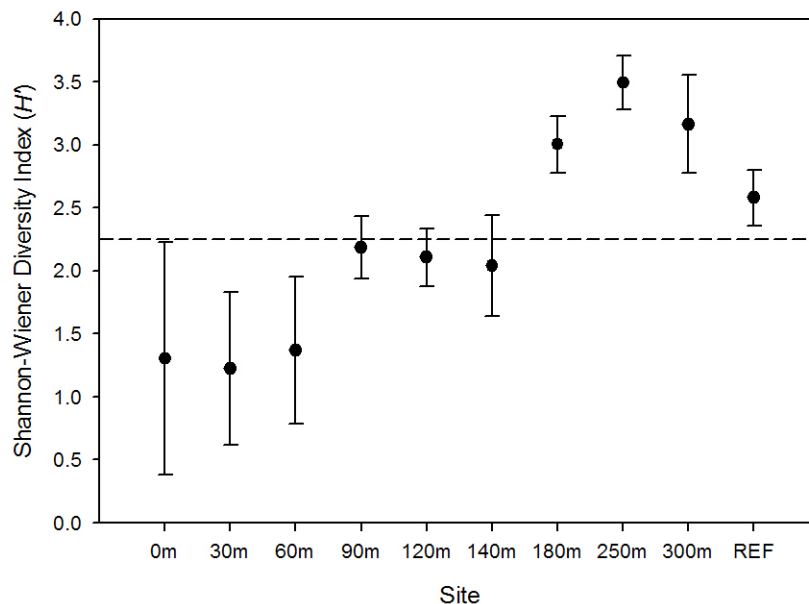


**Figure 4.3 Ambitle Island May/June 2005: Mean macrofaunal diversity  $\pm$  1 standard deviation.**

The Pielou evenness index ( $J'$ ) was significantly lower at the vent site relative to all other sites except the 140 m site (Figure 4.4). All other pair-wise comparisons between sites did not show significant differences in the evenness index. The arc-sine transformed evenness values did not meet the assumptions for ANOVA (normal

distribution or equal variances), however, the statistical power of the analysis was still high ( $1-\beta = 0.94$ ;  $\alpha = 0.05$ ). A non-parametric Kruskal-Wallis ANOVA on ranks also showed a significant difference among sites, but the corresponding pair-wise comparison test only showed a significant difference between the 0 m and 250 m sites.

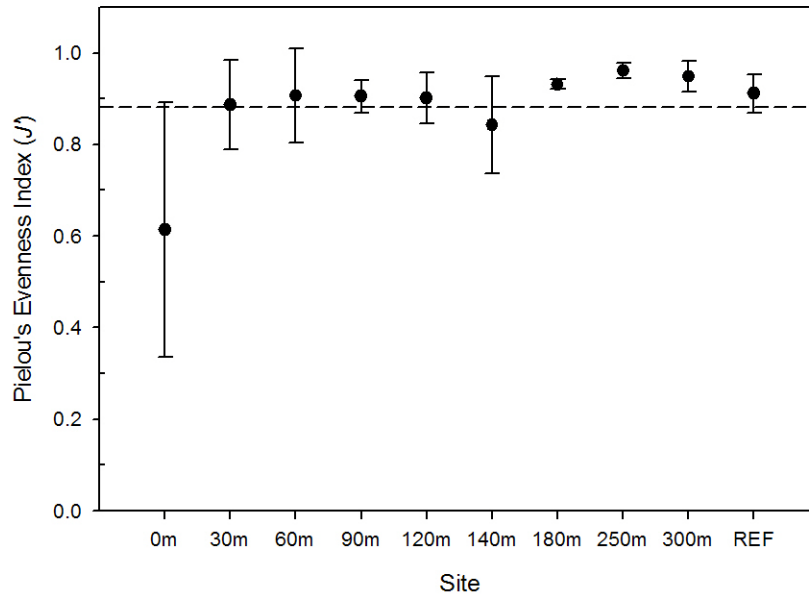


**Figure 4.4 Ambitle Island May/June 2005: Mean macrofaunal evenness  $\pm$  1 standard deviation.**

The non-metric multi-dimensional scaling (MDS) analysis of all 50 samples (Figure 4.5) and of the site averaged data (Figure 4.6a) both suggest that the macrofaunal species composition falls into four distinct faunal communities along the transect and at the reference site. The 0 m and reference sites each comprise their own distinct macrofaunal communities, the 30 m – 140 m transect sites group together as do the 180 m – 300 m sites. Since the environmental characteristics were different at the Danlum Bay reference site relative to the Tutum Bay transect sites, the MDS analysis was also

done omitting the reference site (Figure 4.6b). Excluding the reference site resulted in tighter clustering of the transect sites in the previously defined faunal communities and a lower overall 2D stress for the MDS plot (Figure 4.6b).

The SIMPER analysis defines the average similarity of the samples and the contribution to the species similarity within each defined group (Table 4.3). The 0 m site is defined primarily by the polychaete *Capitella* cf. *capitata*, which accounted for >86% of the similarity among the 0 m samples (Table 4.3). The 30 m – 140 m community is defined by the presence of *Thalassinidea* sp. A and *Platyischnopus* sp. A which contributed 32% and 26% respectively to the similarity among these samples (Table 4.3). Six taxa cumulatively contributed to >50% of the similarity among the samples within the 180 m – 300 m community group (Table 4.3). The amphipod *Cyrtophium?* sp. A and the polychaetes *Typosyllis cornuta* and *Pholoe* sp. A each accounted for >10% of the similarity within this group. The Reference site community was defined by the polychaetes *Litocorsa* sp. A, *Mediomastus* sp. A and Capitellidae w/spatulate chaetae. Cumulatively, these three taxa accounted for >55% of the similarity among the reference site replicates (Table 4.3).

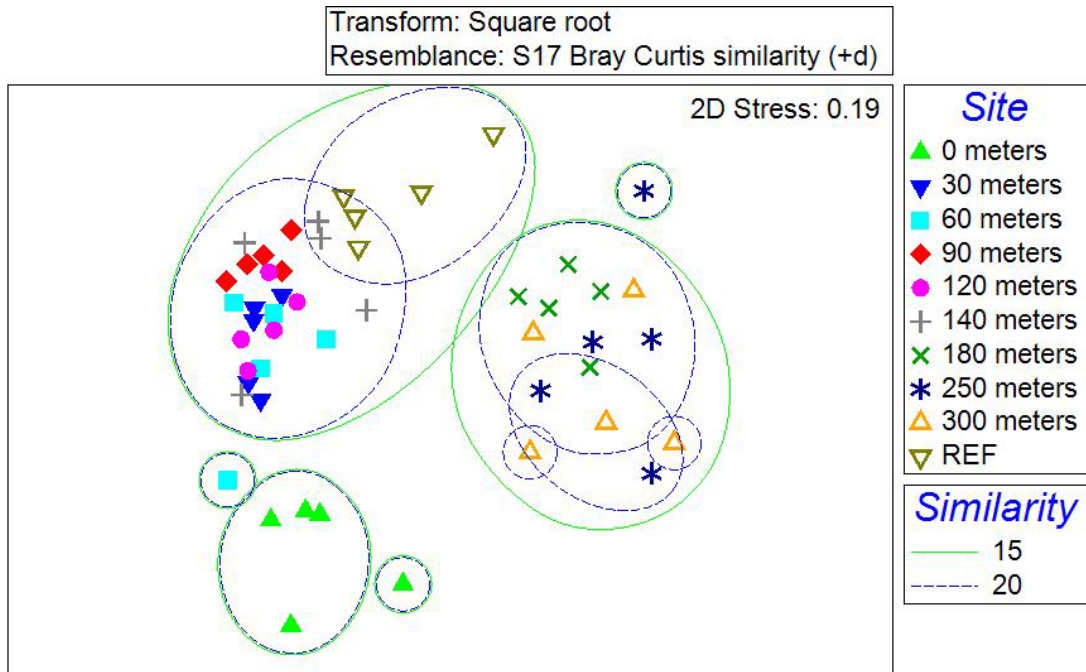


**Figure 4.5 Ambitle Island May/June 2005: Benthic macrofauna multi-dimensional scaling plot based on Bray-Curtis similarity between site replicates.**

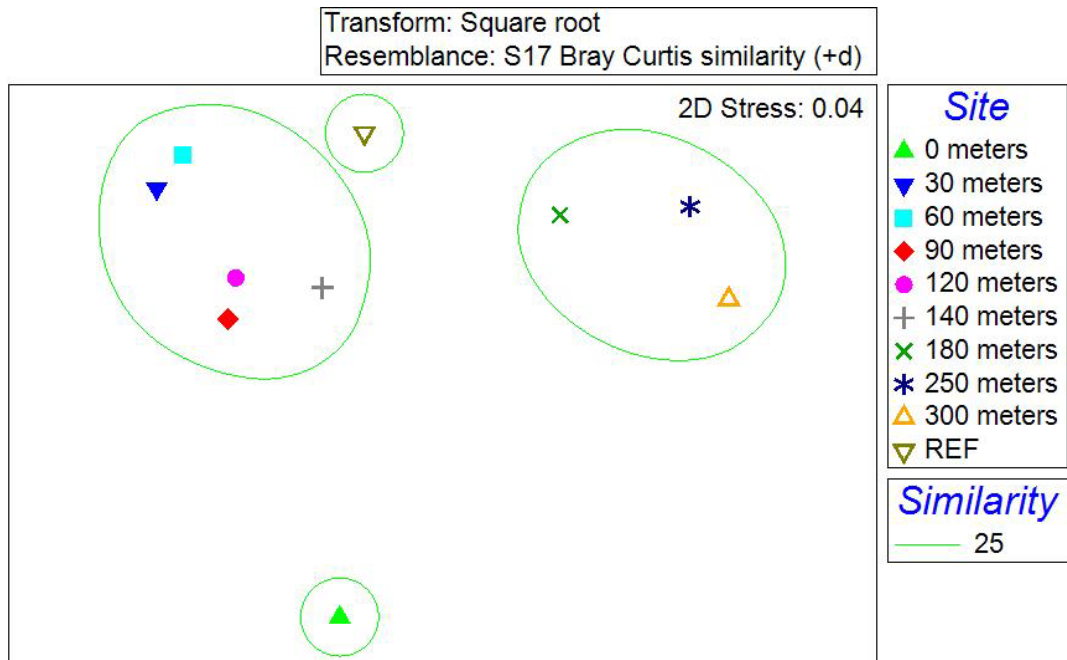


**Figure 4.6a Ambitle Island May/June 2005: Benthic macrofauna multi-dimensional scaling plot based on Bray-Curtis similarity averaged by site.**

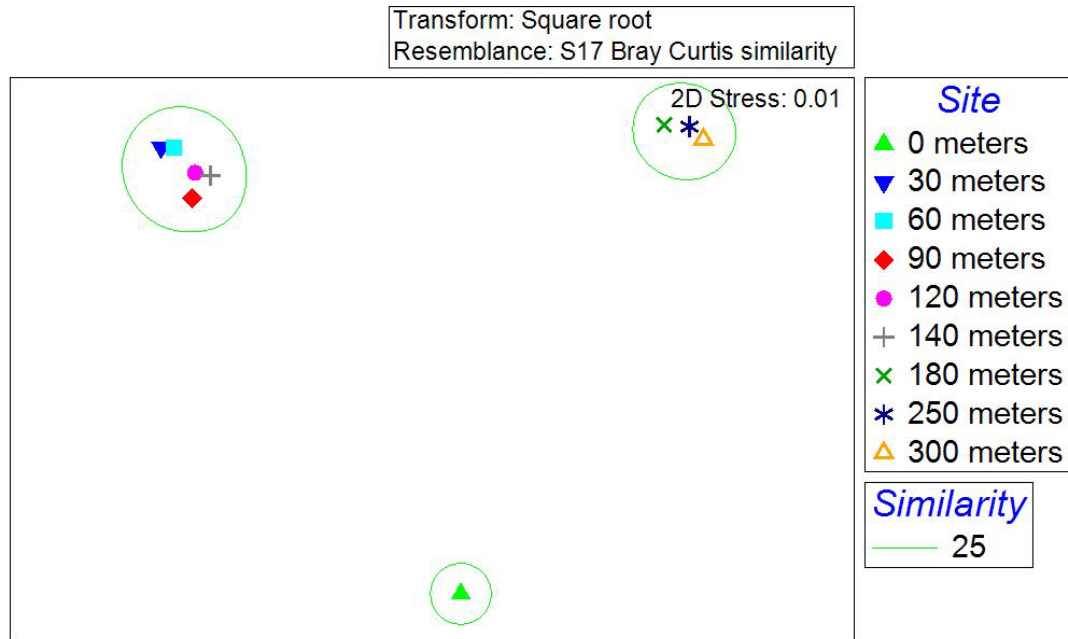


**Figure 4.6b Ambitle Island May/June 2005: Benthic macrofauna multi-dimensional scaling plot based on Bray-Curtis similarity averaged by site; reference site omitted.**

The BIO-ENV analysis comparing the macrofaunal community structure to the physical parameter (Table 4.4a) found the strongest correlation with a combination of total arsenic, % CaCO<sub>3</sub>, and sediment sorting ( $\rho = 0.74$ ). The combination of % CaCO<sub>3</sub>, and sediment sorting only had a slightly weaker correlation with the community structure ( $\rho = 0.74$ ). The % CaCO<sub>3</sub> had the highest correlation of any single variable ( $\rho = 0.67$ ), followed by sediment sorting ( $\rho = 0.63$ ) and median grain size ( $\rho = 0.61$ ). In contrast, total arsenic had a correlation of 0.50 (Table 4.4a). The BIO-ENV analysis was also reevaluated without the reference site (Table 4.4b). Those results generally had slightly higher correlation coefficients and indicated a stronger correlation with the sediment organic content, rather than the % CaCO<sub>3</sub> (Table 4.4b).

The LINKTREE analysis (Figure 4.7) separated the macrofaunal communities at the 180 m, 250 m and 300 m from the remaining sites. These three sites were

characterized by relatively higher pore water pH (>7.74 vs. <7.49), higher sediment CaCO<sub>3</sub> content (>7.4% vs. <6.5%) and lower total arsenic concentrations (<9.9 ppb vs. >11.6 ppb). The 0 m site separated out from the remaining sites due to larger median grain size, higher temperature, higher arsenic concentrations, lower pore water salinity, higher sediment sorting coefficient and lower pore water pH. The reference site split from the remaining sites because of its higher sediment organic content and lower ORP values, higher sediment sorting coefficients and CaCO<sub>3</sub> content, higher pH and lower temperature and arsenic concentrations relative to the remaining transect sites. The final split in the LINKTREE separated the 90 m, 120 m and 140 m sites from the 30 m and 60 m sites, based on slightly lower temperature, and slightly higher median grain size and sediment CaCO<sub>3</sub> content within the 90 m, 120 m, 140 m site group.



**Table 4.3 SIMPER results from macrofaunal community groups defined by Bray-Curtis similarity groupings.**

0 m Average similarity: 16		30 m - 140 m Average similarity: 23		180 m - 300 m Average similarity: 18		Ref Average similarity: 29	
Taxa	%	Taxa	%	Taxa	%	Taxa	%
Capitella cf. capitata	86.9	Thalassinidea sp. A	31.7	Cyrtophium? sp. A	10.9	Litocorsa sp. A	23.9
		Platyischnopus? sp. A	26.4	Typosyllis cornuta	10.6	Mediomastus sp. A	19.5
				Pholoe sp. A	10.1	Capitellidae w/ spatulate chaetae	12.4
				Codakia? sp. A	7.6		
				Grubeosyllis sp. B	6.7		
				Protodorvillea sp. B	6.7		
Cumulative %	86.9	Cumulative %	58.1	Cumulative %	52.5	Cumulative %	55.8

**Table 4.4a BIO-ENV correlations between the benthic macrofaunal community structure and physical parameters.**

Spearman Correlation	Parameters
0.740	Total [As], %CaCO <sub>3</sub> , Sorting
0.735	%CaCO <sub>3</sub> , Sorting
0.732	Total [As], % Organics, %CaCO <sub>3</sub> , Sorting
0.718	ORP, %CaCO <sub>3</sub> , Sorting
0.717	ORP, Total [As], %CaCO <sub>3</sub> , Sorting
0.717	ORP, Total [As], % Organics, %CaCO <sub>3</sub> , Sorting
0.712	Total [As], %CaCO <sub>3</sub>
0.711	pH, Total [As], % Organics, %CaCO <sub>3</sub> , Sorting
0.707	Temperature, %CaCO <sub>3</sub> , Sorting
0.705	Temperature, %CaCO <sub>3</sub> , Median Grain Size, Sorting
0.671	%CaCO <sub>3</sub>
0.626	Sorting
0.604	Median Grain Size
0.551	% Organics
0.496	Total [As]
0.294	pH
0.292	Temperature
0.222	ORP
0.162	Salinity

**Table 4.4b BIO-ENV correlations between the benthic macrofaunal community structure and physical parameters; reference site omitted.**

Spearman Correlation	Parameters
0.790	Total [As], % Organics, %CaCO <sub>3</sub>
0.789	Total [As], % Organics, %CaCO <sub>3</sub> , Sorting
0.780	% Organics, %CaCO <sub>3</sub> , Sorting
0.780	pH, Total [As], % Organics, %CaCO <sub>3</sub> , Sorting
0.774	pH, % Organics, %CaCO <sub>3</sub> , Sorting
0.770	Total [As], %CaCO <sub>3</sub>
0.768	ORP, Total [As], % Organics, %CaCO <sub>3</sub>
0.763	Total [As], %CaCO <sub>3</sub> , Sorting
0.762	ORP, Total [As], % Organics, %CaCO <sub>3</sub> , Sorting
0.758	% Organics, %CaCO <sub>3</sub>
0.746	% Organics
0.726	%CaCO <sub>3</sub>
0.622	Sorting
0.617	Median Grain Size
0.554	Total [As]
0.332	pH
0.320	Temperature
0.249	ORP
0.166	Salinity

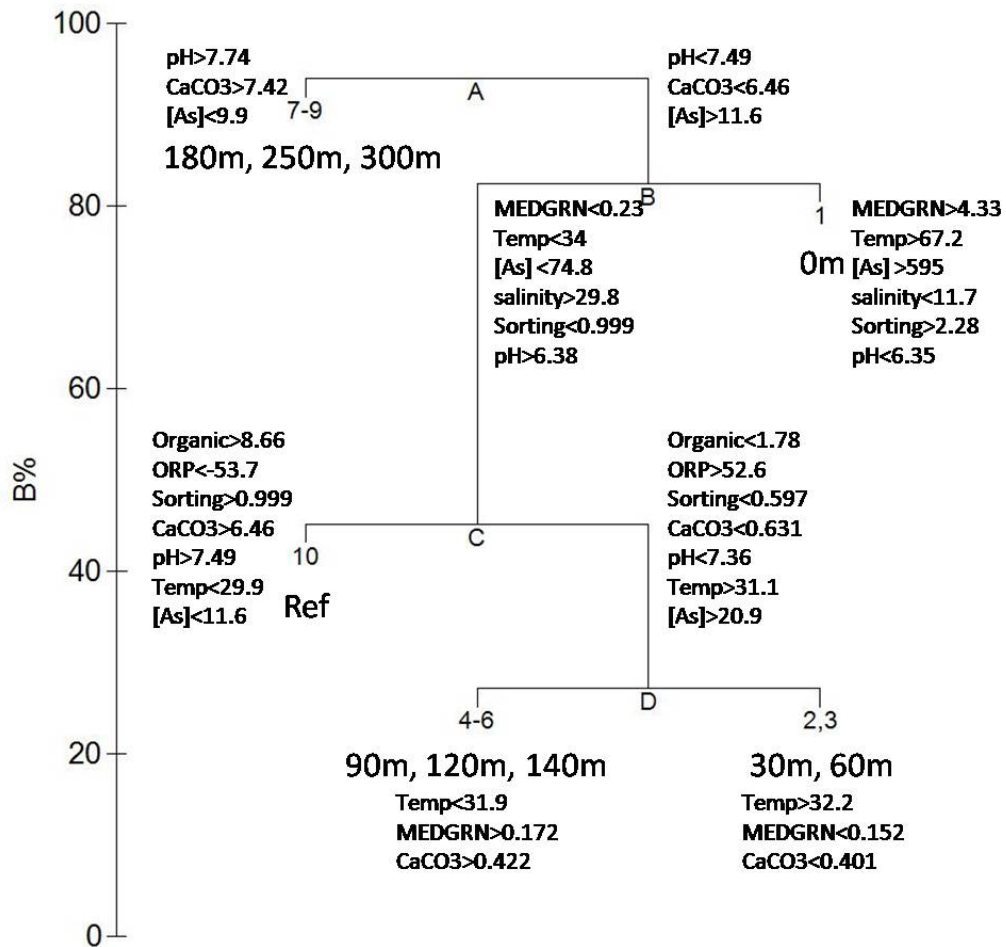


**Figure 4.7 LINKTREE showing physical parameters characterizing site groups based on the benthic macrofauna similarity.**

#### 4.4 Discussion

The benthic macrofaunal communities are known to be good indicators of their surrounding habitat characteristics, and the macrofaunal community structure in Tutum Bay reflects this. Four distinct community assemblages were observed corresponding to different pore water and sediment characters. These communities are defined as the vent community consisting of the 0 m site, the near-vent community consisting of the transect sites from 30 m through 140 m away from the vent, the offshore community consisting of

the transect sites from 180 m through 300 m and the Danlum Bay reference site community.

The vent community unique to the 0 m site had a low species richness and diversity, but high abundance, dominated by a single species. The dominant species at the 0 m site, *Capitella cf. capitata*, has often been associated with disturbed habitats and has been considered to be a pollution indicator species (Grassle and Grassle 1974, 1976). The taxon *Capitella capitata* has long been recognized as a complex of many morphologically similar sibling species (Grassle and Grassle, 1974, Gamenick *et al* 1998b, Blake 2009). Blake (2009) redescribed *Capitella capitata* based on museum specimens collected from Greenland near the original type locality. According to Blake's redescription, *Capitella capitata* has an arctic to subarctic geographical distribution, and other "*Capitella capitata*" reported in the literature from other localities globally are most likely different, but closely related, sibling species. Given this, the specimens identified from Tutum Bay may well represent an undescribed sibling species within the "*Capitella capitata*" species complex that is unique in its tolerance to the extreme environmental conditions near the shallow-water hydrothermal vent.

The near-vent community had low species richness and abundance and was dominated primarily by the burrowing shrimp *Thalassinidea* sp. A and the amphipod *Platyischnopus* sp. A, which seemed to be well adapted to living in the fine-grained sediments characteristic at these sites. The biotic interaction of these two species with other benthic infauna may influence the overall community structure. The constant burrowing activity of thalassinid shrimp, for example, physically disturbs the sediment which can prevent the colonization of that area by other species (Alongi 1986). The same

reworking of the sediment can also affect the geochemical processes and microbial productivity in the sediment column (Lohrer *et al.* 2004, Mermillod-Blondin and Rosenberg, 2006, Jordan *et al.* 2009). In particular, the burrowing activity draws oxygenated water deeper into the sediment which can influence redox reactions. In the case of metals, such as arsenic, this can potentially affect the valence state of the metal and its toxicity and bioavailability.

Species in the amphipod genus *Platyschnopus* are known to be predators on recently settled larvae of other infaunal animals and on meiofauna (J.D. Thomas, personal communication). The presence of this genus in high densities may exclude the colonization by other species, affecting the overall species composition of this community.

The physical characteristics of the pore water and sediment at the near vent sites also influence the benthic community structure at these sites in several possible ways. In addition to the high arsenic concentrations occurring at these sites, the low pH has adverse effects on shell-bearing species. McCloskey (2009) in his corresponding study of the foraminifera in Tutum Bay also found pH to be a controlling factor with foraminifera shells being absent in the sediments as far away as 150 m along the same sampling transect. Engel (2010) studied the effect of short-term (5-day) exposure to the pH and temperature gradient at Tutum Bay on benthic foraminifera. She observed evidence of shell dissolution as far as 30 m from the vent. Most species appeared to be able to survive exposure to low pH but were less tolerant of high temperatures. Dissolution was more apparent on dead shells (Engle 2010).

The offshore community was characterized by higher species richness, abundance and overall species diversity. The sediment characteristics such as CaCO<sub>3</sub> content appeared to be the controlling factor in structuring the macrofaunal community at these sites. This was further related to the higher pore water pH values, reflecting the reduced influence from the hydrothermal vent with distance offshore.

The high organic carbon content in the Danlum Bay sediments was correlated with the macrofaunal community found at the reference site. The macrofaunal community was dominated by several polychaete species, such as *Litocorsa* sp. A (Family Pilargiidae) and representatives in the family Capitellidae including *Mediomastus* sp. A. and a possibly undescribed genus (Capitellidae w/spatulate chaetae). Both of these polychaete families have been classified as deposit feeders by Fauchald and Jumars (1979) and are commonly found in organically enriched environments.

Although arsenic concentrations in the sediments and pore water at Tutum Bay are among the highest recorded in a natural marine system (Pichler and Dix 1996, Pichler *et al* 1999a), this parameter had a lesser influence in structuring the benthic macrofaunal community than expected as seen in the BIO-ENV results. Several factors could explain this. First, the coprecipitation of the arsenic with hydrous ferric oxides (HFOs) binds the arsenic in the sediments reducing its bioavailability to benthic infauna (Pichler and Veizer 1999, Pichler *et al.* 1999a, Price and Pichler 2005). Price and Pichler (2005) found that as much as 98.6% of the arsenic in the vent fluids is precipitated into the sediments. Only a small percentage of the bound arsenic (mean = 3.6%) was found to be easily extractable and still potentially bioavailable to benthic organisms (Price and Pichler 2005). Secondly, because the low salinity and high temperature vent discharge is less

dense than the surrounding seawater it rises to the surface (Price and Pichler 2005) away from the benthic environments.

Many invertebrate organisms have also adapted physiological mechanisms to detoxify or eliminate high concentrations of arsenic and other contaminants (Langdon *et al.* 2003). Most metabolic pathways in marine invertebrates involve the reduction of As(V) to As(III) which is then methylated through a series of organoarsenical compounds typically to arsenobetaine (AB) as the end product (Langdon *et al.* 2003, Argese *et al.* 2005, Grotti *et al.* 2010). Price (2008) looked at the arsenic speciation in tissue samples collected from several sessile organisms living near the Tutum Bay vent and at sites along the transect. He found elevated levels of total arsenic in organisms collected near the vent. Price (2008) further found elevated levels of organoarsenical compounds in the tissue samples from the soft coral *Clavularia* and the ascidian *Polycarpa* suggesting that these organisms were able to detoxify the arsenic via methylation to DMA and AB.

#### **4.5 Summary and conclusions**

The benthic macrofaunal community structure at Tutum Bay was influenced by the environmental gradient along the transect. The community immediately surrounding the focused venting was represented by a few opportunistic species and most notably dominated by the polychaete *Capitella* cf. *capitata*. The transect sites out to 140 m away from the focused vent still showed evidence of hydrothermal influence due to diffuse venting. The macrofaunal community in this area was characterized by low species diversity and abundances and was dominated by *Thalassinidea* sp. A and the amphipod *Platyschnopus* sp. A. This suggests that the community structure at these sites may have

been influenced by a combination of the physical environment and biological interactions due to physical disturbance through bioturbation and by predation of settling larvae. The macrofaunal community farther from the vent, by contrast, had relatively high diversity and abundances.

The preliminary results from the 2003 samples had suggested that pH was a controlling factor in structuring the benthic macrofaunal community at Tutum Bay (Chapter 3; Karlen *et al.* 2010). The results from the 2005 samples, however, do not agree with the earlier findings. Instead, sediment characteristics such as carbonate content, sediment sorting and median grain size appeared to structure the macrofaunal community. These factors in turn were correlated with the pore water pH which suggests that even though pH may not have a direct effect on the community structure it may have an indirect influence by controlling the sediment composition.



## Chapter Five

### Meiofaunal communities associated with the shallow water hydrothermal vent system at Ambitle Island, Papua New Guinea

#### 5.1 Introduction

The meiofauna refers to the size range of organisms occupying the intermediate size range between the smaller microfauna (predominately prokaryotes and “protozoan” eukaryotic groups) and larger macrofauna (predominately invertebrate metazoan groups). The size range that defines the meiofauna varies with different authors, with an upper size limit of either 1 mm or 500  $\mu\text{m}$  (0.5 mm) and a lower limit of ranging from 62 to as small as 42  $\mu\text{m}$  being used (Fenchel 1978, Higgins and Thiel 1988). For this study, meiofauna are defined as organisms within the 50  $\mu\text{m}$  – 500  $\mu\text{m}$  size range. The meiofaunal taxa included in this analysis included the metazoan groups and ciliates. Foraminifera were excluded since this group was analyzed by McCloskey (2009) as part of the larger research effort at Tutum Bay.

Several studies over the past 20 years have looked at the meiofaunal communities associated with shallow-water hydrothermal systems around the world. Past studies have included sites in New Zealand (Kamenev *et al.* 1993), the Aegean Sea (Thiermann *et al.* 1994, 1997), Papua New Guinea (Tarasov *et al.* 1999), Antarctica (Bright *et al.* 2003),

the Kuril Islands, Sea of Okhotsk (reviewed in Tarasov 2006) and Indonesia (Zeppilli and Danovaro 2009).

Kamenev *et al.* (1993) documented the meiofaunal distribution at several sites in the Bay of Plenty, New Zealand. They reported higher densities of nematodes in two samples from a hydrothermally influenced site (McEwen's Bay site 1) relative to an adjacent non-hydrothermal site. Thiermann *et al.* (1994) found no meiofauna present in sediments directly impacted by the venting, while the meiofaunal community farther away was dominated by nematodes. One nematode species, *Oncholaimus camplocercoides*, occurred in high densities at the border of the sulfidic sediment patch surrounding the vent and the nonsulfidic sediment farther from the vent (Thiermann *et al.* 1994).

Tarasov *et al.* (1999) studied the distribution of meiofauna near shallow-water hydrothermal vents at several sites within Matupi Harbor in the Rabaul Caldera, Papua New Guinea. Most of the meiofaunal communities they reported were dominated by nematodes. At one site near the active Tavurvur volcano, the high temperature (85 - 90°C), shallow zone was devoid of infauna, while the area with hydrothermal seeps and slightly cooler temperatures (50 - 60°C) was dominated by nematodes. A second hydrothermal area they sampled was characterized by bacterial mats. The dominant meiofauna living on the mats was a spionid polychaete identified as *Polydora* sp., which formed burrows through the mat down to the underlying sediment. At a third site near the Rabalankaia volcano they found a single species of large nematode (Oncholaimidae) at high densities ( $131 \times 10^3/\text{m}^2$ ) in hydrothermal sediments (50 - 60°C). The meiofaunal densities at the several non-volcanic sites within Matupi Harbor and the Rabaul Caldera

(Blanche Bay) were variable and appeared to be influenced primarily by sediment characteristics and bottom slope (Tarasov *et al.* 1999).

Zeppilli and Danovaro (2009) also found that meiofaunal communities associated with shallow-water hydrothermal vents in Indonesia were dominated by nematodes, with the exception that copepods were dominant 100 cm from the vent in an area of intermediate hydrothermal influence. This they attributed to the alteration of the sediment grain size by hydrothermal fluids. They found a general trend of decreasing abundance and diversity closer to the vent site but noted that the meiofauna abundances they reported were as much as 10x higher than those recorded at other shallow-water vent sites. Zeppilli and Danovaro (2009) also recorded the occurrence of several species of Oncholaimid nematodes near the vent, including *Oncholaimus*, the same genus found by Thiermann *et al.* (1994) at Milos, Greece.

Some meiofaunal communities have adapted to surviving in anoxic sediments below the level of oxygen penetration in the surface sediments. This habitat is characterized by high levels of hydrogen sulfide (H<sub>2</sub>S), and the associated meiofaunal communities are referred to as the “Thiobios” (Fenchel and Riedl 1970). These high sulfide conditions often occur in extreme environments such as hydrothermal vents and brine seeps (Powell and Bright 1981, Powell *et al.* 1983). Several shallow-water hydrothermal vent systems have high levels of H<sub>2</sub>S present, and the associated meiofauna show unique adaptations to these sulfide-enriched environments. The dominant nematodes found near the hydrothermal vents in the Bay of Plenty, New Zealand, were associated with symbiotic sulfur bacteria, which covered the nematodes’ outer cuticle (Kamenev *et al.* 1993, Tarasov 2006). Similarly, Bright *et al.* (2003) discovered that the

outer surface of the dominant meiofaunal flatworm found at Fumarole Bay, Deception Island, Antarctica was associated with symbiotic bacteria which colonized its outer surface. The dominant nematode associated with high sulfidic sediments at Milos, Greece, (*Oncholaimus campylocercoides*) was able to detoxify sulfide by sequestering elemental sulfur as intracellular inclusions in their epidermal cells (Thiermann *et al.* 1994, 2000). At the volcanic site in Rabaul Caldera studied by Tarasov *et al.* (1999), one of the dominant nematodes they found was in the same family (Oncholaimidae) as the species found by Thiermann *et al.* (1994) at Milos, Greece. Additionally, they noted that the dominant meiofaunal polychaete occurring in the bacterial mats (*Polydora* sp.) was associated with filamentous sulfur bacteria that colonized their burrow walls. These observations suggest possible symbiotic relationships between sulfur - metabolizing bacteria and meiofaunal species.

The Ambitle Island vent system was similar to these other sites with regards to its high temperature, but differed in that high levels of hydrogen sulfide were not evident, while arsenic concentrations were high. Because of this, it was expected that the meiofaunal community surrounding the vent would be influenced by the high arsenic, and possibly be associated with arsenic metabolizing bacteria.

## **5.2 Material and methods**

### **5.2.1 Sampling design and field collection**

Sampling and analysis methods for pore water and sediment samples collected at the transect sites and the Danlum Bay reference site are given in Chapter 2.

Sediment samples for meiofaunal community analysis were collected at the nine transect sites and at the Danlum Bay reference site as described in Chapter 2.

Meiofauna samples were collected from a random grid in each of the five quadrats at each site using a 60cc syringe coring tube (diameter = 3cm; area = 7.07 cm<sup>2</sup>). Sediment cores were collected to a depth of 5 cm. The five cores from each site were treated as separate replicate samples. The sediment was sieved through a 500 µm mesh screen onto a 50 µm mesh plankton netting to remove macrofauna and retain meiofaunal sized organisms. The retained meiofauna and sediment was rinsed with filtered seawater into 50 ml HDPE sample bottles and fixed in 10% borax buffered formalin with Rose Bengal stain. Seawater used for sieving and rinsing the samples was filtered through a 50 µm plankton net to remove any planktonic organisms and prevent possible contamination of the samples.

### **5.2.2 Sample processing and identification**

The laboratory processing of the meiofauna samples followed the following procedure: First the formalin was decanted from the sample through a 50 µm mesh piece of plankton netting placed in a funnel. The sediment was rinsed into a 100 ml graduated cylinder with filtered tap water. The graduated cylinder was filled up to the 100 ml mark with filtered tap water then stoppered, and the sediment was mixed by inverting the cylinder 10 times to suspend and separate the meiofauna from the sediment. The water was then decanted through the 50 µm mesh to retain any suspended meiofauna. This float-off procedure was repeated 5 times. The organisms retained on the sieve were rinsed into a gridded petri dish with filtered tap water and sorted into the lowest practical

taxonomic levels and counted. The sediment fraction was also placed in a gridded petri dish and scanned under the dissecting microscope, and any remaining meiofauna were removed. For the meiofauna analysis, “lowest practical taxonomic levels” generally were Orders, although lower taxonomic identifications were made when possible. All specimens were retained and archived for farther taxonomic analysis, and voucher specimens were photographed.

### **5.2.3 Data analysis**

Data analyses were as described in Chapter 4.

## **5.3 Results**

A total of 17,346 meiofaunal specimens were found at all sites, representing 61 higher taxonomic groups. Arthropods and nematodes represented 46% and 40% of the overall meiofaunal abundance respectively (Figure 5.1). Within the arthropods, copepods (predominantly Harpacticoidea) comprised 61% of the abundance, and unidentified crustacean larvae (naupulii) were 27% of the arthropod abundance. The nematode abundance was represented primarily by the order Chromadorida which accounted for 76% of the nematode abundance (Figure 5.1). Arthropods and nematodes were dominant across all sites and accounted for over 80% of the relative abundance at every site (Figure 5.2).

Total number of taxa and abundance pooled for the five replicate cores within each site along with ranked relative abundance are shown in Table 5.1. Chromadorid nematodes and copepods were the top two ranked taxa at all sites except 90 m and

accounted for > 50% of the relative abundance at the most of the sites (Table 5.1). Seven of the 61 identified taxonomic groups were found at all sites. These were Chromadorid, Monhysterid, and Enoplid nematodes; Copepoda, Ostracoda, Platyhelminthes, and unidentified crustacean larvae. Seventeen taxonomic groups were present at a single site, and 12 were represented by a single specimen.

The 0 m site had a total of 17 higher taxa and 382 total individual specimens, with a median richness of 10 taxa/sample and a median abundance of 52 individuals/sample (Tables 5.1 and 5.2). Capitellid polychaetes accounted for nearly 5% of the relative abundance at this site, a much higher contribution than at the other sites where they were present. These were primarily juvenile individuals of *Capitella cf. capitata*. Unique at the 0 m site was a single specimen of the interstitial polychaete family Nautiliniellidae. Taxonomic identifications for the 0 m samples were initially done to lower classification levels when possible. Table 5.3 presents the top ranked taxa at the 0 m site utilizing the lower level identifications. For these calculations, the larval crustaceans were excluded from the total count, resulting in the observed discrepancies with Table 5.1. The harpacticoid copepods here are the highest ranking taxon with 24% of the relative abundance. The chromadorid nematode *Innocuonema* sp. A ranked second, and mites (Acari spp.), juvenile *Capitella cf. capitata*, and the enoplid nematode *Trileptium?* sp. A were among the top five most abundant taxa at the 0 m site.

The 30 m site had a total of 19 higher level taxa and 1,190 individuals, with median taxonomic richness of 11 taxa/sample and median abundance of 210 individual/sample (Tables 5.1 and 5.2). Unique meiofauna taxa at this site included the

interstitial polychaete family Polygordiidae and chaetognaths. Additionally, the interstitial polychaete, *Protodriloides* cf. *chaetifer*, was also found at this site.

A total of 24 higher level taxa and 1,250 individuals were present at the 60 m site (Table 5.1). The median taxonomic richness was 12 taxa/sample and median abundance was 208 individuals/sample (Table 5.2). This site included a decapod and mysid crustaceans which were not found at the other sites (Table 5.1).

The 90 m site had a total of 25 higher level taxa and 2,098 individuals (Table 5.1). Median taxonomic richness was 25 taxa/sample and median abundance was 452 individuals/sample. Crustacean larvae were the second most abundant group at this site, accounting for over 25% of the relative abundance.

The 120 m site had a total of 24 higher level taxa and 2,001 individuals (Table 5.1). Median richness was 15 taxa/sample and median abundance was 419 individuals/sample (Table 5.2). There were no taxa unique to this site.

There were a total of 29 higher level taxa and 2,197 individuals present at the 140 m site (Table 5.1). The median richness and abundance were 15 taxa/sample and 376 individuals/sample respectively. Unique taxa present at this site included an opisthobranch mollusk and a possible chironomid insect larva.

The 180 m site had a total of 32 taxa and 2,294 individuals with a medium taxonomic richness of 17 taxa/sample and a median abundance of 395 individuals/sample (Tables 5.1 and 5.2). Unique taxa at this site included the polychaete families Nereididae and Ampharetidae (Table 5.1).

The 250 m site had a total of 33 higher level taxa and a total abundance of 2,023 individuals (Table 5.1). Median taxonomic richness and median abundance were 18



taxa/sample and 338 individuals/sample respectively (Table 5.2). Copepods were the dominant taxa group at this site, accounting for 38% of the relative abundance (Table 5.1). There were no unique taxa which were found only at the 250 m site, but the interstitial polychaete *Protodriloides* cf. *chaetifer* was recorded (Table 5.1).

The 300 m site had the highest overall taxonomic richness and abundance with a total of 39 higher level taxa and 3,180 individuals (Table 5.1). Median taxonomic richness was 21 taxa/sample and median abundance was 582 individuals/sample (Table 5.2). Copepods were also the most abundant group at this site. Several polychaete families were only found at the 300 m site, including Ctenodrilidae, Fauvelopsidae?, Flabelligeridae? and Maldanidae (Table 5.1). Recently settled trochophore larvae were also recorded at this site (Table 5.1).

The Danlum Bay reference site (Ref) had a total of 24 taxa and a relatively low abundance of 731 individuals (Table 5.1). The median richness was 15 taxa/sample and median abundance was 141 individuals/sample. This site was unique in the strong dominance of copepods, which accounted for 47% of the relative abundance at the reference site.

Table 5.2 presents the summary statistics for the meiofaunal community indices at each site. The higher level taxonomic richness ranged from five taxa/sample at the 0 m site to a maximum of 24 taxa/sample at the 180 m site, with the highest median value at the 300 m site (Table 5.2). The taxonomic richness increased with distance from the vent site (Figure 5.3), and richness at the farthest transect sites (180 m – 300 m) were significantly higher than the 0 m and inner transect sites (ANOVA,  $F=9.45$ ;  $p<0.001$ ).

Taxa richness at the Danlum Bay reference site was similar to the middle transect sites with a median value of 15 taxa/sample (Table 5.2; Figure 5.3).

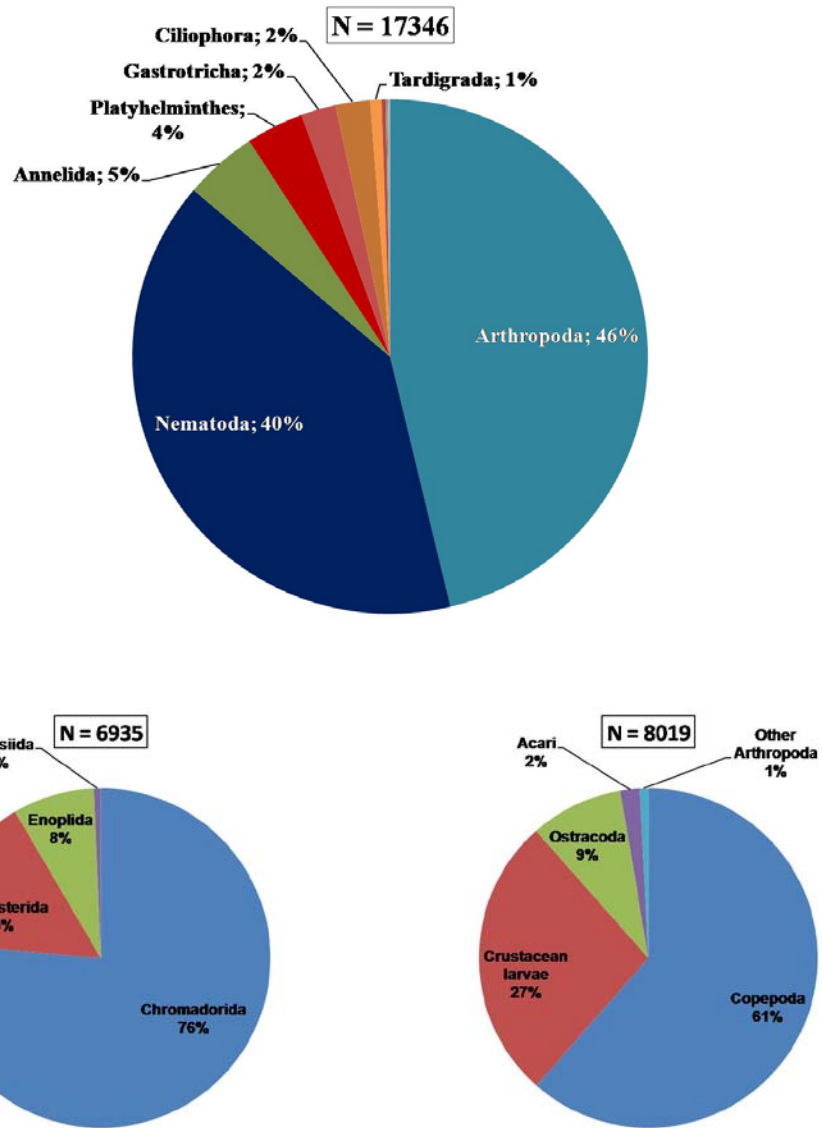


**Figure 5.1** Relative taxonomic composition of total meiofaunal abundance (N = 17,346 individuals) by phylum (top graph) and subsets for Nematoda (bottom left; N = 6,935 individuals) and Arthropoda (bottom right; N = 8,019 individuals).

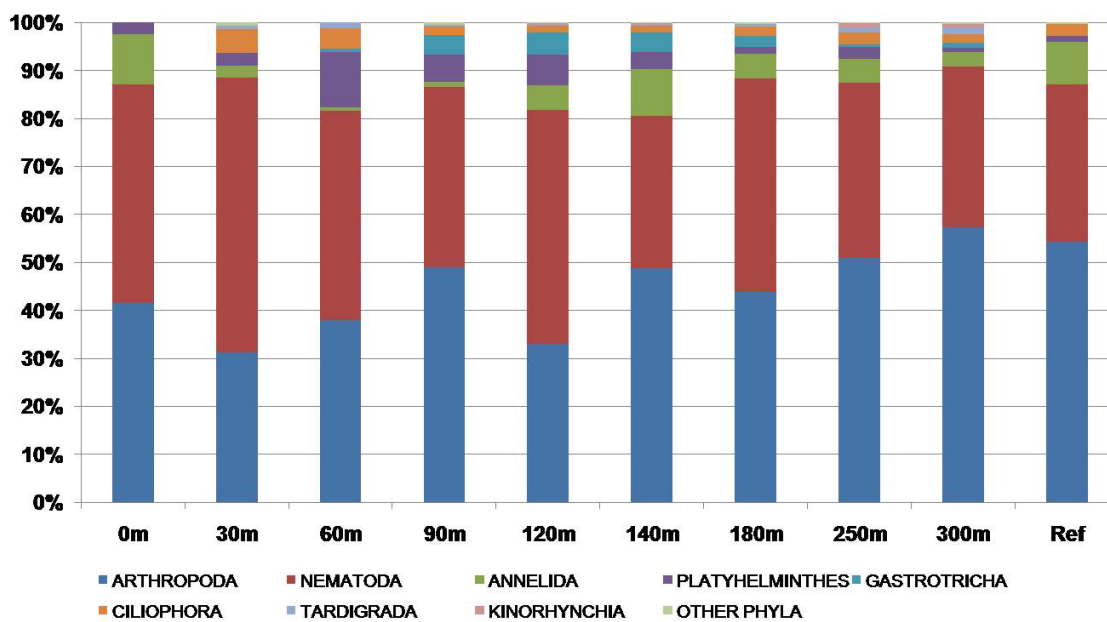


Figure 5.2 Meiofaunal taxonomic composition by site.

**Table 5.1 Meiofaunal total taxa richness (S), abundance (N) and relative abundance (%) by site.**

0 m S = 17 N = 382		Ref S = 24 N = 731	
Taxa	%	Taxa	%
Chromadorida	27.23%	Copepoda	46.92%
Copepoda	23.82%	Chromadorida	17.37%
Enoplida	10.99%	Monhysterida	6.29%
Crustacean larvae	6.54%	Enoplida	5.47%
Monhysterida	6.54%	Crustacean larvae	5.20%
Acari	6.28%	Syllidae	5.06%
Capitellidae	4.97%	Trefusiida	3.69%
Syllidae	3.93%	Ciliophora	2.46%
Ostracoda	2.88%	Hesionidae	1.78%
Platyhelminthes	2.36%	Platyhelminthes	1.37%
Nerillidae	1.31%	Ostracoda	0.96%
Tanaidacea	1.05%	Acari	0.55%
Trefusiida	0.79%	Sabellidae	0.41%
Cumacea	0.52%	Spionidae	0.41%
Gammaridea	0.26%	Tanaidacea	0.41%
Isopoda	0.26%	Capitellidae	0.27%
Nautiliniellidae	0.26%	Polychaete (larvae)	0.27%
		Isopoda	0.27%
		Dorvilleidae	0.14%
		Lumbrineridae	0.14%
		Paraonidae	0.14%
		Pilargiidae	0.14%
		Bivalvia	0.14%
		Gastropoda	0.14%

**Table 5.1 Continued**

30 m S = 19 N = 1190		60 m S = 24 N = 1250	
Taxa	%	Taxa	%
Chromadorida	38.32%	Chromadorida	29.12%
Copepoda	22.52%	Copepoda	26.80%
Monhysterida	14.54%	Platyhelminthes	11.36%
Crustacean larvae	7.82%	Monhysterida	11.12%
Ciliophora	4.87%	Crustacean larvae	10.16%
Enoplida	4.03%	Ciliophora	4.16%
Platyhelminthes	2.69%	Enoplida	3.28%
Polychaeta (larvae)	1.60%	Tardigrada	1.20%
Tardigrada	0.76%	Gastrotricha	0.88%
Ostracoda	0.76%	Ostracoda	0.32%
METAZOA (Undet.)	0.50%	Gammeridea	0.24%
Capitellidae	0.42%	Tubificidae	0.16%
Trefusiida	0.34%	Capitellidae	0.16%
Polygordiidae	0.25%	Glyceridae	0.16%
Chaetognatha	0.17%	Acari	0.16%
Tanaidacea	0.17%	Hesionidae	0.08%
Protodriloides cf. chaetifer	0.08%	Nerillidae	0.08%
Tubificidae	0.08%	Spionidae	0.08%
Caprella	0.08%	Syllidae	0.08%
		Decapoda	0.08%
		Isopoda	0.08%
		Mysidacea	0.08%
		Tanaidacea	0.08%
		Trefusiida	0.08%

**Table 5.1 Continued**

90 m S = 25 N = 2098		120 m S = 24 N = 2001		140 m S = 29 N = 2197	
Taxa	%	Taxa	%	Taxa	%
Chromadorida	28.41%	Chromadorida	34.03%	Copepoda	30.22%
Crustacean larvae	25.60%	Copepoda	21.34%	Chromadorida	28.49%
Copepoda	17.25%	Monhysterida	10.99%	Crustacean larvae	12.56%
Monhysterida	6.20%	Crustacean larvae	7.70%	Hesionidae	7.60%
Ostracoda	5.86%	Platyhelminthes	6.45%	Ostracoda	5.37%
Platyhelminthes	5.67%	Gastrotricha	4.70%	Gastrotricha	4.19%
Gastrotricha	4.00%	Enoplida	3.85%	Platyhelminthes	3.46%
Enoplida	2.96%	Ostracoda	3.45%	Monhysterida	2.00%
Ciliophora	1.81%	Hesionidae	3.20%	Syllidae	1.55%
Tardigrada	0.43%	Ciliophora	1.40%	Ciliophora	1.41%
Syllidae	0.38%	Syllidae	0.90%	Enoplida	1.23%
Cumacea	0.19%	Tardigrada	0.35%	Acari	0.41%
Capitellidae	0.19%	Acari	0.30%	Tardigrada	0.32%
Cnidaria	0.19%	Tubificidae	0.25%	Polychaeta (larvae)	0.23%
Trefusiida	0.14%	Cumacea	0.20%	Nerillidae	0.18%
Orbiniidae	0.14%	Capitellidae	0.20%	Kinorhynchia	0.14%
Sipuncula	0.14%	Enchytraidae	0.20%	Enchytraidae	0.09%
Glyceridae	0.10%	Nerillidae	0.15%	Capitellidae	0.05%
Dorvilleidae	0.05%	Cnidaria	0.10%	Dinophilidae?	0.05%
Paraonidae	0.05%	Glyceridae	0.05%	Glyceridae	0.05%
Polychaeta (larvae)	0.05%	Polychaeta (larvae)	0.05%	Orbiniidae	0.05%
Sabellidae	0.05%	Kinorhynchia	0.05%	Pisionidae	0.05%
Enchytraidae	0.05%	Gastropoda	0.05%	Gammeridea	0.05%
Nemertea	0.05%	Nemertea	0.05%	Caprella	0.05%
Porifera	0.05%			Tanaidacea	0.05%
				Insect larvae	0.05%
				Gastropoda	0.05%
				Opisthobranchia	0.05%
				Nemertea	0.05%

**Table 5.1 Continued**

180 m S = 32 N = 2294		250 m S = 33 N = 2023		300 m S = 39 N = 3180	
Taxa	%	Taxa	%	Taxa	%
Chromadorida	38.54%	Copepoda	37.52%	Copepoda	34.37%
Copepoda	25.59%	Chromadorida	29.81%	Chromadorida	26.95%
Crustacean larvae	9.94%	Crustacean larvae	8.80%	Crustacean larvae	16.07%
Ostracoda	7.24%	Monhysterida	4.35%	Ostracoda	5.03%
Monhysterida	3.97%	Platyhelminthes	2.47%	Enoplida	3.43%
Syllidae	2.75%	Enoplida	2.42%	Monhysterida	3.02%
Gastrotricha	2.40%	Ciliophora	2.37%	Ciliophora	1.82%
Enoplida	2.01%	Syllidae	2.32%	Syllidae	1.76%
Ciliophora	1.92%	Ostracoda	2.17%	Tardigrada	1.42%
Platyhelminthes	1.48%	Acari	1.93%	Acari	1.38%
Nerillidae	0.92%	Polychaeta (larvae)	1.09%	Gastrotricha	1.04%
Acari	0.92%	Tardigrada	1.04%	Platyhelminthes	0.79%
Tardigrada	0.48%	Kinorhynchia	0.99%	Kinorhynchia	0.66%
Hesionidae	0.22%	Gastrotricha	0.54%	Hesionidae	0.44%
Polychaeta (larvae)	0.22%	Hesionidae	0.40%	Cumacea	0.31%
Sabellidae	0.22%	Dorvilleidae	0.35%	Dorvilleidae	0.22%
Spionidae	0.22%	Cumacea	0.35%	Trefusiida	0.16%
Dorvilleidae	0.13%	Capitellidae	0.15%	Polychaeta (larvae)	0.13%
Cumacea	0.13%	Cirratulidae`	0.15%	Enchytraidae	0.09%
Pisionidae	0.09%	Spionidae	0.10%	Caprella	0.09%
Cnidaria	0.09%	Isopoda	0.10%	Pisionidae	0.06%
Nereididae	0.09%	Dinophilidae?	0.05%	Sabellidae	0.06%
Rotifera	0.09%	Nerillidae	0.05%	Tanaidacea	0.06%
Ampharetidae	0.04%	Paraonidae	0.05%	Cnidaria	0.06%
Cirratulidae`	0.04%	Pilargiidae	0.05%	Rotifera	0.06%
Paraonidae	0.04%	Pisionidae	0.05%	Trochophore larvae?	0.06%
Polynoidae	0.04%	Polynoidae	0.05%	Bivalvia	0.06%
Gammaridea	0.04%	Protodriloides cf. chaetifer	0.05%	Capitellidae	0.03%
Kinorhynchia	0.04%	Sabellidae	0.05%	Ctenodrilidae	0.03%
Trefusiida	0.04%	Tubificidae	0.05%	Dinophilidae?	0.03%
Nemertea	0.04%	Enchytraidae	0.05%	Fauveliopsidae?	0.03%
Priapulida	0.04%	Cnidaria	0.05%	Flabelligeridae?	0.03%
		Rotifera	0.05%	Maldanidae	0.03%
				Paraonidae	0.03%
				Pilargiidae	0.03%
				Polynoidae	0.03%
				Gastropoda	0.03%
				Sipuncula	0.03%
				Priapulida	0.03%



**Table 5.2 Median, minimum and maximum meiofaunal community index values for taxa richness, raw abundance counts, Shannon diversity index (base e), and evenness by site.**

Site	n	Taxa Richness		Abundance		Shannon Diversity		Evenness	
0 m	5	10		52		1.93		0.87	
		5	15	11	178	1.41	2.17	0.67	0.94
30 m	5	11		210		1.81		0.74	
		11	16	96	370	1.58	2.05	0.63	0.76
60 m	5	12		208		1.87		0.71	
		10	15	168	361	1.63	1.94	0.69	0.78
90 m	5	16		452		1.96		0.71	
		14	16	244	515	1.72	2.06	0.65	0.76
120 m	5	15		419		1.93		0.70	
		14	16	229	573	1.67	2.05	0.62	0.76
140 m	5	15		376		1.71		0.61	
		11	18	158	727	1.43	2.06	0.59	0.80
180 m	5	17		395		1.87		0.61	
		15	24	332	745	1.60	1.95	0.59	0.70
250 m	5	18		338		1.86		0.62	
		17	23	253	619	1.73	1.94	0.57	0.66
300 m	5	21		582		1.81		0.60	
		19	23	468	971	1.64	1.99	0.56	0.65
Ref	5	15		141		1.77		0.64	
		12	16	118	176	1.52	2.06	0.58	0.76

**Table 5.3 Relative abundance of dominant taxa representing >50% relative abundance at the 0 m site (excluding crustacean larvae).**

Taxon	Phylum	Relative Abundance (N = 357)	Cumulative Abundance
Harpacticoidea spp.	Arthropoda	24.09%	24.09%
<i>Innocuonema</i> sp. A	Nematoda	12.89%	36.97%
Acari spp.	Arthropoda	6.72%	43.70%
<i>Capitella</i> cf. <i>capitata</i>	Annelida	5.32%	49.02%
<i>Trileptium?</i> sp. A	Nematoda	3.92%	52.94%

The meiofaunal abundance ranged from as few as 11 specimens/sample at one of the 0 m replicates to 971 individuals/sample at the 300 m site (Table 5.2). Meiofaunal abundance increased with distance from the vent but was highly variable at each individual site (Figure 5.4). There was a significant difference in abundance among sites

(ANOVA,  $F = 4.158$ ;  $p < 0.001$ ), with abundances at the 300 m, 180 m and 120 m sites being significantly higher than at the 0 m and reference sites (Holm-Sidak multiple comparison test;  $p < 0.001$ ). Meiofaunal abundance at the reference site was lower than at all the transect site except 0 m, and was less variable among replicate samples (Table 5.2; Figure 5.4).

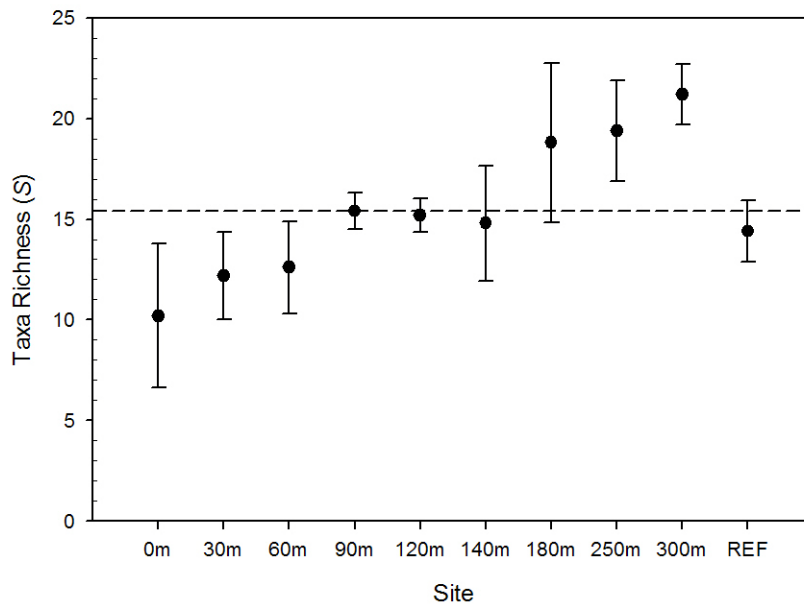


**Figure 5.3 Ambitle Island May/June 2005: Mean meiofaunal taxa richness  $\pm$  1 standard deviation.**

The Shannon diversity index values were highly variable among the replicate samples at each site (Figure 5.5) and there was not a significant difference between sites (Kruskal-Wallis ANOVA:  $H = 6.352$ ;  $df = 9$ ;  $p = 0.704$ ). Evenness values showed a decreasing trend with distance from the vent (Table 5.2; Figure 5.6), There were significant differences in the evenness values among sites (ANOVA:  $F = 6.030$ ;  $p < 0.001$ ), with the 0 m site being significantly higher than the 120 m through 300 m transect sites and the reference site.

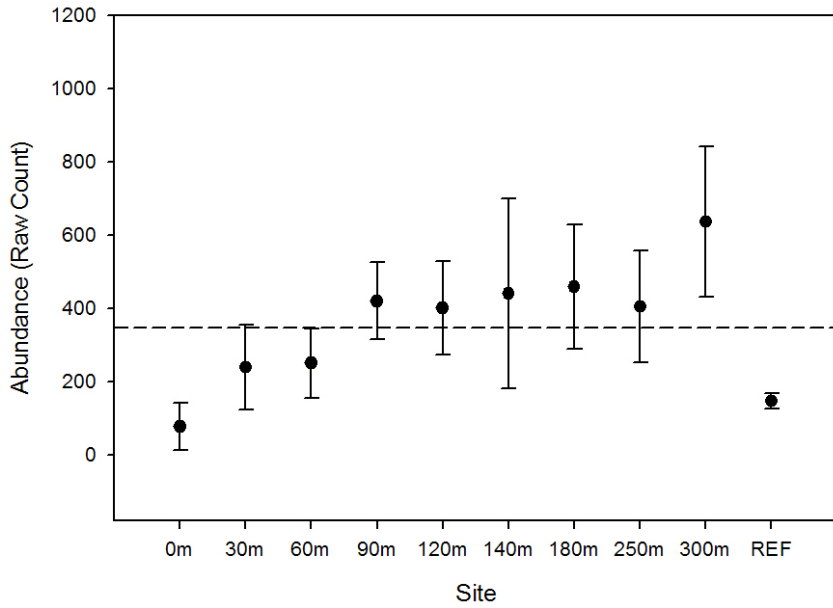


**Figure 5.4 Ambitle Island May/June 2005: Mean meiofaunal abundance  $\pm$  1 standard deviation. Abundance presented as individuals/sample.**

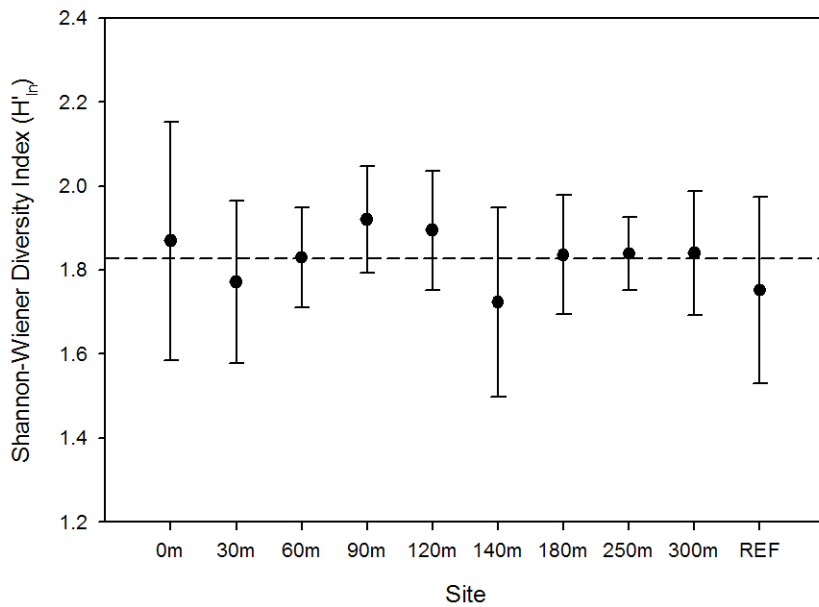


**Figure 5.5 Ambitle Island May/June 2005: Mean meiofaunal Shannon diversity index  $\pm$  1 standard deviation.**

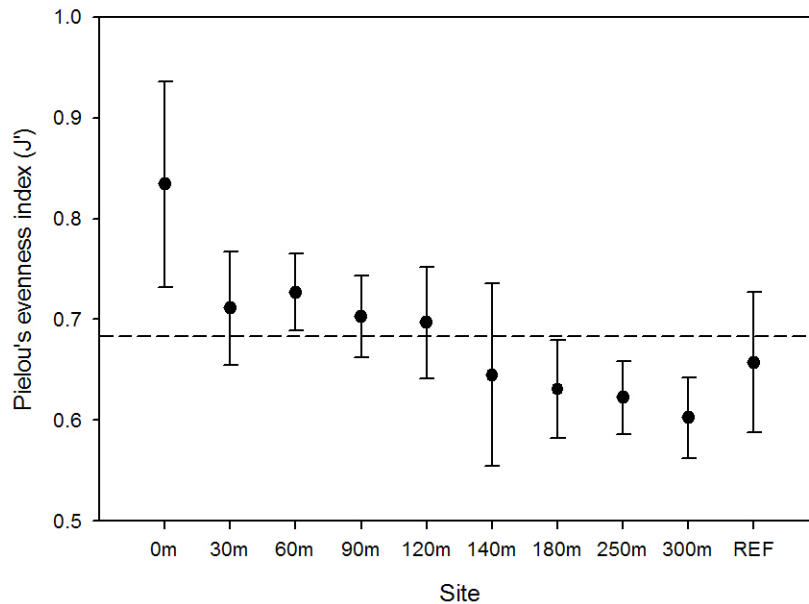


**Figure 5.6 Ambitle Island May/June 2005: Mean meiofaunal evenness  $\pm$  1 standard deviation.**

The ratio of nematode to copepod abundance has been used as a measure of environmental stress (Rafaelli and Mason 1981). The abundance values for nematodes and copepods and the nematode:copepod ratios are presented in Table 5.4. Both nematodes and copepod abundances increased with distance from the vent (Figures 5.7 and 5.8). Nematode abundances were significantly different among sites (ANOVA:  $F = 4.158$ ;  $p < 0.001$ ), with the 120 m, 180 m and 300 m sites having significantly higher nematode abundance than at the 0 m and reference sites (Holm-Sidak multiple comparison test;  $p < 0.001$ ). The copepod abundance among sites was also significantly different (Kruskal-Wallis:  $H = 28.281$ ;  $df = 9$ ;  $p < 0.001$ ). The copepod abundance was significantly higher at the 300 m site than the 0 m and 30 m sites and the 250 m site also had higher copepod abundance than at the 0 m site (Tukey Test;  $p < 0.05$ ). The nematode:copepod ratio exhibited a decreasing trend with distance from the vent site

(Figure 5.9), approaching a 1:1 ratio at the 250 m and 300 m sites. The reference site had a ratio value < 1 (Table 5.2; Figure 5.7). There were significant differences among sites (Kruskal-Wallis:  $H = 25.802$ ;  $df = 9$ ;  $p = 0.002$ ), with the 30 m site being significantly higher than the reference site (Tukey Test;  $p < 0.05$ ).

**Table 5.4 Median, minimum and maximum values for nematode and copepod abundances (individuals/sample) and the nematode:copepod ratio at each site.**

Site	n	TOTAL_NEMATODA		COPEPODA		N_C_RATIO	
0 m	5	18		10		2.00	
		2	106	1	43	1.13	2.47
30 m	5	99		45		2.83	
		60	223	20	106	1.94	3.60
60 m	5	84		60		1.63	
		71	195	43	119	1.01	2.91
90 m	5	170		75		2.00	
		65	226	53	85	1.23	3.32
120 m	5	186		81		2.11	
		86	278	49	121	1.16	5.67
140 m	5	140		134		1.09	
		43	257	5	260	0.74	8.60
180 m	5	202		119		1.70	
		140	315	74	185	1.56	2.08
250 m	5	133		120		1.11	
		100	251	77	255	0.53	1.30
300 m	5	249		205		0.99	
		101	330	141	333	0.52	1.77
Ref	5	42		68		0.67	
		30	66	52	84	0.44	1.27

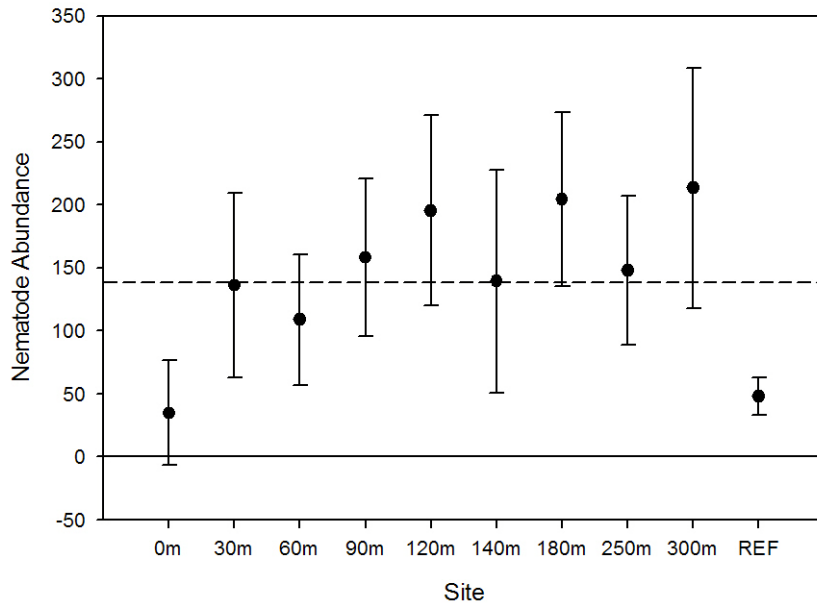


**Figure 5.7 Ambitle Island May/June 2005: Mean nematode abundance  $\pm$  1 standard deviation. Abundance presented as individuals/sample.**

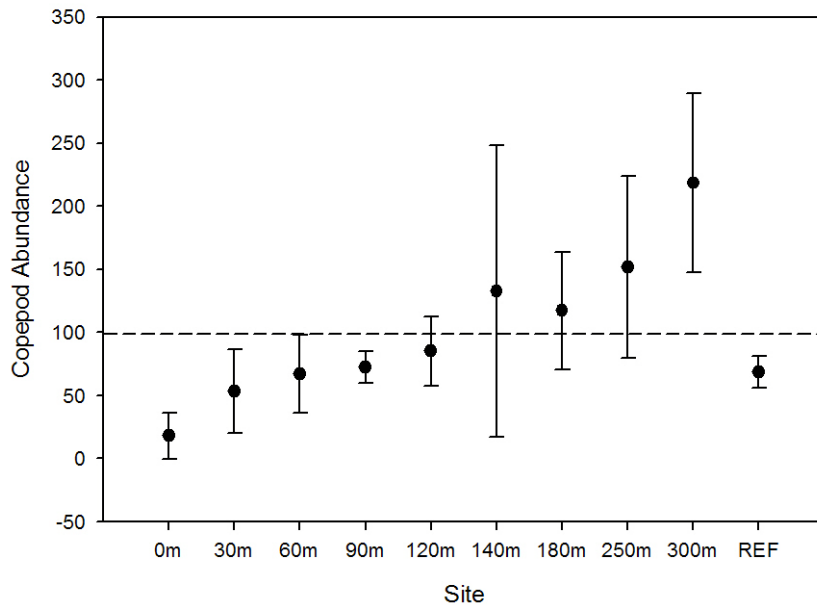


**Figure 5.8 Ambitle Island May/June 2005: Mean copepod abundance  $\pm$  1 standard deviation. Abundance presented as individuals/sample.**

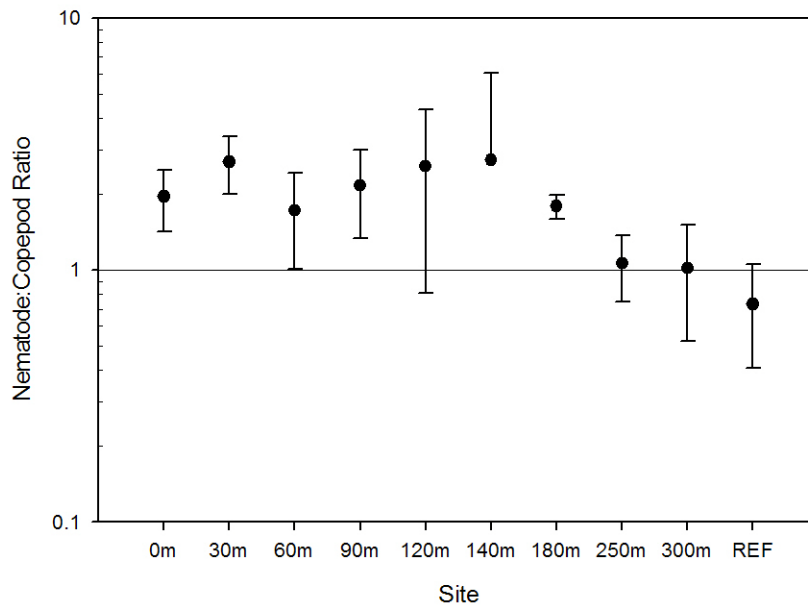


**Figure 5.9 Ambitle Island May/June 2005: Mean nematode:copepod ratio  $\pm$  1 standard deviation.**

Figures 5.10 and 5.11a show the similarity analysis based on all replicates and on site averaged abundance data respectively. The results for both analyses show the sites generally grouping together relative to their distance from the vent based on Bray-Curtis similarity values  $>60$  and SIMPROF test groupings, with more variability seen in the complete dataset. The analysis for the complete dataset shows one replicate from the vent site (0-B) as an outlier. This sample had the fewest taxa and lowest abundance which separated it out from the other samples. Several replicates from the 120 m and 140 m sites also were outliers, but overall replicate samples tended to group together within their sites or with adjacent sites. The results for the group - averaged data suggest that the meiofauna form four distinct communities relative to the distance along the transect, with the Danlum Bay reference site grouping with the 0 m site (Figure 5.11a). The four meiofaunal communities identified consisted of the 0 m site + the Danlum Bay reference

site (Group A); the 30 m + 60 m sites (Group B); the 90 m, 120 m + 140 m sites (Group C); and the 180 m + 250 m + 300 m sites (Group D). Removing the reference site data from the analysis still resulted in the same site groups (Figure 5.11b).

SIMPER analysis of the defined meiofaunal community groups (Table 5.5) showed that several taxa were common across all communities including harpacticoid copepods, chromadorid nematodes, monhysterid and enoplid nematodes, larval crustaceans, and flatworms (Platyhelminthes). The group A community was characterized by the contribution of trefusiid nematodes and marine mites (*Acari* spp.) to the similarity among the 0 m and reference sites (Table 5.5). The group B community also had ciliates (Ciliophora) and tardigrades contributing to the similarity among the 30 m and 60 m sites. The Group C community included gastrotrichs, ostracods and the polychaete families Syllidae and Hesionidae. The group D community was the most diverse with 15 taxa cumulatively contributing to >90% of the similarity among the 180 m, 250 m and 300 m sites. This community also was characterized by tardigrades, mites, cumaceans and kinorhynchs.

The BIO-ENV analysis (Table 5.6a) correlating the meiofaunal community structure with the physical parameters measured at each site shows that the strongest correlation ( $\rho = 0.565$ ) was with the combination of temperature, ORP, pore water salinity, and sediment organic carbon. The combinations of temperature, pore water salinity, sediment organic carbon and median grain size had only a slightly lower correlation ( $\rho = 0.564$ ). The pore water salinity had the highest correlation of a single variable ( $\rho = 0.512$ ) followed by temperature ( $\rho = 0.496$ ). Reanalysis of the BIO-ENV without the reference site (Table 5.6b) showed a stronger correlation with the combined



variables of pore water temperature and salinity ( $\rho = 0.664$ ), with salinity having the highest single variable correlation ( $\rho = 0.623$ ).

The LINKTREE analysis (Figure 5.12) separated the 0 m and reference site meiofaunal communities from the remaining sites. These two sites had lower ORP readings relative to the other sites. Node B of the LINKTREE separated the 30 m and 60 m meiofaunal community from the other sites based on slightly higher temperature, smaller median grain size and lower  $\text{CaCO}_3$  sediment content at those two sites. Node C of the link tree divided the remaining sites into two groups: the 180 m, 250 m and 300 m group and the 90 m, 120 m and 140 m group. The 180 m, 250 m, 300 m group was characterized by higher sediment sorting coefficients, higher sediment organic content, higher pH, higher  $\text{CaCO}_3$  content, lower arsenic concentrations, and larger median grain size relative to the other remaining sites.

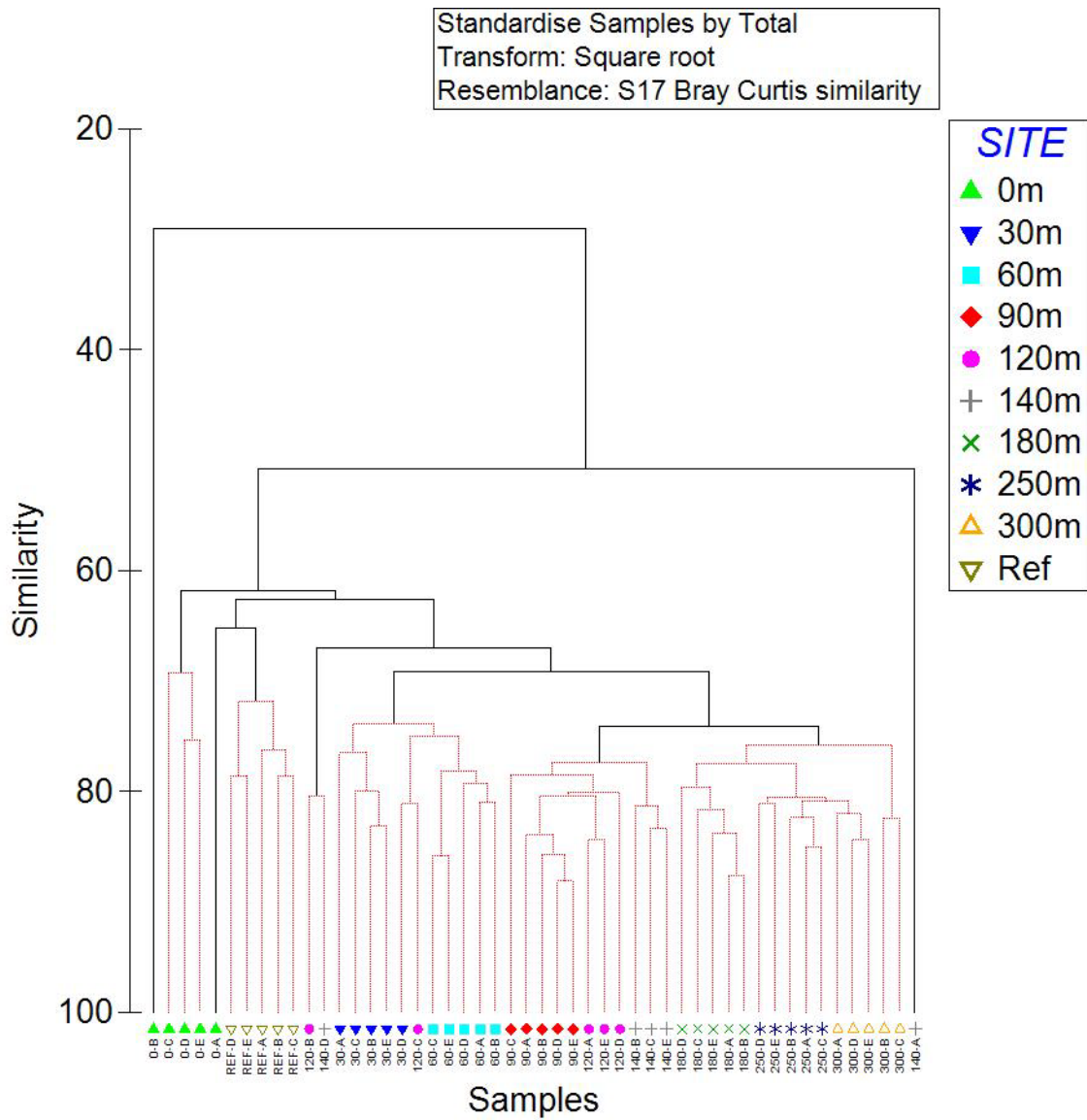


**Figure 5.10 Ambitle Island May/June 2005: Meiofaunal Bray Curtis similarity cluster analysis.**

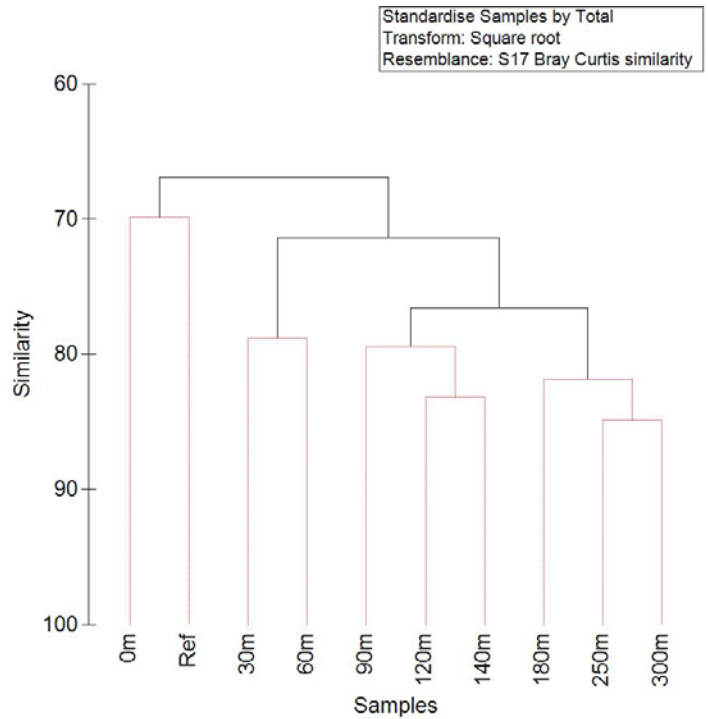


**Figure 5.11a Ambitle Island May/June 2005: Meiofaunal Bray Curtis similarity cluster analysis averaged by site.**

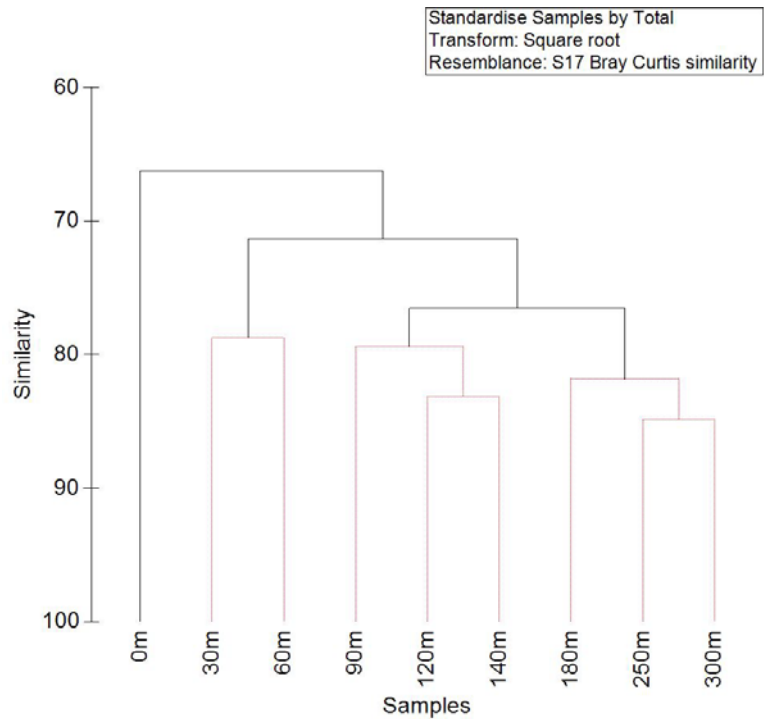


**Figure 5.11b Ambitle Island May/June 2005: Meiofaunal Bray Curtis similarity cluster analysis averaged by site; reference site omitted.**

**Table 5.5 SIMPER results for meiofaunal community groupings.**

Group A 0 m+ Ref Average similarity: 70		Group B 30 m+60 m Average similarity: 79		Group C 90 m+120 m+140 m Average similarity: 81		Group D 180 m+250 m+300 m Average similarity: 83	
Taxa	Contrib%	Taxa	Contrib%	Taxa	Contrib%	Taxa	Contrib%
Copepoda	20.7	Nematoda/Chromadorida	22.1	Nematoda/Chromadorida	19.9	Copepoda	18.3
Nematoda/Chromadorida	17.7	Copepoda	19.4	Copepoda	16.0	Nematoda/Chromadorida	18.1
Nematoda/Monhysterida	10.6	Nematoda/Monhysterida	13.6	Crustacean larvae	11.3	Crustacean larvae	10.4
Nematoda/Enoplida	9.9	Crustacean larvae	11.4	Platyhelminthes	7.6	Nematoda/Monhysterida	6.3
Crustacean larvae	9.7	Ciliophora	8.3	Gastrotricha	7.5	Ostracoda	5.9
Syllidae	8.4	Nematoda/Enoplida	7.4	Ostracoda	7.5	Nematoda/Enoplida	5.0
Platyhelminthes	5.0	Platyhelminthes	6.7	Nematoda/Monhysterida	6.6	Syllidae	4.8
Ostracoda	4.2	Tardigrada	3.6	Nematoda/Enoplida	4.9	Ciliophora	4.7
Nematoda/Trefusiida	3.8			Ciliophora	4.4	Acari	3.5
Acari	3.1			Syllidae	2.7	Platyhelminthes	3.4
				Hesionidae	2.2	Gastrotricha	2.9
						Tardigrada	2.8
						Hesionidae	1.8
						Cumacea	1.5
						Kinorhynchia	1.4
Cumulative %	92.9	Cumulative %	92.6	Cumulative %	90.6	Cumulative %	90.7

**Table 5.6a BIO-ENV Spearman correlations and best fit of physical parameters with the meiofaunal community structure.**

Spearman Correlation	Parameters
0.565	Temperature, ORP, Salinity, % Organics
0.564	Temperature, Salinity,% Organics, Median Grain Size
0.563	Temperature, ORP, Salinity, % Organics, Median Grain Size
0.560	Temperature,pH,Salinity,% Organics, Median Grain Size
0.559	Temperature,pH,ORP, Salinity, % Organics
0.557	Temperature, Salinity, % Organics
0.557	Salinity, % Organics, Median Grain Size
0.556	pH,ORP, Salinity, % Organics, Median Grain Size
0.556	ORP, Salinity, % Organics, Median Grain Size
0.553	pH, Salinity, % Organics, Median Grain Size
0.512	Salinity
0.496	Temperature
0.344	ORP
0.342	Median Grain Size
0.327	Sorting
0.326	Total [As]
0.244	pH
0.239	% Organics
0.100	%CaCO <sub>3</sub>

**Table 5.6b BIO-ENV Spearman correlations and best fit of physical parameters with the meiofaunal community structure; reference site omitted.**

Spearman Correlation	Parameters
0.664	Temperature, Salinity
0.623	Salinity
0.622	Temperature,pH,Salinity, Total [As], Median Grain Size
0.621	Temperature,pH,Salinity, Median Grain Size
0.619	Temperature,pH, ORP,Salinity, Total [As]
0.618	Temperature
0.617	pH, Salinity,Median Grain Size
0.617	pH, ORP,Salinity, Total [As], Median Grain Size
0.616	pH, Salinity, Total [As],Median Grain Size
0.614	Temperature,pH, ORP,Salinity, Median Grain Size
0.510	Median Grain Size
0.450	Total [As]
0.396	Sorting
0.350	ORP
0.318	pH
0.112	% Organics
0.105	%CaCO <sub>3</sub>

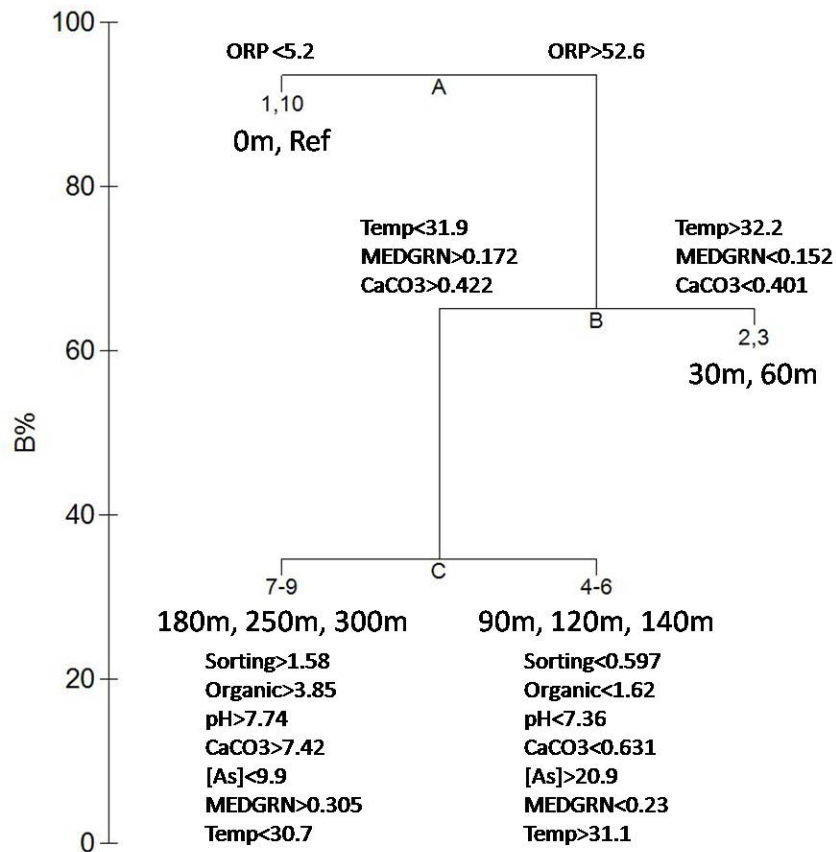


**Figure 5.12 LINKTREE diagram of meiofaunal community site groupings and corresponding physical characteristics.**

## 5.4 Discussion

Meiofaunal communities at Tutum Bay were dominated by nematodes and copepods, reflecting a global pattern typical of most meiofaunal communities (Riemann 1988). Nematodes were dominant at the vent and at most of the inner transect sites which were influenced by diffuse venting. This trend of nematode dominance is similar to other hydrothermal vent systems, both shallow-water and deep-sea, which also host meiofaunal communities dominated by nematodes (Kamenev *et al.* 1993, Thiermann *et al.* 1994, Vanreusel *et al.* 1997). The trend of low taxonomic richness and abundance at the vent site and increasing richness and abundance away from the focused venting is also

characteristic of other shallow-water hydrothermal systems (Kamenev *et al.* 1993, Thiermann *et al.* 1994).

Present among the meiofaunal community were juvenile *Capitella cf. capitata*, which were present at 9 of the 10 sites and indicates a continued recruitment of this polychaete throughout the system. Juveniles were most abundant at the 0 m site, which accounted for 46% of the specimens found. The dominance of adult *Capitella cf. capitata* at the vent site, and its relatively low abundance at the other sites in the macrofauna samples indicate the ability of this species to tolerate the extreme conditions at the vent while being out competed at the other sites.

The meiofaunal communities at the inner transect sites from 30 m to 140 m away from the vent were similar. These sites split into two subgroups. The meiofaunal community at the 30 m and 60 m sites had fewer taxa and lower abundances than the 90 m – 140 m sites, which also had relatively fewer taxa but increased abundances. This trend possibly reflects the sensitivity of the meiofaunal taxa to the pore water conditions and reflects the influence of diffuse venting along this zone of the transect. At all sites, nematodes were proportionally most abundant, but there was an increasing number of arthropods with distance along the transect. This may reflect the gradual increase in sediment grain size observed along the transect. The meiofaunal community in this zone may also have been influenced by the dominant macrofaunal taxa through physical disturbance by the burrowing activities of thalassinid shrimp and direct predation. The negative influence of bioturbation by the thalassinid shrimp *Callianassa* on nematode communities was reported by Alongi (1986) on the Great Barrier Reef, where he found reduced densities of nematodes associated with high densities of *Callianassa* burrows.

The meiofaunal communities at the 180 m – 300 m sites had higher taxonomic richness than the other transect sites but the abundances were similar to the 90 m – 140 m sites. These offshore transect sites had nearly equal proportion of nematodes and copepods. The higher abundance of copepods and of many typically interstitial phyla might have been due to the larger median grain size and higher sorting coefficient of the sediments, resulting in more interstitial space between sediment grains to support meiofaunal diversity.

The meiofaunal community at the Danlum Bay reference site had a relatively low number of taxa and abundance and grouped with the 0 m vent site in terms of its species similarity. This site was unique in the strong dominance of copepods, which accounted for 47% of the relative abundance. Copepods are typically more abundant in coarser, well oxygenated sediments, or associated with phytal habitats (Hicks and Coull, 1983), so their dominance at the Danlum Bay site is enigmatic and may be an artifact of the low overall meiofaunal abundance at this site.

## **5.5 Summary and conclusions**

The meiofaunal communities in Tutum Bay and at the Danlum Bay reference site reflect the complex interactions among the physical and biological components of the system. The meiofauna were most strongly correlated with pore water characteristics such as temperature and salinity as well as with the sediment parameters such as organic content and median grain size. Biological interactions with the macrofaunal community also may play an important role in structuring the meiofaunal community, especially at sites where high densities of thalassinid shrimp rework the sediments.



## Chapter Six

### **Molecular diversity of eukaryotic and bacterial communities associated with the shallow-water hydrothermal vent at Ambitle Island, Papua New Guinea**

#### **6.1 Introduction**

Molecular methods have been used for a number of years to measure bacterial diversity and over the last decade have been used increasingly more to measure micro-eukaryotic diversity in different environments such as soils (Wu *et al.* 2009). In the marine environment, molecular surveys of eukaryotic diversity have focused on extreme habitats such as anoxic and sulfide environments (Dawson and Pace 2002, Stoeck and Epstein 2003, Behnke *et al.* 2006, Takishita *et al.* 2007a), deep-sea hydrothermal vents (Atkins *et al.* 2000, Edgcomb *et al.* 2002, López-García *et al.* 2003, 2007, Takishita *et al.* 2005, Le Calvez *et al.* 2009), and deep-sea methane cold seeps (Takishita *et al.* 2007b and 2010). One common finding in molecular surveys is the unexpectedly high diversity of eukaryotic groups and the discovery of new lineages. Examples include early molecular surveys of marine picoplankton (López-García *et al.* 2001, Moon-van der Staay *et al.* 2001) which found high diversities of previously unknown taxa in samples collected from Antarctica and the equatorial Pacific respectively, and a global survey of the protozoan phylum Cercozoa (Bass and Cavalier-Smith 2004). Despite the high diversity discovered in these studies, molecular methods tend to underestimate the actual diversity believed to be present in the habitat (Potvin and Lovejoy 2009).

Molecular analysis of 18S and 16S rDNA was employed in this study in order to

describe the composition of the sediment microeukaryotic and bacterial communities along the hydrothermal gradient at Tutum Bay. Additionally, I wanted to evaluate the effectiveness of using molecular methods as a measure of meiofaunal diversity in comparison to traditional techniques by focusing on the metazoan component of the eukaryotic analysis. The results of this comparison will be presented in Chapter 7.

## **6.2 Material and methods**

### **6.2.1 Sampling design and field collection**

Sampling and analysis methods for pore water and sediment samples collected at the transect sites and the Danlum Bay reference site are given in Chapter 2.

Sediment samples for meiofaunal community analysis were collected at the nine transect sites and at the Danlum Bay reference site as described in Chapter 2.

Sediment samples for DNA extractions were collected from a random grid in each of the five quadrats at each site using a 60cc syringe coring tube (diameter = 3cm).

Sediment cores were collected to a depth of 5 cm. The five sediment cores from each site were pooled into a single sample and sieved through a 500  $\mu\text{m}$  mesh screen onto a 50  $\mu\text{m}$  mesh plankton netting to remove macrofauna and retain meiofaunal sized organisms.

Seawater used for sieving and rinsing the samples was filtered through a 50  $\mu\text{m}$  plankton net to remove any planktonic organisms and prevent possible contamination of the samples. The retained sediment was split into three aliquots, two of which were kept frozen and the third was preserved in 95% ETOH. The frozen samples were hand carried back to the United States and stored at  $-80^{\circ}\text{C}$  upon return to USF.

## 6.2.2 DNA extraction and amplification

Sediment DNA was extracted from a 0.5g subsample from each site using a MoBio UltraClean Soil DNA isolation kit following the alternate protocol for maximum yield with the following modification: Step # 15 of the protocol was repeated one extra time. The 18S rDNA fraction of the extracted sediment DNA was PCR amplified using 18S4 and 18S5 primers following the following PCR mixture:

5.00 $\mu$ l	10x buffer
1.00 $\mu$ l	dXTPs
0.50 $\mu$ l	Taq
1.25 $\mu$ l	18S4 Primer
1.25 $\mu$ l	18S5 Primer
2.00 $\mu$ l	MgCl <sub>2</sub>
2.00 $\mu$ l	extracted sediment DNA
37.00 $\mu$ l	ultrapure H <sub>2</sub> O
<hr/>	
50.00 $\mu$ l	Total PCR reaction mix

18S4: 5'-CCGGAATTCAAGCTTGCTTGCTTGTCTCAAAGATTAAGCC-3'

18S5: 5'-CCGGAATTCAAGCTTACCATACTCCCCCGGAACC-3'

The PCR reaction was cycle sequenced using the following reaction: 95°C denaturing for 15 seconds, 50°C annealing for 1 minute, 72°C polymerization for 1 minute x 45 cycles followed by 72°C extension for 7 minutes (Figure 6.1).

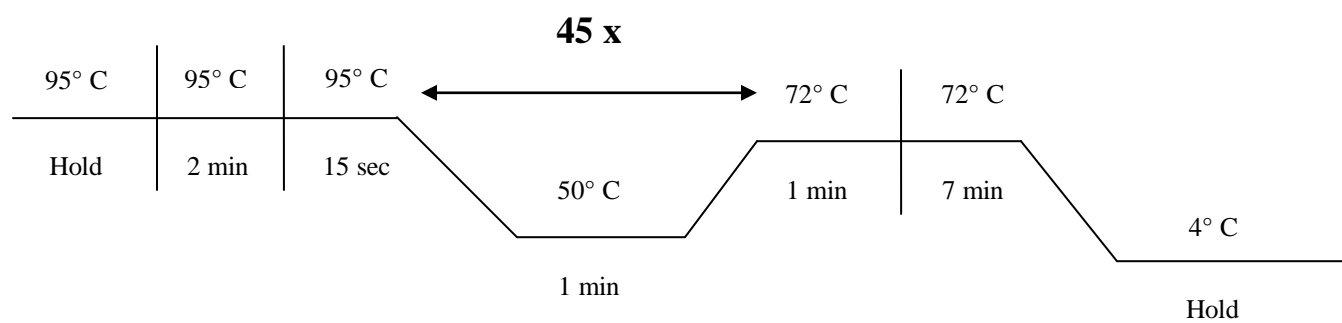


**Figure 6.1 Cyclesequencing reaction for eukaryotic 18S gene amplification.**

A 45 µl subsample of the final PCR product was used for gel purification of the 18S rDNA using a Qiagen Gel Extraction Kit. The purified PCR product (4 µl) was cloned into TOPO<sup>®</sup> cloning vector and transformed into chemically competent TOP10 strain *E. coli* using an Invitrogen TOPO Cloning Kit. Clones were minipreped in 96 well plates using the Eppendorf Perfectprep Plasmid 96 Vac miniprep kit.

The final sequencing was done by Polymorphic DNA Technologies, Inc. (Alameda, CA). Final 18S sequences were trimmed to a final length of 576 bp around the 18S6 region (150 bp before, and 400 bp after) using ANCHOR software (Garey Lab proprietary software). Operational Taxonomic Units (OTUs) were assembled based on 99% sequence similarity using SEQUENCHER 4.7 (Gene Codes, Ann Arbor, MI). The assembled OTU sequences were BLAST searched against the NCBI database (GENBANK) for tentative taxonomic and phylogenetic identifications.

Sediment samples for bacterial community analysis using 16S r-DNA were collected at selected sites along the transect. Results and community analysis are presented here for comparison with the eukaryotic sequence trends along the transect. The DNA was extracted from approximately 1 gram of sediment sample using the MoBio UltraClean Soil DNA isolation kit protocols. PCR amplification of the 16S rDNA was done using primers 27F (5' - AGA GTT TGA TCC TGG CTC AG - 3') and 1492R (5' - GGT TAC CTT CTT ACG ACT T - 3') and using the following thermocycling procedure: 95°C denaturing for 15 seconds, 45°C annealing for 1 minute, 72°C polymerization for 2 minutes x 40 cycles followed by 72°C extension for 7 minutes (Figure 6.2).

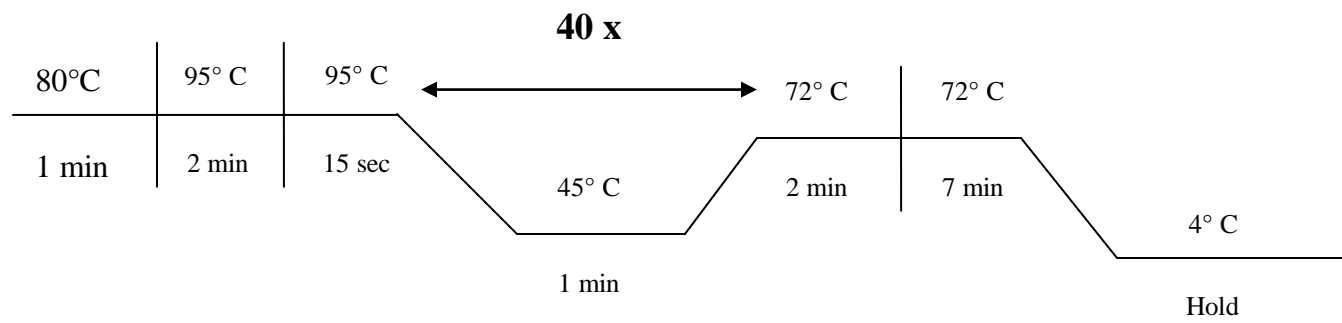


**Figure 6.2 Cyclesequencing reaction for bacterial 16S gene amplification.**

The purified PCR product was transformed using an Invitrogen TOPO Cloning Kit and clones were minipreped in 96 well plates using the Eppendorf Perfectprep Plasmid 96 Vac miniprep kit as described for the 18S r-DNA methods. The final sequencing was done by Polymorphic DNA Technologies, Inc. (Alameda, CA). Operational Taxonomic Units (OTUs) were assembled based on 97% sequence similarity using SEQUENCHER 4.7 (Gene Codes, Ann Arbor, MI). The assembled OTU sequences were BLAST searched against the NCBI database (GENBANK) for tentative taxonomic and phylogenetic identifications.

### **6.3 Results**

A total of 3,840 eukaryotic sequences were initially obtained from all ten sites. After trimming to the final 576 bp sequence length, 3,004 sequences remained which were assembled into 971 OTUs based on 99% sequence similarity. The dataset was further reduced by removing questionable or non-target sequences (i.e. cloning vector, terrestrial organisms, vertebrate sequences) after BLAST searching the GENBANK database, leaving a final dataset of 2,987 sequences and 923 OTUs. The number of useable sequences obtained per site was variable and ranged from 224 to 362 at 120 m and 0 m respectively (Figure 6.3). The number of OTUs per site was also variable, ranging from 68 at the 60 m site to 144 at the 250 m site (Figure 6.4). There was no significant correlation between the number of sequences and corresponding number of OTUs ( $R^2 = 0.174$ ) as shown in the linear regression analysis (Figure 6.5).

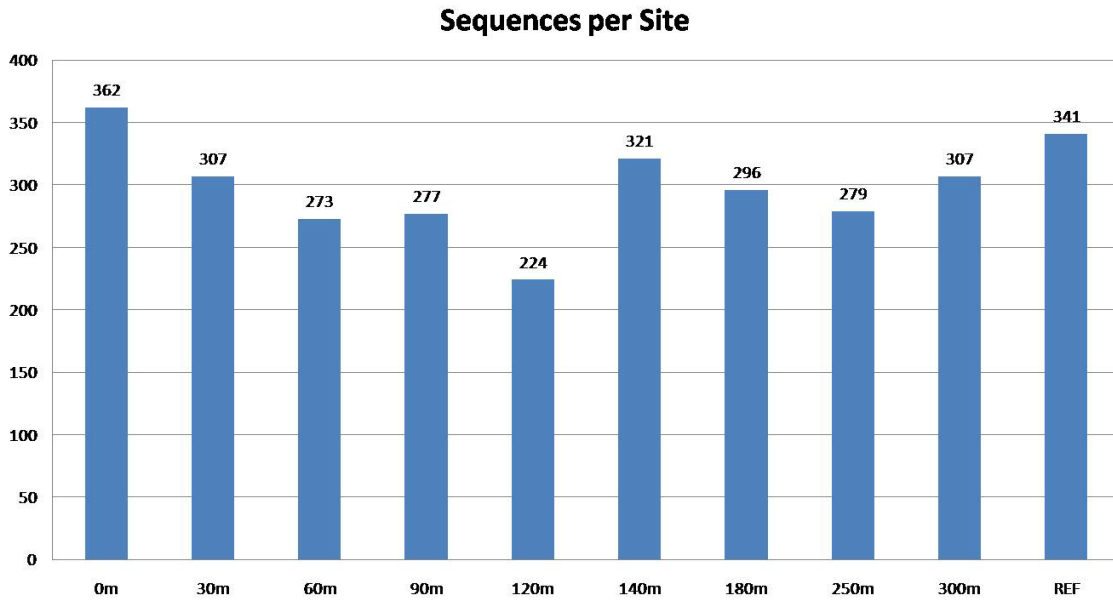


**Figure 6.3 Ambitle Island May/June 2005: Number of eukaryotic sequences obtained per site.**

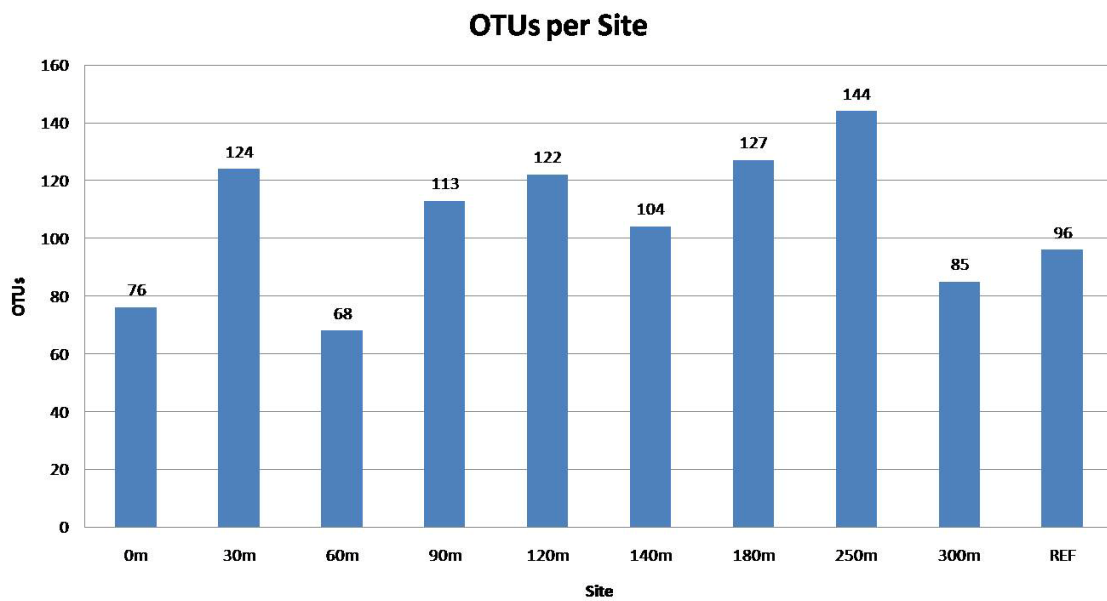


**Figure 6.4 Ambitle Island May/June 2005: Number of eukaryote operational taxonomic units (OTUs) obtained per site.**



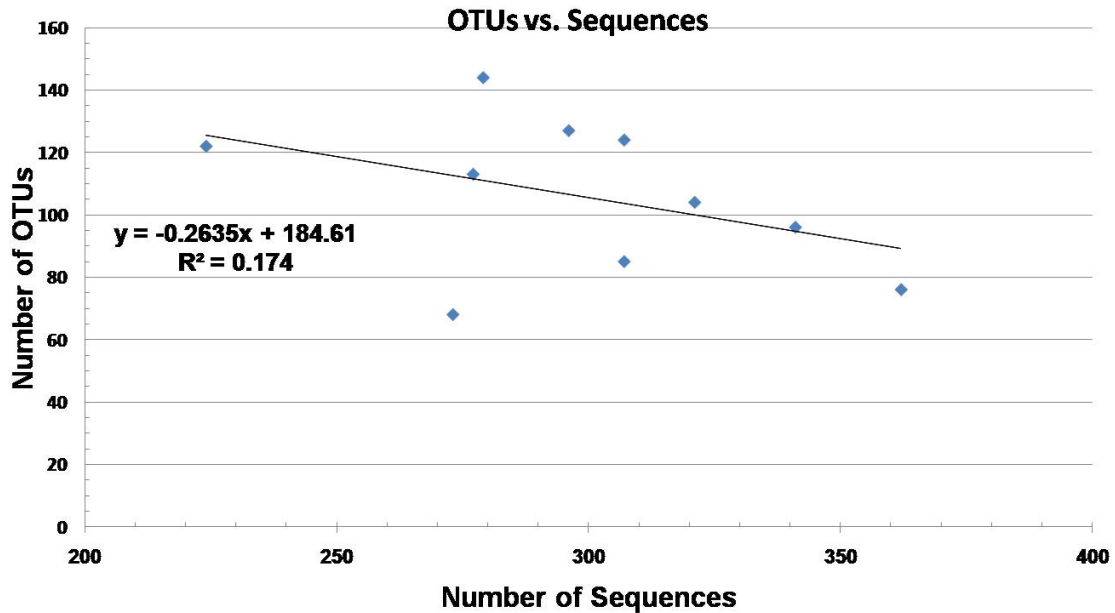


**Figure 6.5 Linear regression analysis of OTUs vs. number of sequences.**

Metazoans were represented by 35% of the overall sequences, followed by Fungi (30%), and Stramenopiles (17%). “Uncultured Eukaryota” from environmental sequences and Alveolata each comprised 7% of the total sequences (Figure 6.6). The sequence composition at each site was variable, with Metazoans comprising over half of the sequences at the 0 m site as well as at the 250 m and 300 m sites (Figure 6.7) while Fungi accounted for the majority of sequences at the 120 m and the reference sites and Stramenopile sequences were prevalent at 30 m and Alveolates at 180 m (Figure 6.7).

Metazoans comprised the largest fraction of the OTUs (30%), followed by the Fungi and Stramenopiles (Figure 6.8). The OTU composition was dominated by metazoans at the 0 m site as well as at 140 m, 180 m, 250 m and 300 m. Fungi OTUs were dominate at 120 m and at the reference site and Stramenopiles comprised the largest percentage of OTUs at the 30 m, 60 m and 90 m sites (Figure 6.9).

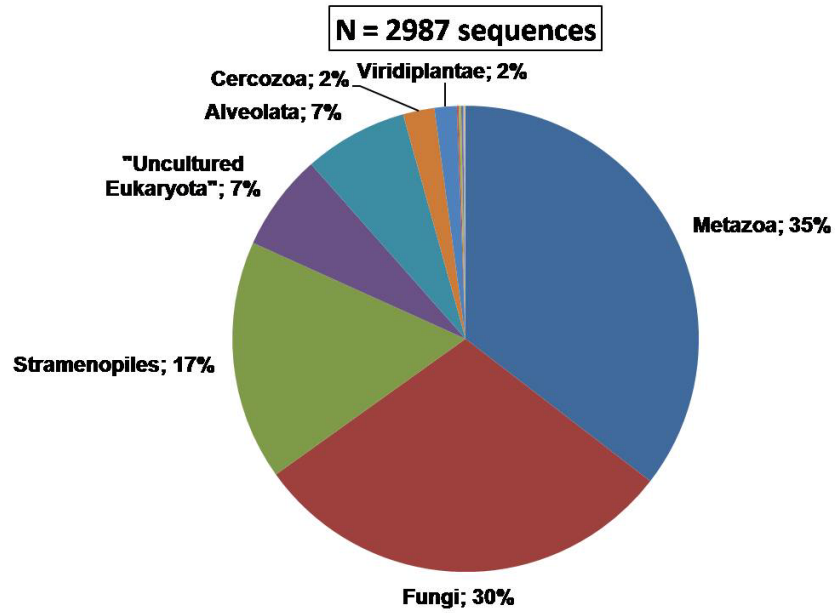


Figure 6.6 Ambitle Island May/June 2005: Percentage of eukaryote sequences by kingdom level taxonomic category for all sites combined.

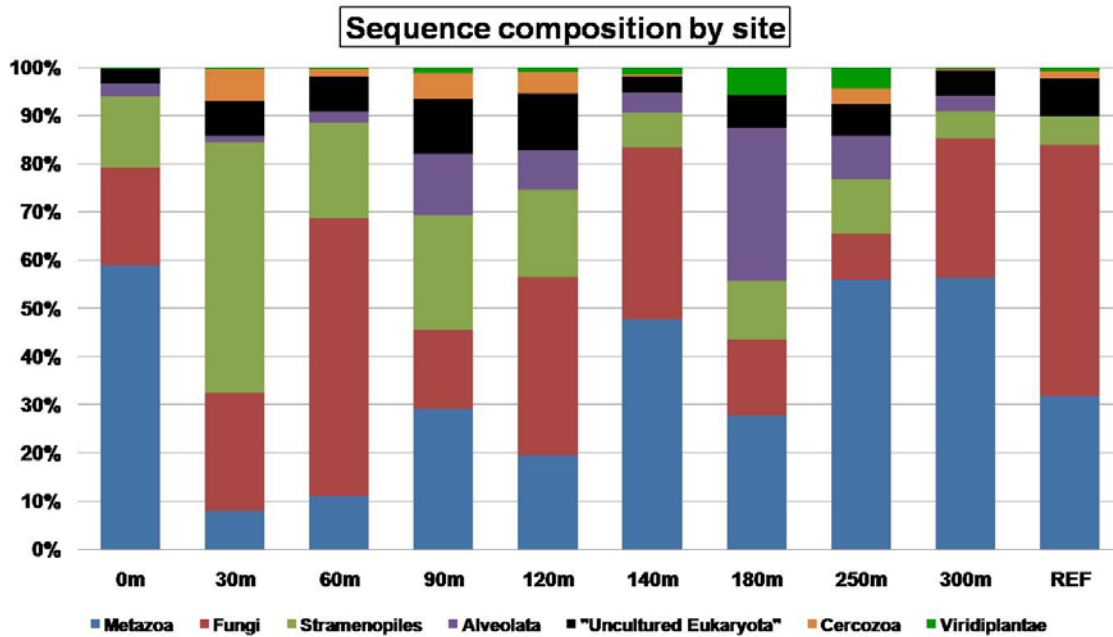


Figure 6.7 Ambitle Island May/June 2005: Percentage of eukaryote sequences by kingdom level taxonomic category at each site.

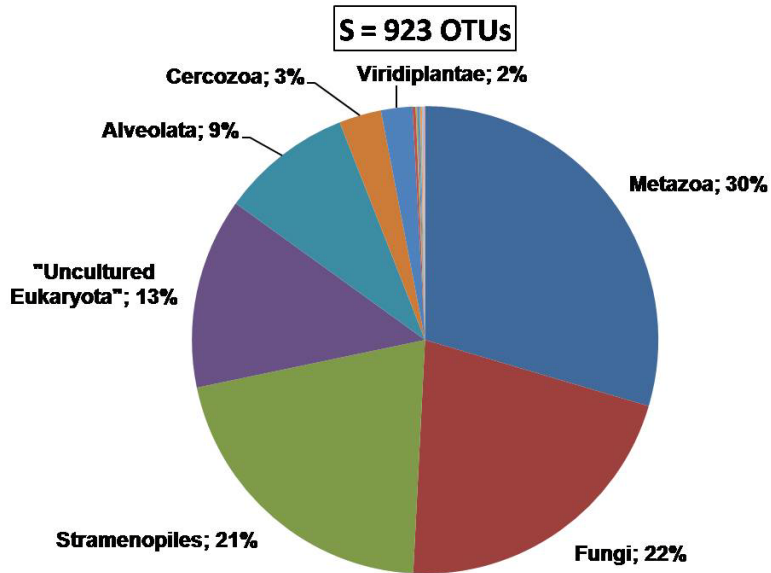


Figure 6.8 Ambitle Island May/June 2005: Percentage of eukaryote OTUs by kingdom level taxonomic category for all sites combined.

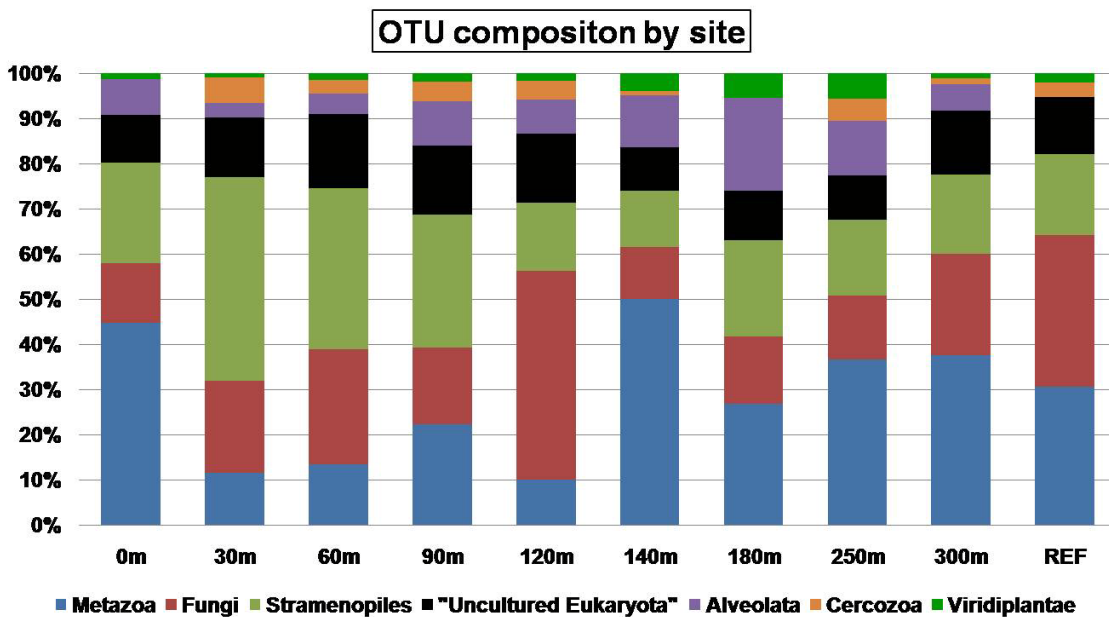


Figure 6.9 Ambitle Island May/June 2005: Percentage of eukaryote sequences by kingdom level taxonomic category at each site.

Thirty-three OTUs (3.6%) accounted for 50% of the sequences, with the top four ranked OTUs making up 25% of the sequences (Table 6.1). The majority of OTUs were found at only one site (851; 92.2%) and 72.3% (667) of the OTUs were represented by a single sequence. The most abundant OTU was Contig [0002] identified as the fungus *Paecilomyces* sp. (GENBANK Accession # DQ401104). This OTU comprised over 12% of the total sequences and was present at 8 of the 10 sites. This OTU was absent at 0 m and 90 m and most abundant at 60 m where it accounted for 50% of the sequences at that site. Other top-ranked OTUs were provisionally identified as the fungus *Cladosporium cladosporioides* (Contig [0008]; GENBANK Accession # EF114717), the nematode *Viscosia viscosa* (AY854198; Contig [0006]), and the bivalve mollusk *Astarte castanea* (AF120551; Contig [0001]).

No OTUs were present at all ten sites. The most frequently occurring OTUs were the fungi *Paecilomyces* sp. (Contig [0002]) and *Penicillium chrysogenum* (Contig [0013]), each present at eight sites (Table 6.1), while *Cladosporium cladosporioides* (Contig [0008]) was present at seven sites (Table 6.1). Cumulatively these three OTUs accounted for over 20% of the sequences.

Additionally, seven OTUs were found at five of the ten sites. These included two OTUs (Contigs [0644] and [0541]) which were also identified as *Paecilomyces* sp. Three were identified as stamenopiles, including two as the same “unclassified” diatom (Contigs [0172] and [0235]; GENBANK Accession number AB18359) and the third (Contig 0184) as the oomycotes *Phytophthora infestans* (Accession number AY742744). The remaining two OTUs were Contig [0042] identified as the nematode

*Chromadorita tentabundum* (AY854208) and Contig[0074], identified as the chlorophyte *Cladophora glomerata*, (AB062706).

The 0 m site had a total of 362 sequences in 76 OTUs. Metazoans dominated both the number of sequences (213; 59%) and the OTUs (34; 45%). Six OTUs accounted for >50% of the sequences at the 0 m site (Table 6.2). The top two OTUs were both metazoans: Contig[0058] was identified as the nematode *Viscosia viscosa* (AY854198) and comprised 14% of the sequences and Contig[0066] which was identified as the polychaete *Capitella capitata* (U67323). These two taxa accounted for > 25% of the eukaryotic sequences at the 0 m site.

There were 307 sequences representing 124 OTUs at the 30 m site. Fifteen OTUs accounted for >50% of the sequences. Stramenopiles were dominant in both the number of sequences and OTUs comprising 52% and 44% respectively. The top two OTUs were Contig[0068] identified as the diatom *Pauliella toeniata* (AY485528) and Contig[0002] identified as the fungus *Paecilomyces* sp. 080834, (DQ401104). These two OTUs comprised nearly 24% of the total sequences at the 30 m site (Table 6.2).

The 60 m site had a total of 273 sequences and had the fewest OTUs with 68. Fungi comprised 58% of the sequences, while Stramenopiles had the largest percentage of OTUs (35%). A single OTU, the fungus *Paecilomyces* sp. (Contig[0002]) dominated the site, accounting for over 50% of the sequences (Table 6.2).

The 90 m site had a total of 277 sequences and 113 OTUs. Metazoans comprised the largest proportion of the sequences (29%) while Stramenopiles made up the largest percentage of OTUs (29.2%). A total of 21 OTUs accounted for >50% of the sequences.

The dominant OTU was Contig[0042] identified as the nematode *Chromadorita tentabundum* (AY854208) which accounted for 8.3% of the sequences (Table 6.2).

The 120 m site had the fewest amplified sequences with 224 and a total of 122 OTUs. Fungi dominated both the number of sequences (37%) and accounted for 45% of the OTUs. Twenty-five OTUs made up >50% of the sequences. Two OTUs tied as the top ranked taxon each accounting for 7.6% of the sequences (Table 6.2). These were Contig[0002] identified as the fungus *Paecilomyces* sp. (DQ401104) and Contig[0010] identified as the acoel flat worm *Pseudaphanostoma smithrii* (AY078375).

The 140 m site had a total of 321 sequences and 104 OTUs. Metazoans made up the largest percentage of sequences (47.7%) and accounted for half of the OTUs. Three OTUs accounted for over 50% of the sequences. The top ranked OTU was the fungus *Paecilomyces* sp. (Contig [0002]) which comprised nearly 30% of the sequences. The other two top ranked OTUs were Contig [0006] identified as the nematode *Viscosia viscosa* (AY854198) and Contig [0001] identified as a bivalve mollusk (*Astarte castanea* AF120551). These comprised 15.9% and 10.9% of the sequences respectively (Table 6.2).

There were 296 sequences and 127 OTUs at the 180 m site. The sequences were dominated by Alveolates (31.8%), while Metazoans comprised 26.8% of the OTUs. Fourteen OTUs accounted for >50% of the sequences. The top ranked OTU was Contig [0054] identified as the ciliate *Strombidinopsis acuminata* (AJ877014) and incorporated 14.2% of the sequences (Table 6.2).

The 250 m site had 279 sequences and the most OTUs of the ten sites, with 144. Metazoans dominated both the number of sequences (55.2%) and OTUs (36.1%).

Fourteen OTUs accounted for >50% of the sequences. The top ranked OTU was Contig [0006], identified as the nematode *Viscosia viscosa* (AY854198), which comprised 28.7% of the sequences (Table 6.2).

The 300 m site had 307 sequences and 85 OTUs. Metazoans made up 56.4% of the sequences and 37.7% of the OTUs. Three taxa accounted for >50% of the sequences, with Contig [0002] – *Paecilomyces* sp. (DQ401104) being the most abundant with 22.80% of the sequences). Contig [0001], identified as the bivalve mollusk *Astarte castanea* (AF120551) and Contig [0107], identified as the turbellarian flatworm *Schizorhynchoides caniculatus* (AY775748) ranked second and third comprising 17.3% and 11.7% of the sequences respectively (Table 6.2).

The reference site had 341 sequences and 96 OTUs. Fungi dominated the site comprising 51.3% of the sequences and 33.3% of the OTUs. Three OTUs accounted for >50% of the sequences. The most abundant OTU was Contig [0008] identified as the fungus *Cladosporium cladosporioides* (EF114717) and comprising 31.4% of the sequences. Contig [0018], identified as a polychaete annelid worm (*Amphicorina mobilis*, AY611449), ranked second and had 13.2% of the sequences. The third most abundant OTU was Contig [0013] identified as the fungus *Penicillium chrysogenum* (EU203859) and accounted for 8.50% of the sequences (Table 6.2).

**Table 6.1 Ranked OTUs representing 50% of the 2,987 total sequences. OTUs ranked by percent abundance and then by number of sites at which they occur. Tied ranks indicated by an asterisk.**

Rank	Sequence	BLAST ID	Accession #	Kingdom	Phylum	Percent	Cumulative	Sites
1	Contig[0002]	Paecilomyces sp. 080834	DQ401104	Fungi	Dikarya	12.06%	12.06%	8
2	Contig[0008]	Cladosporium cladosporioides	EF114717	Fungi	Dikarya	5.76%	17.82%	7
3	Contig[0006]	Viscosia viscosa	AY854198	Metazoa	Nematoda	5.10%	22.92%	3
4	Contig[0001]	Astarte castanea	AF120551	Metazoa	Mollusca	3.20%	26.12%	4
5	Contig[0013]	Penicillium chrysogenum	EU203859	Fungi	Dikarya	2.33%	28.45%	8
6	Contig[0058]	Viscosia viscosa	AY854198	Metazoa	Nematoda	1.67%	30.11%	1
7	Contig[0107]	Schizorhynchoides caniculatus	AY775748	Metazoa	Platyhelminthes	1.57%	31.68%	3
8	Contig[0042]	Chromadorita tentabundum	AY854208	Metazoa	Nematoda	1.53%	33.21%	5
9	Contig[0066]	Capitella capitata	U67323	Metazoa	Annelida	1.53%	34.74%	1
10	Contig[0018]	Amphicorina mobilis	AY611449	Metazoa	Annelida	1.50%	36.24%	1
11	Contig[0068]	Pauliella toeniata	AY485528	Stramenopiles	Bacillariophyta	1.43%	37.67%	2
12	Contig[0054]	Strombidinopsis acuminata	AJ877014	Alveolata	Ciliophora	1.40%	39.07%	1
13	Contig[0003]	Cheliplana cf. orthocirra	AJ012507	Metazoa	Platyhelminthes	0.93%	40.01%	1
14	Contig[0059]	Cheliplana cf. orthocirra	AJ012507	Metazoa	Platyhelminthes	0.70%	40.71%	3
15	Contig[0056]	Parodontophora sp. PB-2005	AM234630	Metazoa	Nematoda	0.70%	41.41%	1
16	Contig[0644]	Paecilomyces sp. 080834	DQ401104	Fungi	Dikarya	0.63%	42.04%	5
17	Contig[0541]	Paecilomyces sp. 080834	DQ401104	Fungi	Dikarya	0.57%	42.60%	5
18	Contig[0116]	uncultured alveolate	AF372785	Alveolata	Alveolata	0.57%	43.17%	4
19	Contig[0010]	Pseudaphanostoma smithii	AY078375	Metazoa	Platyhelminthes	0.57%	43.74%	1
20*	Contig[0015]	uncultured cercozoan	AY620357	Cercozoa	Cercozoa	0.53%	44.27%	4
20*	Contig[0046]	Navicula ramosissima	AY485512	Stramenopiles	Bacillariophyta	0.53%	44.80%	4
21	Contig[0189]	Haliphthoros sp. NJM 0034	AB178865	Stramenopiles	Oomycetes	0.50%	45.30%	4
22	Contig[0175]	Atolla vanhoeffeni	AF100942	Metazoa	Cnidaria	0.50%	45.80%	1
23	Contig[0027]	Navicula sp. CCMP2746	EF106790	Stramenopiles	Bacillariophyta	0.47%	46.27%	4
24	Contig[0016]	Strombidium sp. SNB99-2	AY143564	Alveolata	Ciliophora	0.47%	46.74%	1
25	Contig[0074]	Cladophora glomerata	AB062706	Viridiplantae	Chlorophyta	0.43%	47.17%	5
26*	Contig[0113]	Pseudechiniscus islandicus	AY582119	Metazoa	Tardigrada	0.43%	47.60%	1
26*	Contig[0557]	Strombidinopsis acuminata	AJ877014	Alveolata	Ciliophora	0.43%	48.03%	1
27	Contig[0112]	Pseudechiniscus islandicus	AY582119	Metazoa	Tardigrada	0.40%	48.43%	3
28	Contig[0060]	Schizosaccharomyces japonicus	AB243296	Fungi	Dikarya	0.40%	48.83%	2
29*	Contig[0011]	Exophiala salmonis	EF413608	Fungi	Dikarya	0.40%	49.23%	1
29*	Contig[0367]	Cheliplana cf. orthocirra	AJ012507	Metazoa	Platyhelminthes	0.40%	49.63%	1
30	Contig[0439]	Diascorhynchus rubrus	AJ012508	Metazoa	Platyhelminthes	0.37%	50.00%	2



**Table 6.2 Relative abundance the top five ranked OTUs (including ties) at each site**

0 m				30 m			
OTU	BLAST ID	Accession #	%	OTU	BLAST ID	Accession #	%
Contig[0058]	<i>Viscosia viscosa</i>	AY854198	13.81%	Contig[0068]	<i>Pauliella toeniata</i>	AY485528	12.38%
Contig[0066]	<i>Capitella capitata</i>	U67323	12.71%	Contig[0002]	<i>Paecilomyces</i> sp. 080834	DQ401104	11.40%
Contig[0008]	<i>Cladosporium cladosporioides</i>	EF114717	10.22%	Contig[0215]	<i>Dickieia ulvacea</i>	AY485462	2.61%
Contig[0056]	<i>Parodontophora</i> sp. PB-2005	AM234630	5.80%	Contig[0081]	<i>Protaspis grandis</i>	DQ303924	2.61%
Contig[0013]	<i>Penicillium chrysogenum</i>	EU203859	5.80%	Contig[0585]	<i>Pauliella toeniata</i>	AY485528	2.28%
Contig[0175]	<i>Atolla vanhoeffeni</i>	AF100942	4.14%	Contig[0686]	<i>Pauliella toeniata</i>	AY485528	2.28%
				Contig[0541]	<i>Paecilomyces</i> sp. 080834	DQ401104	2.28%
				Contig[0644]	<i>Paecilomyces</i> sp. 080834	DQ401104	2.28%
				Contig[0027]	<i>Navicula</i> sp. CCMP2746	EF106790	2.28%
				Contig[0015]	uncultured cercozoan	AY620357	1.95%

**Table 6.2 Continued**

60 m				90 m			
OTU	BLAST ID	Accession #	%	OTU	BLAST ID	Accession #	%
Contig[0002]	<i>Paecilomyces</i> sp. 080834	DQ401104	50.92%	Contig[0042]	<i>Chromadorita tentabundum</i>	AY854208	8.30%
Contig[0042]	<i>Chromadorita tentabundum</i>	AY854208	4.03%	Contig[0016]	<i>Strombidium</i> sp. SNB99-2	AY143564	5.05%
Contig[0189]	<i>Haliphthoros</i> sp. NJM 0034	AB178865	2.20%	Contig[0060]	<i>Schizosaccharomyces japonicus</i>	AB243296	3.61%
Contig[0119]	<i>Montastraea annularis</i>	AF238267	2.20%	Contig[0222]	<i>Pseudaphanostoma smithrii</i>	AY078375	3.25%
Contig[0112]	<i>Pseudechiniscus islandicus</i>	AY582119	2.20%	Contig[0046]	<i>Navicula ramosissima</i>	AY485512	2.89%
Contig[0055]	Uncultured stramenopile clone CCI6	AY179998	1.83%				
Contig[0068]	<i>Pauliella toeniata</i>	AY485528	1.83%				
Contig[0203]	<i>Amphidinium</i> sp. PEL-2	AB092335	1.47%				
Contig[0328]	Uncultured eukaryotic picoplankton clone VN3	DQ409093	1.47%				

**Table 6.2 Continued.**

120 m				140 m			
OTU	BLAST ID	Accession #	%	OTU	BLAST ID	Accession #	%
Contig[0010]	<i>Pseudaphanostoma smithii</i>	AY078375	7.59%	Contig[0002]	<i>Paecilomyces</i> sp. 080834	DQ401104	29.91%
Contig[0002]	<i>Paecilomyces</i> sp. 080834	DQ401104	7.59%	Contig[0006]	<i>Viscosia viscosa</i>	AY854198	15.89%
Contig[0023]	<i>Apodachlya brachynema</i>	AJ238663	2.68%	Contig[0001]	<i>Astarte castanea</i>	AF120551	10.90%
Contig[0046]	<i>Navicula ramosissima</i>	AY485512	2.68%	Contig[0107]	<i>Schizorhynchoides caniculatus</i>	AY775748	3.12%
Contig[0013]	<i>Penicillium chrysogenum</i>	EU203859	2.68%	Contig[0644]	<i>Paecilomyces</i> sp. 080834	DQ401104	2.49%
Contig[0541]	<i>Paecilomyces</i> sp. 080834	DQ401104	2.23%				
Contig[0229]	<i>Bacillariophyta</i> sp. MBIC10102	AB183593	1.79%				
Contig[0001]	<i>Astarte castanea</i>	AF120551	1.79%				
Contig[0116]	uncultured alveolate	AF372785	1.79%				
Contig[0117]	<i>Gammarus duebeni</i>	AF419227	1.79%				
Contig[0416]	uncultured alveolate	AF530536	1.79%				
Contig[0112]	<i>Pseudechiniscus islandicus</i>	AY582119	1.79%				
Contig[0139]	<i>Xenotrichula</i> sp. aff. <i>Velox</i>	AY963686	1.79%				
Contig[0251]	Uncultured eukaryote clone D1P02C04	EF100195	1.79%				
Contig[0189]	<i>Haliphthoros</i> sp. NJM 0034	AB178865	1.34%				

**Table 6.2 Continued**

180 m				250 m			
OTU	BLAST ID	Accession #	%	OTU	BLAST ID	Accession #	%
Contig[0054]	<i>Strombidinopsis acuminata</i>	AJ877014	14.19%	Contig[0006]	<i>Viscosia viscosa</i>	AY854198	28.67%
Contig[0008]	<i>Cladosporium cladosporioides</i>	EF114717	5.74%	Contig[0115]	<i>Thalassarachna basteri</i>	AY692342	2.51%
Contig[0557]	<i>Strombidinopsis acuminata</i>	AJ877014	4.39%	Contig[0606]	<i>Neochromadora BHMM-2005</i>	AY854210	2.51%
Contig[0113]	<i>Pseudechiniscus islandicus</i>	AY582119	4.39%	Contig[0087]	<i>Leptolaimus</i> sp. LeLaSpl	EF591323	2.51%
Contig[0011]	<i>Exophiala salmonis</i>	EF413608	4.05%	Contig[0093]	<i>Trichosporon porosum</i>	AB051045	2.15%
Contig[0012]	<i>Bradya</i> sp. Greenland-RJH-2004	AY627016	3.04%	Contig[0110]	<i>Chromadorita tentabundum</i>	AY854208	1.79%
				Contig[0075]	<i>Gymnodinium dorsalisulcum</i>	DQ837534	1.79%
				Contig[0711]	<i>Psammodictyon panduriforme</i>	AY485485	1.43%
				Contig[0321]	uncultured eukaryote	EU087264	1.43%
				Contig[0218]	<i>Polytoma oviforme</i>	U22936	1.43%

**Table 6.2 Continued**

300 m				Ref			
OTU	BLAST ID	Accession #	%	OTU	BLAST ID	Accession #	%
Contig[0002]	Paecilomyces sp. 080834	DQ401104	22.80%	Contig[0008]	Cladosporium cladosporioides	EF114717	31.38%
Contig[0001]	Astarte castanea	AF120551	17.26%	Contig[0018]	Amphicorina mobilis	AY611449	13.20%
Contig[0107]	Schizorhynchoides caniculatus	AY775748	11.73%	Contig[0013]	Penicillium chrysogenum	EU203859	8.50%
Contig[0006]	Viscosia viscosa	AY854198	7.17%	Contig[0003]	Cheliplana cf. orthocirra	AJ012507	8.21%
Contig[0059]	Cheliplana cf. orthocirra	AJ012507	5.86%	Contig[0099]	Uncultured marine eukaryote clone SA2_2G5	EF527173	2.64%

The non-metric multidimensional scaling analysis grouped the sites into three main eukaryotic communities based on a Bray-Curtis similarity index value of 5 (Figure 6.10a). These groups consisted of the 0 m + Reference sites, the 180 m + 250 m sites, and the six remaining sites (30 m – 140 m + 300 m). This latter grouping formed two distinct subgroups consisting of the 30 m + 60 m sites and the 140 m + 300 m sites. Leaving out the reference site from the analysis did not alter the overall site groupings (Figure 6.10b)

The SIMPER analysis revealed that the 0 m + Ref grouping was due primarily to the presence of two fungi, *Cladosporium cladosporioides* (Contig [0008]) and *Penicillium chrysogenum* (Contig[0013]). The grouping of the 180 m + 250 m sites was due in part to the presence of the fungus *Cladosporium cladosporioides* (Contig[0008]), the Chlorophytes *Polytoma oviforme* (Contig[0218]) and *Cladophora glomerata* (Contig[0074]) and a Metazoan sequence, a marine mite, *Thalassarachna basteri* (Contig[0115]). The 30 m – 140 m + 300 m grouping was due primarily to the presence of the fungus *Paecilomyces* sp. (Contig[0002]). Two additional contributing OTUs, Contig[0541] and Contig[0644], were also identified in GENBANK as *Paecilomyces* sp. (DQ401104). Two Metazoan sequences also contributed to the similarity among the sites in this group, the nematode *Chromadorita tentabundum* (Contig[0042]) and the bivalve mollusk *Astarte castanea* (Contig[0001]), as well as Contig[0184], a Stramenopile (Oomycetes) which closely matched *Phytophthora infestans* (AY742744).

The subgroup consisting of the 30 m + 60 m sites was defined by the fungus *Paecilomyces* sp. (Contig[0002]) as well as by several OTUs identified as Stramenopiles. These included sequences identified as the diatoms *Pauliella toeniata* (Contig[0068]),

*Navicula* sp. (Contig[0027]) and Bacillariophyta sp. (Contig[0172]). Other contributing OTUs included an Oomycetes closely matching *Haliphthoros* sp. NJJM0034 (AB178865; Contig[0189]) and an uncultured Stramenopile clone (AY179998; Contig[0055]) and an uncultured cercozoan (AY620357; Contig[0015]).

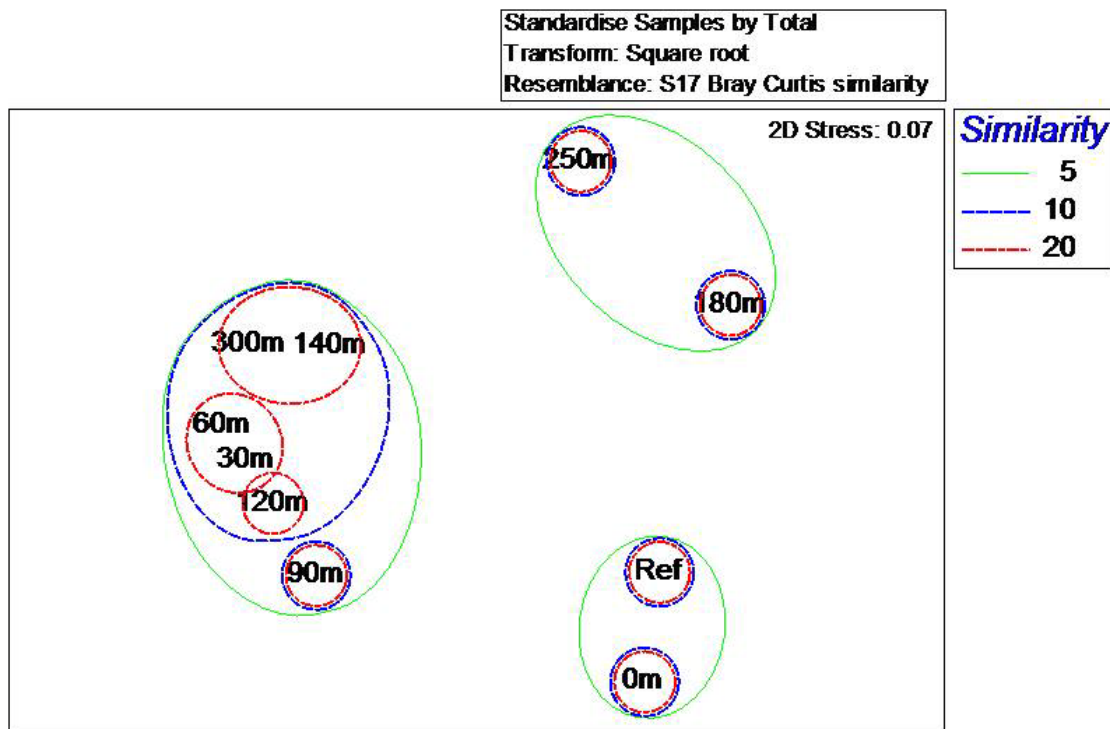


**Figure 6.10a Ambitle Island May/June 2005: Multi-Dimensional Scaling (MDS) of eukaryotic community structure based on Bray-Curtis similarity among sites.**

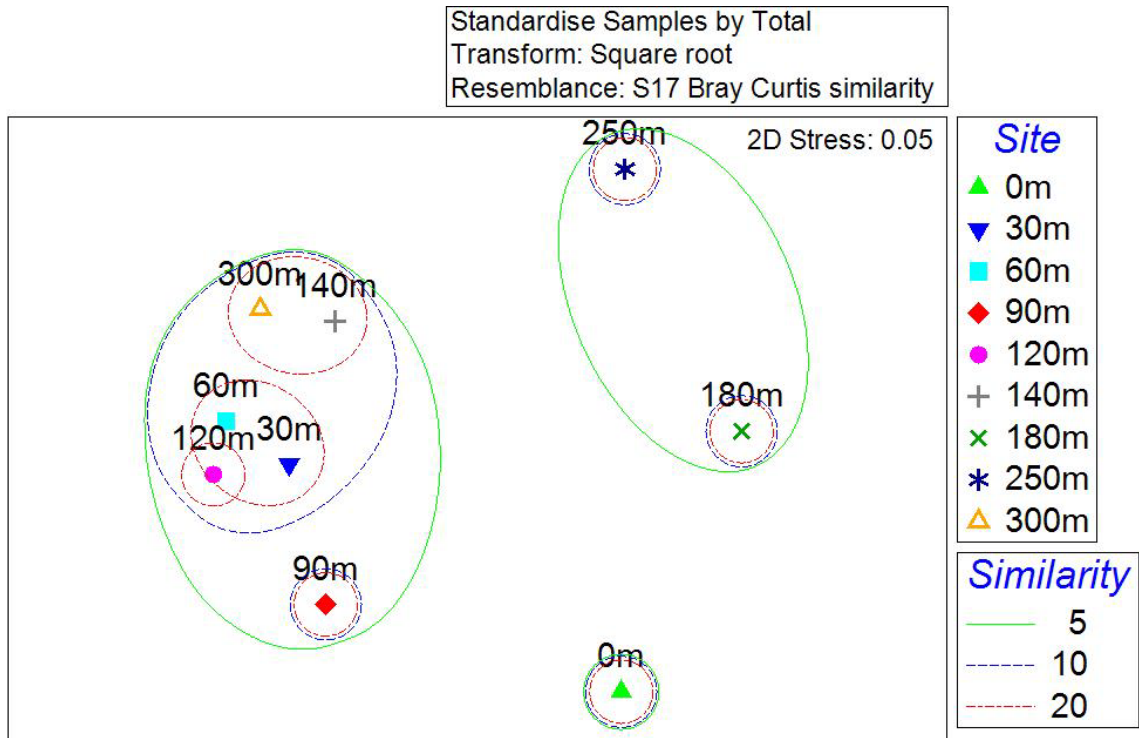


**Figure 6.10b Ambitle Island May/June 2005: Multi-Dimensional Scaling (MDS) of eukaryotic community structure based on Bray-Curtis similarity among sites; reference site omitted.**

The subgroup consisting of the 140 m + 300 m sites was defined by the fungus *Paecilomyces* sp. (Contig[0002]), the bivalve mollusk *Astarte castanea* (Contig[0001]), and the nematode *Viscosia viscosa* (Contig[0006]).

The BIO-ENV results correlating the eukaryotic molecular community structure and the physical variables are presented in Table 6.3a. The overall correlations were low, but the strongest correlation was with the combination of pore water salinity, median grain size and sorting coefficient ( $\rho = 0.447$ ). The combination of median grain size and sorting coefficient had a slightly lower correlation ( $\rho = 0.444$ ). The sediment sorting coefficient had the highest correlation for single variables ( $\rho = 0.394$ ), followed by total pore water arsenic ( $\rho = 0.358$ ), median grain size ( $\rho = 0.324$ ) and percent  $\text{CaCO}_3$  ( $\rho = 0.313$ ).

**Table 6.3a BIO-ENV correlations between eukaryotic community structure and physical parameters.**

Spearman Correlation	Parameters
0.447	Salinity, Median Grain Size, Sorting
0.444	Median Grain Size, Sorting
0.442	ORP, Total [As], %CaCO <sub>3</sub> , Median Grain Size, Sorting
0.441	Salinity, %CaCO <sub>3</sub> , Median Grain Size, Sorting
0.438	Salinity, %CaCO <sub>3</sub> , Sorting
0.437	Temperature, Median Grain Size, Sorting
0.437	ORP, Total [As], %CaCO <sub>3</sub> , Sorting
0.434	ORP, Salinity Total [As], %CaCO <sub>3</sub> , Sorting
0.433	Total [As], Sorting
0.433	Temperature, Salinity, Median Grain Size, Sorting
0.394	Sorting
0.358	Total [As]
0.324	Median Grain Size
0.313	%CaCO <sub>3</sub>
0.241	ORP
0.241	% Organics
0.190	Temperature
0.169	Salinity
0.158	pH

**Table 6.3b BIO-ENV correlations between eukaryotic community structure and physical parameters; reference site omitted.**

Spearman Correlation	Parameters
0.510	ORP, Total [As], %CaCO <sub>3</sub> , Median Grain Size, Sorting
0.508	Total [As], Sorting
0.506	ORP, Salinity, Total [As], Sorting
0.505	ORP, Total [As], Sorting
0.504	pH, ORP, Salinity, Sorting
0.504	pH, ORP, Sorting
0.504	Temperature, pH, ORP, Salinity, Sorting
0.503	pH, ORP, Salinity, Total [As], Sorting
0.502	Total [As], %CaCO <sub>3</sub> , Median Grain Size, Sorting
0.501	Temperature, ORP, Total [As], Sorting
0.457	Total [As]
0.432	Median Grain Size
0.430	Sorting
0.321	% Organics
0.310	%CaCO <sub>3</sub>
0.286	Salinity
0.283	ORP
0.277	Temperature
0.202	pH

The BIO-ENV results excluding the reference site had higher correlations between the community structure and physical parameters (Table 6.3b). The arsenic concentration had the strongest correlation ( $\rho = 0.457$ ) for a single parameter, along with median grain size ( $\rho = 0.432$ ) and sorting ( $\rho = 0.430$ ).

The LINKTREE analysis (Figure 6.11) separated the 180 m + 250 m site grouping out from the other sites at the first split of the LINKTREE (node "A"), based on differences in pore water pH, with the 180 m and 250 m sites having  $\text{pH} > 7.8$  vs.  $< 7.74$  at the other sites. The split at node B separated out the 0 m + Ref grouping from the other sites based on the oxygen-reduction potential (ORP) values, with the 0 m and reference sites having ORP values  $< 5.2$  mV while the remaining sites had  $\text{ORP} > 52$  mV. Node C separated the 90 m site based on the ORP being  $> 156$  mV vs.  $< 118$  mV and pore water salinity being  $> 34.1$  psu (vs.  $< 33.9$  psu). The final division in the LINKTREE separated the 140 m + 300 m community from the 30 m+60 m + 120 m grouping based on the pH being  $> 7.06$  ( vs.  $< 6.59$ ), the sorting coefficient  $> 0.597$  ( vs.  $< 0.449$ ), the ORP  $< 91.2$  ( vs.  $> 98.4$ ), the pore water total arsenic  $< 25.8$  ppb (vs.  $> 43.5$  ppb), pore water temperature  $< 31.5^\circ$  (vs.  $> 31.9^\circ\text{C}$ ), median grain size  $> 0.23$  mm (vs.  $< 0.198$  mm),  $\text{CaCO}_3 > 0.631\%$  (vs.  $< 0.422\%$ ) and pore water salinity  $> 31.6$  psu (vs.  $< 31.5$  psu).



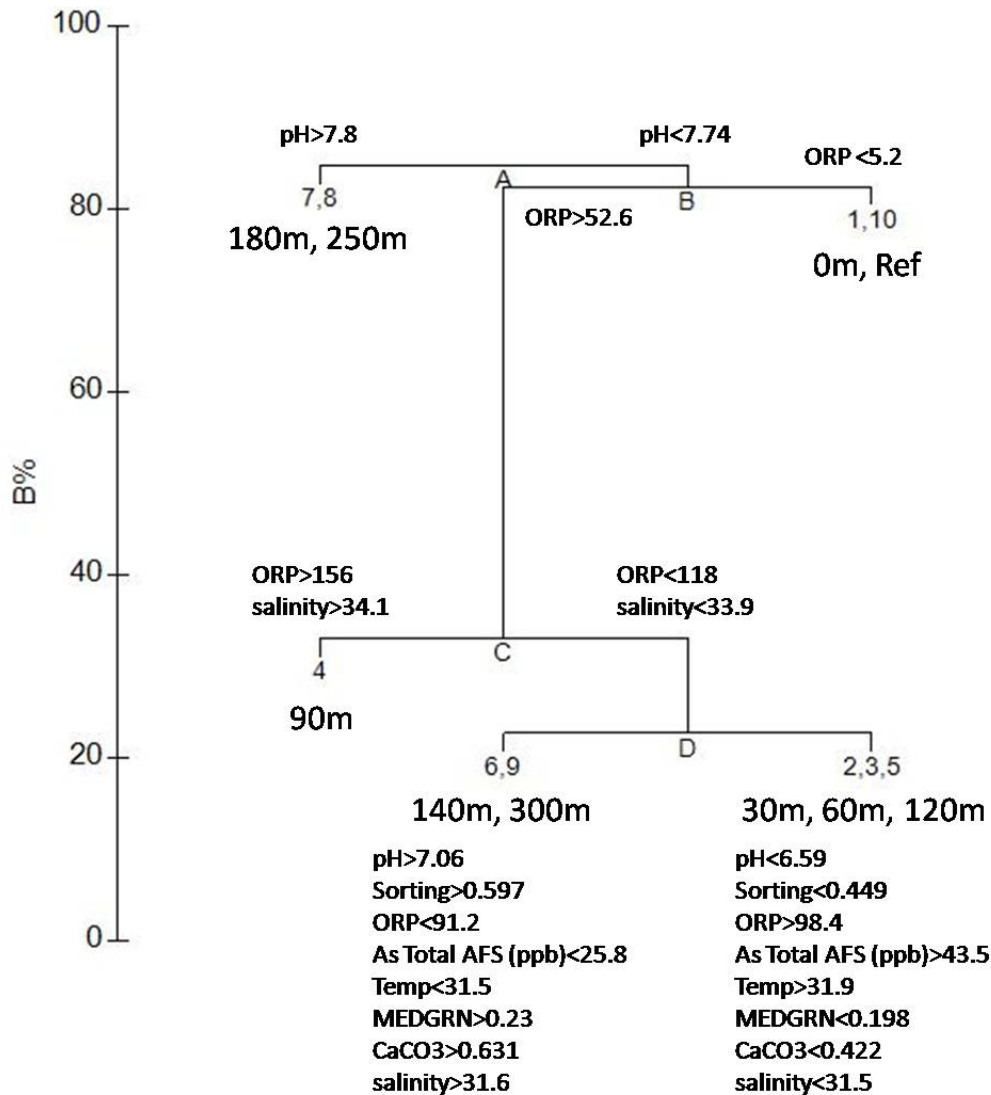


**Figure 6.11 LINKTREE results showing physical characteristics between eukaryotic community site groups.**

The analysis was reevaluated looking only at the metazoan sequences in order to better compare the molecular results with the meiofaunal and macrofaunal community analysis. There were a total of 1,059 metazoan sequences and 273 metazoan OTUs from the ten sites. Nematodes dominated both the number of sequences and OTUs followed by Platyhelminthes and Annelida (Figures 6.12 and 6.13). Ten OTUs (3.66%) accounted for >50% of the sequences (Table 6.4), while 201 OTUs (73.63%) were represented by a

single sequence. The most abundant metazoan sequence was Contig[0006] identified as the nematode *Viscosia viscosa* and comprised 14.45% of the sequences. This OTU occurred at three sites: 140 m 250 m and 300 m. Contig[0058] ranked third overall and was also matched to *Viscosia viscosa*. This OTU was only present at the 0 m site. The second ranked OTU was Contig[0001] which was identified as the bivalve mollusk *Astarte castanea* and represented over 9% of the sequences.

**Table 6.4 Top ten ranked metazoans comprising >50% of the 1,059 metazoan sequences.**

OTU	BLAST ID (Phyla)	Accession #	Percent	Cumulative	Freq
Contig[0006]	<i>Viscosia viscosa</i> (Nematoda)	AY854198	14.45%	14.45%	3
Contig[0001]	<i>Astarte castanea</i> (Mollusca)	AF120551	9.07%	23.51%	4
Contig[0058]	<i>Viscosia viscosa</i> (Nematoda)	AY854198	4.72%	28.23%	1
Contig[0107]	<i>Schizorhynchoides caniculatus</i> (Platyhelminthes)	AY775748	4.44%	32.67%	3
Contig[0042]	<i>Chromadorita tentabundum</i> (Nematoda)	AY854208	4.34%	37.02%	5
Contig[0066]	<i>Capitella capitata</i> (Annelida)	U67323	4.34%	41.36%	1
Contig[0018]	<i>Amphicorina mobilis</i> (Annelida)	AY611449	4.25%	45.61%	1
Contig[0003]	<i>Cheliplana</i> cf. <i>orthocirra</i> (Platyhelminthes)	AJ012507	2.64%	48.25%	1
Contig[0059]	<i>Cheliplana</i> cf. <i>orthocirra</i> (Platyhelminthes)	AJ012507	1.98%	50.24%	3
Contig[0056]	<i>Parodontophora</i> sp. PB-2005 (Nematoda)	AM234630	1.98%	52.22%	1

Most of the OTUs (95.97%) only occurred at a single site. The most frequently occurring OTU was Contig[0042] identified as the nematode *Chromadorita tentabundum*. This OTU was the only one present at five of the ten sites, with its highest abundance at the 90 m site. The second most frequently occurring OTU was

Contig[0001] (*Astarte castanea*) which was found at four sites with its highest numbers at the 300 m and 140 m sites.

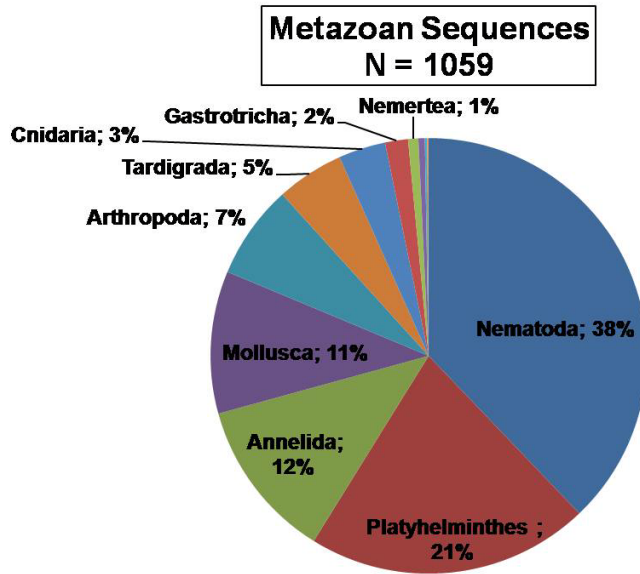


Figure 6.12 Proportion of metazoan sequences by phyla.

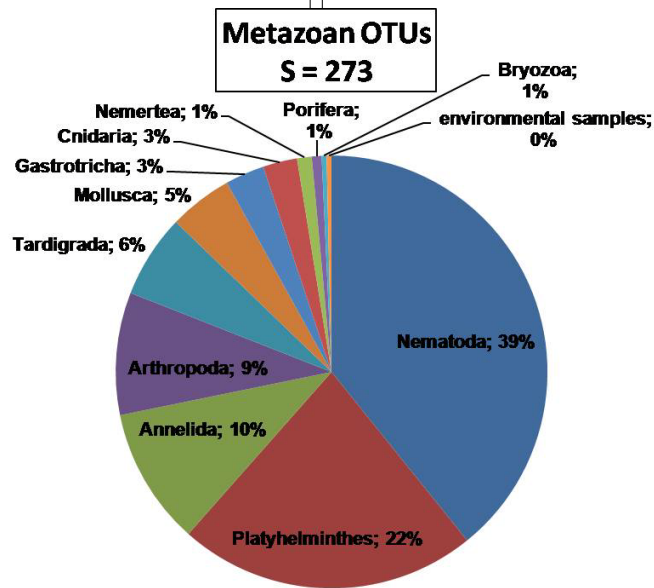


Figure 6.13 Proportion of metazoan OTUs by phyla.

The composition of metazoan sequences was variable between sites (Figures 6.14 and 6.15). The 0 m site had 213 metazoan sequences and 34 OTUs. Nematodes dominated both the number of sequences and OTUs, making up 37% and 27% respectively. Annelids comprised 25% of the sequences, while annelids and platyhelminthes each made up 23.5% of the OTUs. Three OTUs accounted for >50% of the sequences. The most abundant OTUs were Contig[0058], which was close to the nematode *Viscosia viscosa* and represented 23.5% of the sequences, followed by Contig[0066] identified as the polychaete annelid *Capitella capitata*, accounting for 22%.

The 30 m site had only 24 metazoan sequences and 14 OTUs. Platyhelminthes accounted for 62.5% of the sequences and 57% of the OTUs at this site. The most abundant OTU was Contig[0365] identified as the acoel platyhelminthes *Pseudaphanostoma smithrii* (AY078375) which represented 17% of the sequences. This was closely followed by Contig[0523], identified as the acoel *Philocelis karlingi* (AJ845243) and Contig[0152], and identified as the acoel *Pelophila lutheri* (AY078366). Each represented 12.5% of the sequences at the 30 m site.

There were 30 metazoan sequences and 9 OTUs at the 60 m site. Three OTUs accounted for >75% of the sequences at that site. Nematoda represented 40% of the sequences, while Cnidarians comprised 33% of the OTUs. The most abundant OTU was Contig[0042] identified as the nematode *Chromadorita tentabundum* (AY854208) which represented 37% of the sequences. Contig[0119], a cnidarian sequence near *Montastraea annularis* (AF238267) and Contig[0112], a tardigrade near *Pseudechiniscus islandicus* (AY582119) each comprised 20% of the sequences at the 60 m site.

The 90 m site had 80 metazoan sequences represented by 25 OTUs. Nematoda and Platyhelminthes comprised 35% and 30% of the sequences respectively. These two phyla also made up 20% and 36% of the OTUs respectively. Four OTUs accounted for >50% of the sequences. The most abundant OTU was Contig[0042] identified as the nematode *Chromadorita tentabundum* (AY854208) which comprised 29% of the sequences at that site.

The 120 m site had 43 metazoan sequences in 12 OTUs. Platyhelminthes comprised 49% of the sequences and 25% of the OTUs. Three OTUs accounted for >50% of the sequences. The dominant OTU was Contig[0010] identified as the acoelomate flatworm *Pseudaphanostoma smithii* (AY078375) and representing 39.5% of the sequences.

There were 153 metazoan sequences and 52 OTUs at the 140 m site. Nematodes dominated the site, accounting for 54% of the sequences and 58% of the OTUs. Two OTUs made up >50% of the sequences. The most abundant OTU was Contig[0006] identified as the nematode *Viscosia viscosa* (AY854198) and represented a third of the sequences. The second most abundant OTU was Contig[0001] identified as the bivalve mollusk *Astarte castanea* (AF120551) and comprising 23% of the sequences. It should also be noted that in addition to Contig[0006], 22 additional OTUs at the 140 m site also had BLAST search results for the same *Viscosia viscosa* sequence in GenBank. None of these OTUs were the same as Contig[0058] which was also identified as *Viscosia viscosa* (AY854198) from the 0 m site.

The 180 m site had 82 metazoan sequences and 34 OTUs. Tardigrades made up 46% of the sequences and 38% of the OTUs. Five OTUs accounted for >50% of the

sequences. The dominant OTU was Contig[0113] identified as the tardigrade *Pseudechiniscus islandicus* (AY582119), which represented 16% of the sequences.

There were 154 metazoan sequences and 52 OTUs at the 250 m site. The site was strongly dominated by nematodes, which comprised 89% of the sequences and 79% of the OTUs. Contig[0006], identified as the nematode *Viscosia viscosa* (AY854198) accounted for 52% of the sequences. Additionally, 29 singleton OTUs from this site also had BLAST search results for *Viscosia viscosa* (AY854198).

The 300 m site had 173 metazoan sequences and 32 OTUs. Platyhelminthes accounted for 43% of the sequences and 41% of the OTUs. Two OTUs comprised >50% of the sequences. The most abundant OTU was Contig[0001] identified as the bivalve mollusk *Astarte castanea* (AF120551) and making up 31% of the sequences. Contig[0107], identified as the Turbellarian flatworm *Schizorhynchoides caniculatus* (AY775748) represented 21% of the sequences.

The reference site had 107 metazoan sequences and 29 OTUs. Polychaete annelids comprised 51% of the sequences and 34.5% of the OTUs. Platyhelminthes additionally accounted for 36.5% of the sequences and 41% of the OTUs. Two OTUs represented >50% of the sequences. The most abundant OTU was Contig[0018], identified as a polychaete close to *Amphicorina mobilis* (AY611449) and accounting for 42% of the sequences. The second most abundant OTU was Contig[0003] identified as a turbellarian flatworm close to *Cheliplana cf. orthocirra* (AJ012507) and comprising 26% of the sequences. Nine additional singleton OTUs from the reference site also had BLAST results for *Amphicorina mobilis* (AY611449) and ten singleton OTUs were also identified as *Cheliplana cf. orthocirra* (AJ012507).

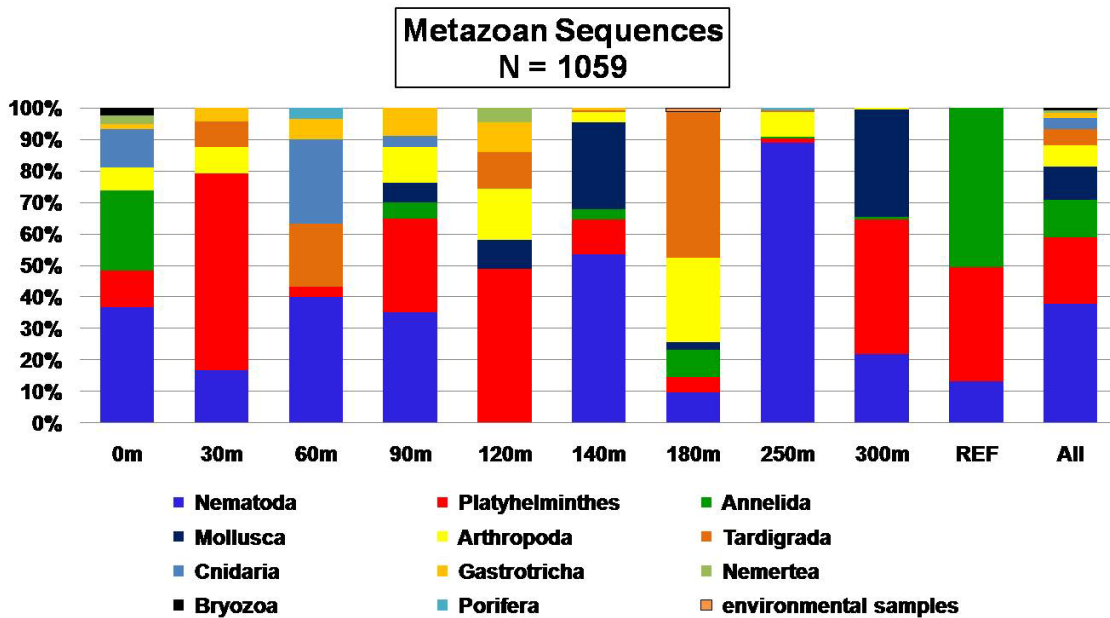


Figure 6.14 Percentage of metazoan sequences by phyla at each site and all sites combined (All).

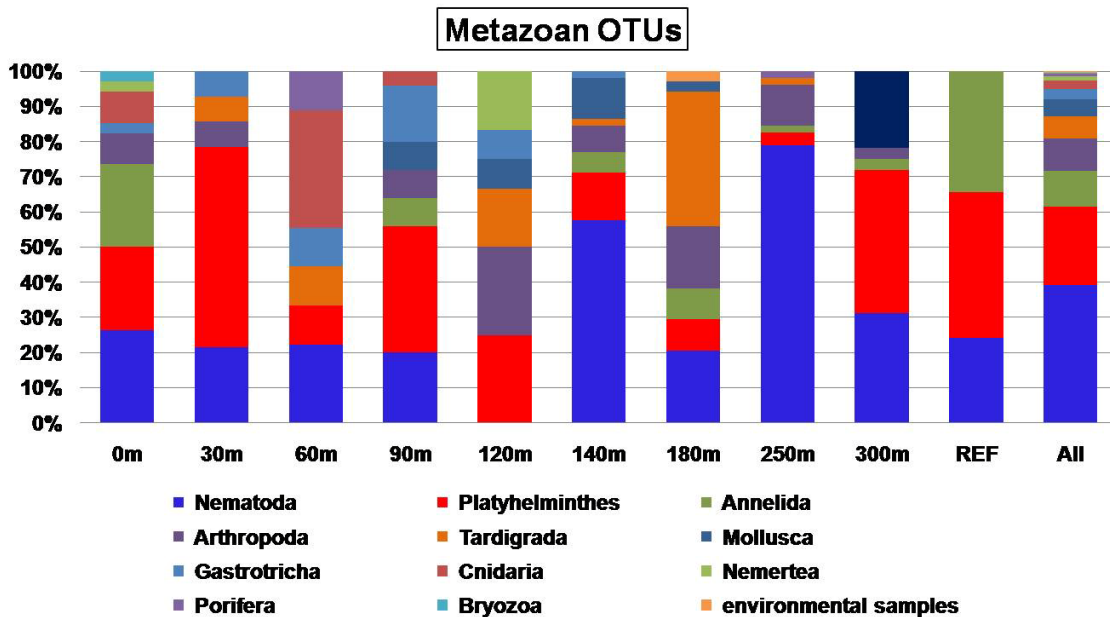
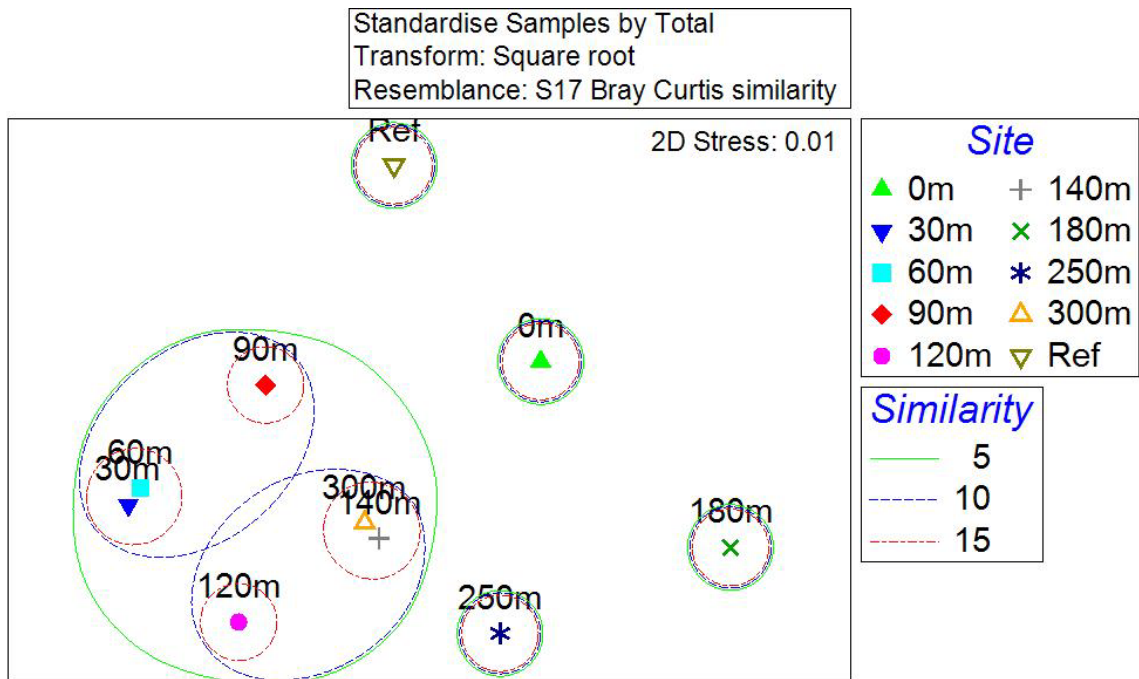


Figure 6.15 Percentage of metazoan OTUs by phyla at each site and for all sites combined (All).1

The MDS analysis based on the metazoan sequence similarity between sites grouped the 30 m – 140 m sites together with the 300 m site at a Bray-Curtis similarity of 5 (Figure 6.16a). Within this grouping, the 30 m, 60 m and 90 m sites formed a subgroup at a similarity value of 10, as did the 120 m, 140 and 300 m sites (Figure 6.16a). The 0 m, 180 m, 250 m and Reference sites each fell out as their own groups in this analysis (Figure 6.16a). Excluding the reference site from the analysis did not change the overall site groupings in the MDS analysis (Figure 6.16b).



**Figure 6.16a Non-metric Multi-Dimensional Scaling (MDS) plot of metazoan sequence Bray-Curtis similarity between sites. Sequence data standardized by site total and square root transformed.**



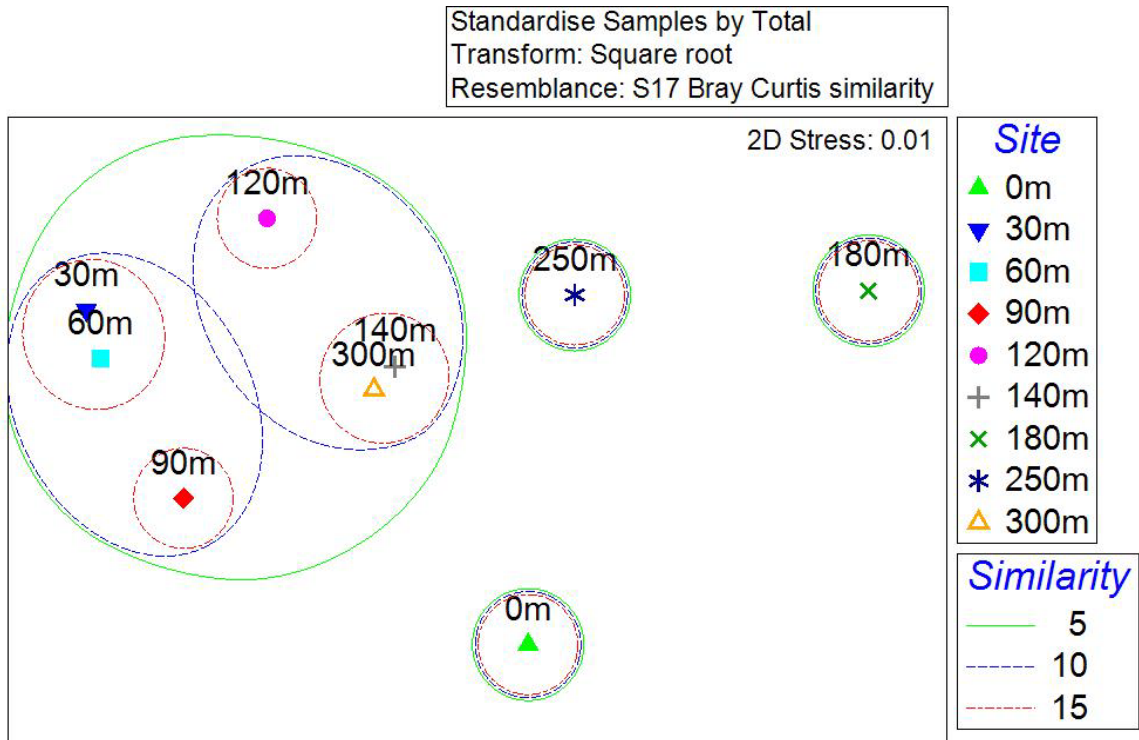


**Figure 6.16b Non-metric Multi-Dimensional Scaling (MDS) plot of metazoan sequence Bray-Curtis similarity between sites; reference site omitted. Sequence data standardized by site total and square root transformed.**

SIMPER results of the site groupings shown in the MDS analysis found that the grouping of the 30 m, 60 m and 90 m sites was due to Contig[0042] identified as the nematode *Chromadorita tentabundum* (AY854208) which contributed 77.5% to the similarity among these sites. The grouping of the 120, 140 m and 300 m sites was due to Contig[0001] identified as the bivalve mollusk *Astarte castanea* (AF120551) and Contig [0059] identified as the turbellarian flatworm *Cheliplana cf. orthocirra* (AJ012507). These two OTUs contributed 48% and 18% respectively to the among site similarity.

The BIO-ENV analysis between the metazoan sequences and the physical parameters found three combinations of physical variables that had equally strong

correlations to the metazoan community structure (Table 6.5a). The combination of pore water salinity + percent organics + median grain size, the combination of pore water temperature + sediment sorting, and the combination of ORP + percent organics + median grain size each had a correlation of 0.440. Sediment sorting had the highest correlation of any single variable ( $\rho = 0.413$ ), followed by total arsenic concentration ( $\rho = 0.352$ ).

**Table 6.5a BIO-ENV correlations between metazoan community structure and physical parameters.**

Spearman Correlation	Parameters
0.440	Salinity, % Organics, Median Grain Size
0.440	Temperature, Sorting
0.440	ORP, % Organics, Median Grain Size
0.437	Total [As], Median Grain Size, Sorting
0.436	Salinity, Total [As], Median Grain Size, Sorting
0.435	% Organics, Median Grain Size
0.435	Temperature, pH, % Organics, Median Grain Size, Sorting
0.434	Temperature, Total [As], Median Grain Size, Sorting
0.433	Salinity, Median Grain Size, Sorting
0.433	pH, % Organics, Median Grain Size, Sorting
0.413	Sorting
0.352	Total [As]
0.293	Median Grain Size
0.281	ORP
0.274	% Organics
0.215	Temperature
0.212	%CaCO <sub>3</sub>
0.201	pH
0.183	Salinity

The BIO-ENV results excluding the reference site had stronger correlations overall (Table 6.5b). These results show pH in combination with other parameters correlating more strongly with the community structure while the percent organics had a weaker correlation (Table 6.5b).

**Table 6.5b BIO-ENV correlations between metazoan community structure and physical parameters; reference site omitted.**

Spearman Correlation	Parameters
0.538	pH, ORP, Sorting
0.534	Temperature, pH, ORP, Sorting
0.532	pH, ORP, Total [As], Sorting
0.531	pH, ORP, Salinity, Total [As], Sorting
0.530	Total [As], Median Grain Size, Sorting
0.529	pH, ORP, Salinity, Sorting
0.529	ORP, Salinity, Total [As], Sorting
0.529	Salinity, Total [As], Median Grain Size, Sorting
0.528	ORP, Total [As], Sorting
0.528	Temperature, pH, ORP, Salinity, Sorting
0.491	Sorting
0.458	Total [As]
0.434	Median Grain Size
0.336	ORP
0.319	Salinity
0.307	Temperature
0.247	pH
0.232	% CaCO <sub>3</sub>
0.179	% Organics

The LINKTREE analysis based on the metazoan -only sequence similarity (Figure 6.17) separated the 0 m and Reference site out from the other sites at node A based on their lower ORP measurements (ORP < 5.2 vs. >52.6). Node B split out the 180 m + 250 m sites from the remaining sites based on their higher pH values (>7.8 vs. <7.74). The final node separated the 30 m + 60 m + 90 m sites from the 120 m + 140 m + 300 m sites base on differences in the median grain size.

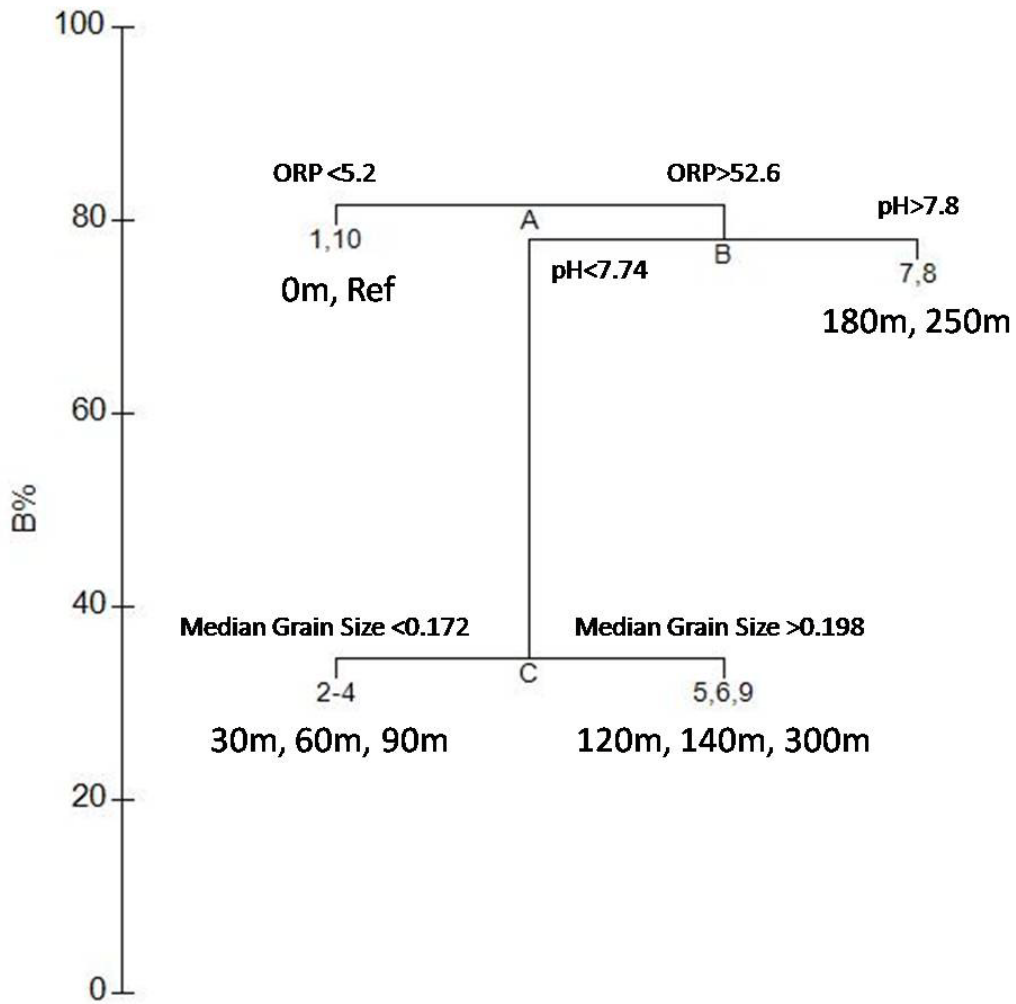


**Figure 6.17 LINKTREE results showing physical characteristics between metazoan sequence community site groups.**

A total of 25 bacterial phyla were found, representing 1,973 sequences in 1,081 OTUs (Table 6.6). The  $\gamma$ -Proteobacteria had the largest percentage of OTUs and sequences, followed by the Actinobacteria (Figures 6.18 and 6.19). Most phyla ranked similarly in the percentage of OTUs and percentage of sequences they represented (Figures 6.17 and 6.18). One notable exception were the Firmicutes, which comprised only 4% of the OTUs but represented 14% of the sequences (Figures 6.18 and 6.19).

There was a decreasing trend in the number of phyla found at each site with distance from the vent (Figure 6.20). The number of OTUs per site was higher at the intermediate sites, peaking at 20 m (Figure 6.21). The farthest site from the vent (180 m) had only 4 phyla represented and also had the lowest number of OTUs (Table 6.6; Figures 6.20 and 6.21). The trends in the distribution of OTUs and sequences among phyla at each site are shown in Figures 6.22 and 6.23. Actinobacteria dominated at the 7.5 m site in both the number of OTUs and sequences, while Chloroflexi was dominant at the 12 m site (Table 6.6; Figures 6.22 and 6.23). The  $\gamma$ -Proteobacteria and  $\delta$ -Proteobacteria together represented a large percentage of the bacterial composition at the 20 m through 120 m sites along the transect (Table 6.6; Figures 6.22 and 6.23). The 180 m site was strongly dominated by Firmicutes, which represented 89% of the OTUs and 99% of the sequences at that site (Table 6.6; Figures 6.22 and 6.23).

The cluster analysis results indicate the bacteria form three distinct groups in relation to their distance along the transect (Figure 6.24). The two sites closest to the focused venting (7.5 m and 12 m) had a distinct bacterial community, the 20 m through 120 m sites formed a distinct community, and the 180 m site separated out as a unique community. SIMPER analysis indicated that the similarity among the 7.5 m and 12 m

sites was defined by the presence of Chlorobi and Chloroflexi. The similarity among the 20 m through 120 m sites was due to OTUs within the Actinobacteria and  $\gamma$ -Proteobacteria phyla, while the bacterial community at the 180 m site was defined by the dominance of Firmicutes at that site.

**Table 6.6 Number of OTUs (S) and sequences (N) for bacterial phyla for all sites (Total) and individual sites.**

	Total		7.5 m		12 m		20 m		30 m	
	S	N	S	N	S	N	S	N	S	N
Acidobacteria	140	205	19	32	3	3	30	36	35	42
Actinobacteria	164	311	40	71	10	11	48	65	35	47
Bacteroidetes	43	58	7	11	15	18	4	4	7	9
Chlamydiae	7	7	2	2	0	0	1	1	0	0
Chlorobi	26	106	13	28	15	78	0	0	0	0
Chloroflexi	60	109	11	22	33	65	10	11	3	3
Cyanobacteria	2	2	1	1	0	0	1	1	0	0
Deferribacteres	5	5	3	3	1	1	1	1	0	0
Deinococcus-Thermus	2	3	2	3	0	0	0	0	0	0
Fibrobacteres	2	2	0	0	0	0	1	1	1	1
Firmicutes	46	278	4	5	4	8	3	3	4	4
Gemmatimonadetes	8	15	3	8	1	1	3	3	1	1
Nitrospirae	12	27	1	1	2	3	1	1	2	5
Planctomycetes	104	116	17	22	5	5	19	19	13	13
Proteobacteria	3	3	0	0	0	0	1	1	1	1
Spirochaetes	1	1	0	0	0	0	0	0	0	0
Thermodesulfobacteria	4	4	1	1	1	1	1	1	0	0
Thermotogae	1	1	0	0	1	1	0	0	0	0
Verrucomicrobia	16	24	1	1	1	3	2	2	4	5
$\alpha$ -Proteobacteria	67	115	1	1	15	31	7	7	13	21
$\beta$ -Proteobacteria	3	4	0	0	3	4	0	0	0	0
$\gamma$ -Proteobacteria	204	358	15	20	3	3	44	56	45	67
$\delta$ -Proteobacteria	153	209	17	21	14	30	33	37	31	33
$\epsilon$ -Proteobacteria	4	6	2	2	1	3	0	0	1	1
Bacteria Undet.	4	4	1	1	1	1	2	2	0	0
Total	1081	1973	161	256	129	270	212	252	196	253
Number of Phyla	25		20		19		19		15	

**Table 6.6 Continued.**

	60 m		90 m		120 m		180 m	
	S	N	S	N	S	N	S	N
Acidobacteria	25	29	19	25	30	38	0	0
Actinobacteria	31	52	26	40	21	25	0	0
Bacteroidetes	7	7	5	5	4	4	0	0
Chlamydiae	0	0	1	1	3	3	0	0
Chlorobi	0	0	0	0	0	0	0	0
Chloroflexi	1	2	4	4	2	2	0	0
Cyanobacteria	0	0	0	0	0	0	0	0
Deferribacteres	0	0	0	0	0	0	0	0
Deinococcus-Thermus	0	0	0	0	0	0	0	0
Fibrobacteres	0	0	0	0	0	0	0	0
Firmicutes	3	8	5	6	3	5	24	239
Gemmatimonadetes	0	0	2	2	0	0	0	0
Nitrospirae	1	1	4	7	4	9	0	0
Planctomycetes	13	13	10	12	29	32	0	0
Proteobacteria	0	0	1	1	0	0	0	0
Spirochaetes	0	0	0	0	1	1	0	0
Thermodesulfobacteria	1	1	0	0	0	0	0	0
Thermotogae	0	0	0	0	0	0	0	0
Verrucomicrobia	4	4	3	5	3	4	0	0
$\alpha$ -Proteobacteria	17	19	12	14	16	21	1	1
$\beta$ -Proteobacteria	0	0	0	0	0	0	0	0
$\gamma$ -Proteobacteria	33	45	38	78	58	88	1	1
$\delta$ -Proteobacteria	31	34	21	26	20	26	1	2
$\epsilon$ -Proteobacteria	0	0	0	0	0	0	0	0
Bacteria Undet.	0	0	0	0	0	0	0	0
Total	167	215	152	226	193	258	27	243
Number of Phyla	12		14		13		4	

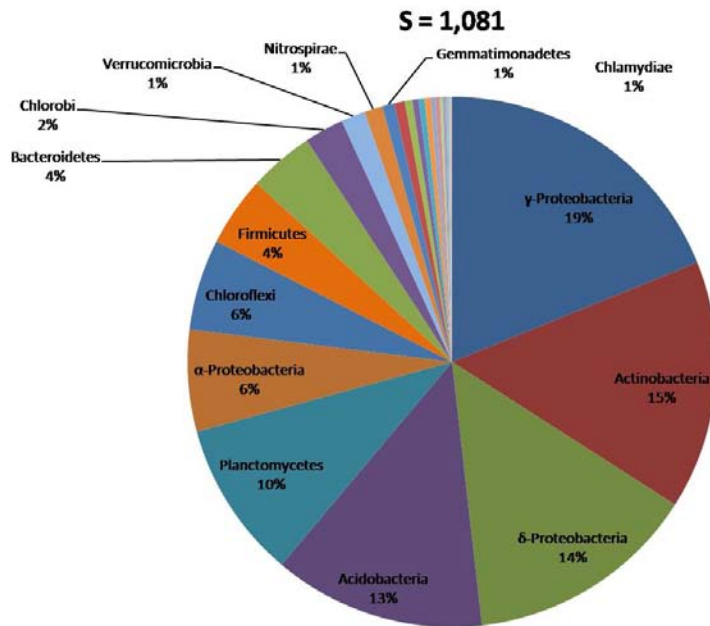


**Figure 6.18** Percentage of total bacterial OTUs (S = 1,081) by phyla.

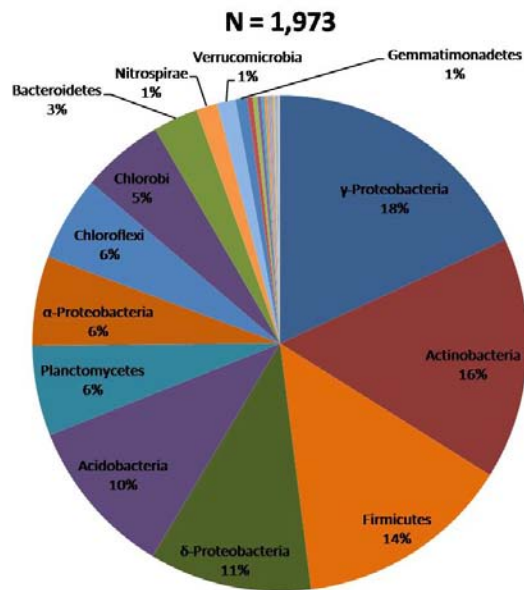


**Figure 6.19** Percentage of total bacterial sequences (N = 1,973) by phyla.



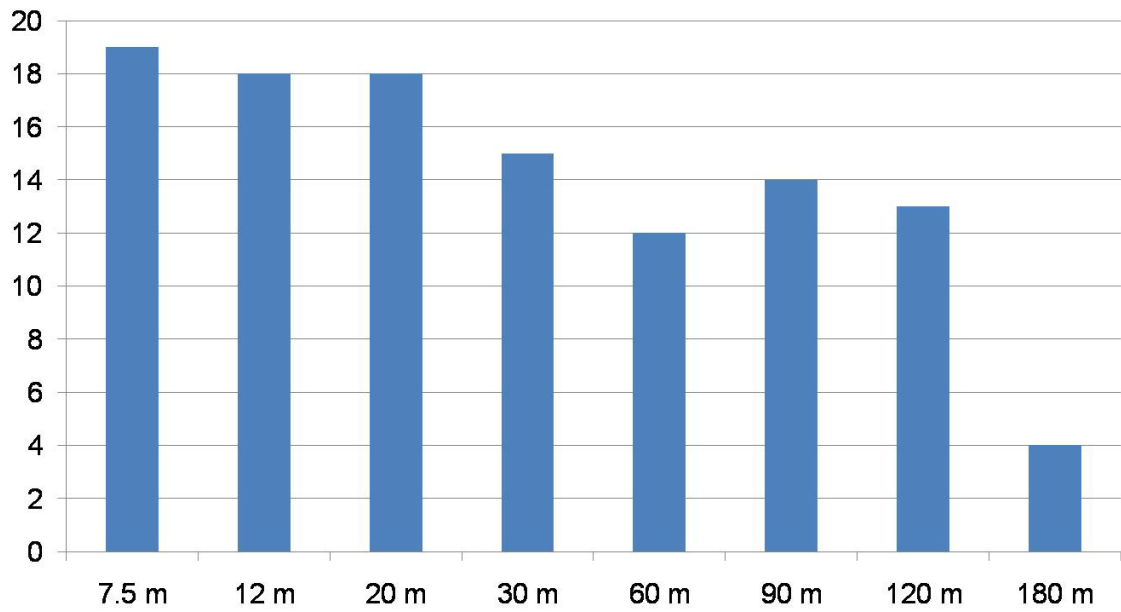


**Figure 6.20 Total number of bacterial phyla represented at each transect site.**

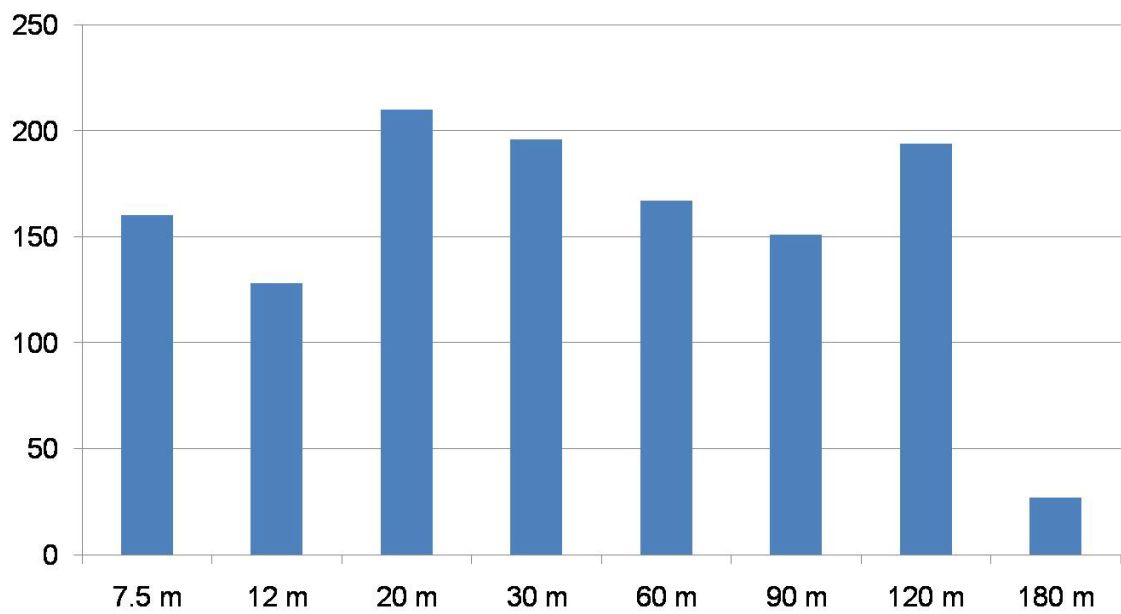


**Figure 6.21 Total number of bacterial OTUs represented at each transect site.**

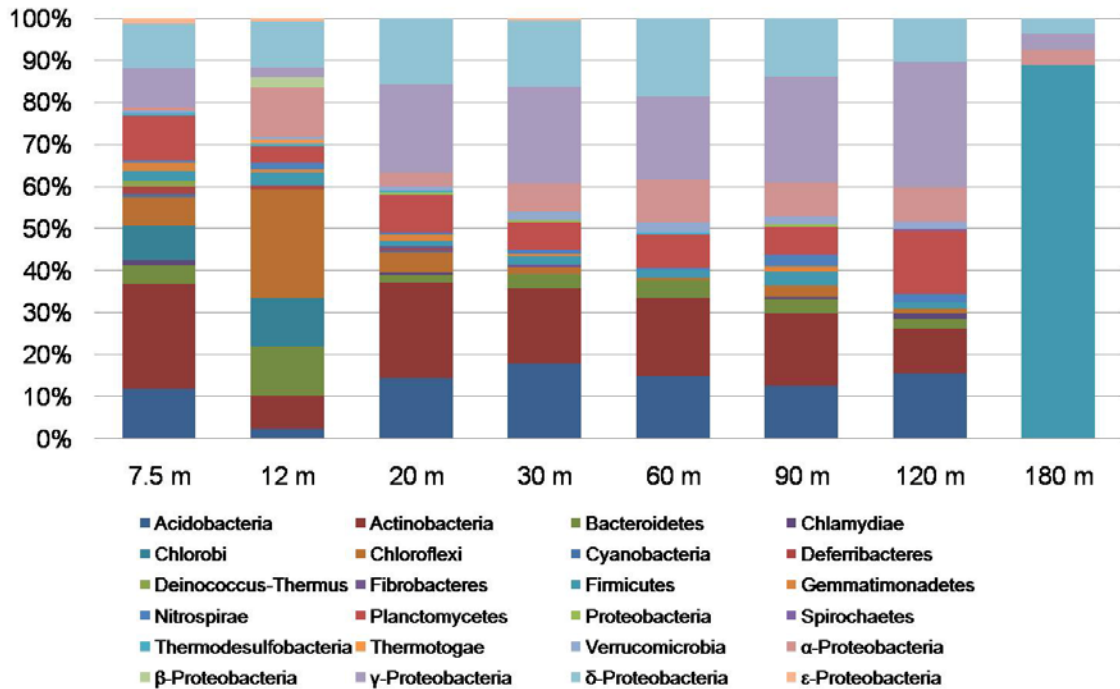


Figure 6.22 Percentage of bacterial OTUs by phyla at each transect site.

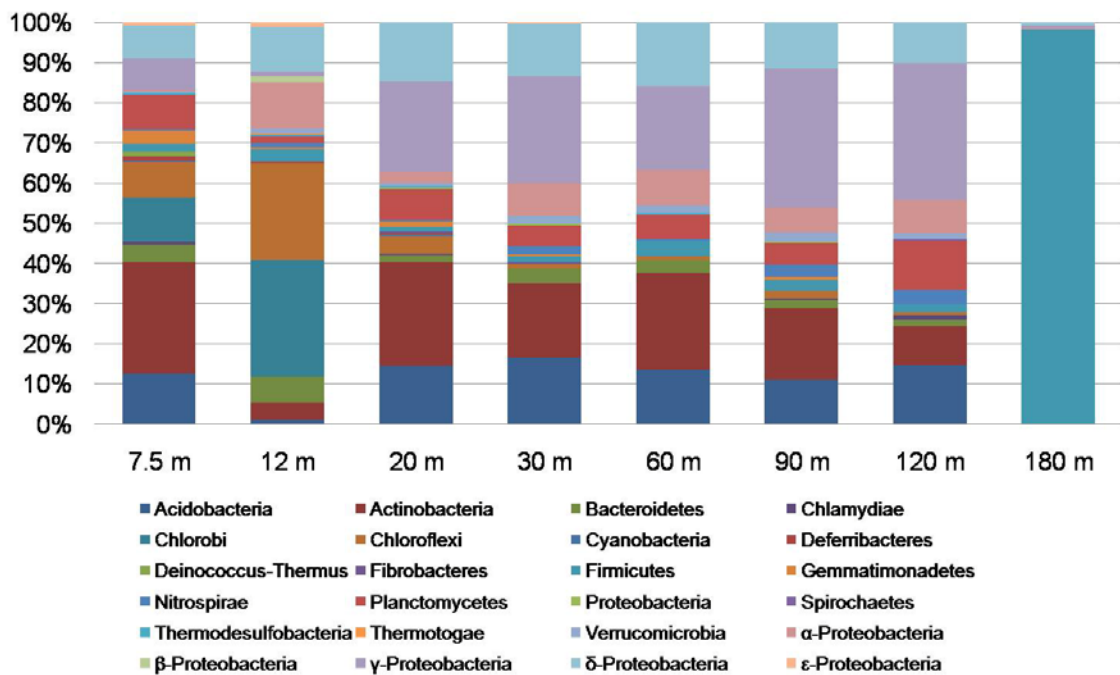
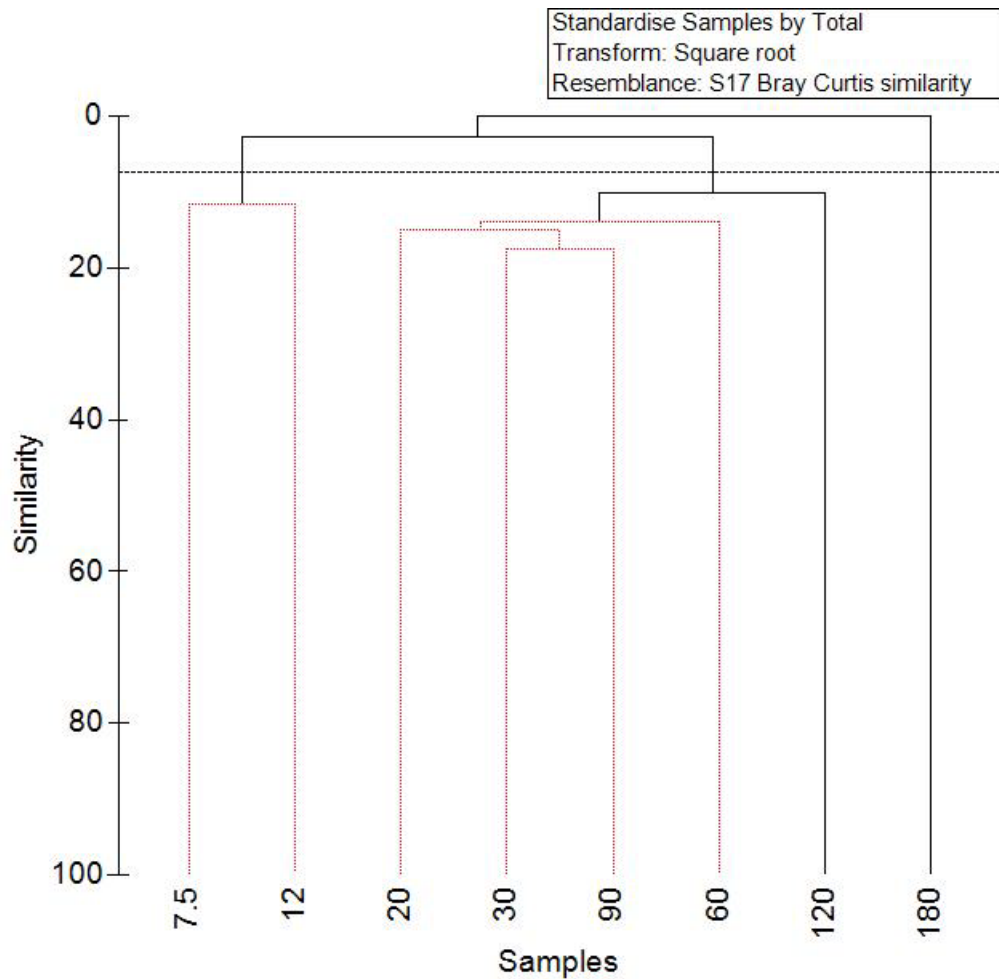


Figure 6.23 Percentage of bacterial sequences by phyla at each transect site.



**Figure 6.24 Cluster analysis of bacterial sequence Bray-Curtis similarity between sites. Sequence data was standardized by site totals and square root transformed. Dashed horizontal line demarcates 7.5 Bray –Curtis similarity. Red dendrogram branches indicate significant SIMPROF groupings.**

## 6.4 Discussion

The molecular eukaryotic diversity at the vent site was very similar to the macrofaunal and meiofaunal communities at that site. There was a relatively low number of OTUs dominated by metazoans. The dominant OTUs were provisionally identified as the nematode (*Viscosia viscosa*) and the polychaete (*Capitella capitata*), which are close matches to the taxa found in the macrofaunal and meiofaunal samples at this site. Both of

these taxa are relatively large and were abundant, which may have also contributed to their representation in the 18S rDNA extractions.

The eukaryotic community in inner transect zone, which included the 30 m through 140 m sites also encompassed the 300 m site. This community was defined by the presence of an OTU provisionally identified as the fungus *Paecilomyces* sp. and two metazoan OTUs provisionally identified as the nematode *Chromadorita tentabundum* and the bivalve mollusk *Astarte castanea*, as well as a Stramenopile (Oomycetes) which closely matched *Phytophthora infestans*. The presence of the molluscan sequence in this zone is enigmatic since there were few mollusks found in the corresponding meiofaunal samples. These sequences may represent recently settled larvae, which may not survive to the adult stage in the low pH environment. The 30 m and 60 m sites formed a subgroup defined by the fungus *Paecilomyces* sp. and several stramenopile OTUs provisionally identified as the diatoms *Pauliella toeniata*, *Navicula* sp., and unidentified Bacillariophyta. The presence of diatom sequences suggests that the benthic microalgal community is important in primary production at these sites.

The eukaryotic community at the 180 m and 250 m sites had the most OTUs, which suggests the eukaryotic diversity is higher farther from the vent, although this pattern was very variable at the other transect sites. The dominant eukaryotes included OTUs closely matching the fungus *Cladosporium cladosporioides*, the chlorophytes (green algae) *Polytoma oviforme* and *Cladophora glomerata* and a marine mite, *Thalassarachna basteri*. The presence of chlorophyte sequences at these sites suggests that macroalgae from the surrounding reef system are important contributors to the primary production at these sites. This may be either through photosynthetic or detrital

pathways and further suggests that the fungal OTUs present at that site may be associated with decomposing algal detritus.

The eukaryotic community at the Danlum Bay reference site was dominated by fungi, which are probably associated with the breakdown of detritus found at that site. Among the most abundant OTUs were the fungi provisionally identified as *Cladosporium cladosporioides* and *Penicillium chrysogenum*. The eukaryotic community was most similar to the 0 m site due to the presence of common fungal sequences. This is possibly due to the proximity to shore of both of these sites and the input of terrestrial detrital material from Ambitle Island.

One unexpected finding from the eukaryotic diversity was the large proportion of fungal sequences. Fungi are an often overlooked component of the biodiversity in marine environments (Le Calvez *et al.* 2009), and this finding highlights the utility of using molecular techniques in evaluating marine biodiversity. The most abundant sequence found was provisionally identified as the fungus *Paecilomyces*, and several OTUs had BLAST matches with this fungus. The genus *Paecilomyces* is a speciose and wide spread group of fungi which includes many thermophilic species (Sampson 1974). *Paecilomyces* spp. have been recorded in other similar studies including in marine sediment samples from the continental slope of the Bay of Bengal in India (Das *et al.* 2009), and sequences of this fungus have been reported to co-amplify with targeted nematode 18S rRNA in marine environmental samples (Bhadury *et al.* 2006).

The analysis of the bacterial sequence data also indicated that the environmental gradient along the transect influenced the bacterial community structure. Several studies at other similar shallow-water hydrothermal vent systems had found that molecular

microbial diversity in the sediment was highest near the vent, suggesting the hydrothermal influence stimulates microbial activity (Sievert *et al.* 2000, Manini *et al.* 2008). An earlier study at the vent system in Milos, Greece by Sievert *et al.* (1999) however, found bacterial cell counts were highest in the intermediate zone between the strongly hydrothermally influenced sediments and the normal marine sediments, while diversity was lowest near the vent. Corresponding work done at Ambitle Island looked at the possibility of microbial metabolism of arsenic in the sediments. Price *et al.* (2007) looked at the distribution of As(V) and As(III) in sediment pore waters collected along the transect at Tutum Bay. Their findings suggested that the higher concentrations of As(V) in pore waters near the vent could be due to microbial oxidation of As(III) from the hydrothermal fluid (Price *et al.* 2007). More recently, an arsenic metabolizing  $\gamma$ -Proteobacterium, *Marinobacter santoriniensis*, was isolated and described from a shallow-water hydrothermal vent in Santorini, Greece (Handley *et al.* 2009). The high percentage of  $\gamma$ -Proteobacteria sequenced from the Tutum Bay sediments suggests that a similar species could be present here as well.

## **6.5 Summary and conclusions**

The molecular survey of eukaryotes and bacteria showed a high diversity for both of these domains and revealed the contribution of often overlooked lineages to the biodiversity of the shallow-water vent system. The results for the eukaryotes did show some similarities to the macrofaunal and meiofaunal communities, particularly with the metazoans at the vent site. There were several incongruencies in the proportions of metazoan sequences recovered which showed a bias in the molecular methods used. In

particular, the metazoan sequence dataset appeared to undersample arthropods, while having a disproportionately high number of flatworm sequences compared to the meiofaunal results. The molecular results however did show the contribution of fungi and other eukaryotic groups as well as the bacteria to the overall diversity of the system, a finding that would have otherwise been overlooked by traditional benthic survey methods.

## Chapter Seven

### **Biocomplexity of the communities associated with the shallow-water hydrothermal system at Tutum Bay, Ambitle Island, Papua New Guinea.**

#### **7.1 Comparison of different biological communities and physical parameters.**

One goal of this project was to evaluate different methods for measuring biotic communities in particular the use of molecular techniques as a measure of the meiofaunal metazoan community vs. morphological identifications. To do this, I used second stage multi-dimensional scaling analysis (PRIMER v6) to find correlations between the underlying distance measures of the physical variables and the similarity measures of each community: macrofauna, meiofauna, molecular eukaryotic and molecular metazoan. The bacterial sequence data were excluded since they were not available from all sites, and several sites did not match the other datasets and lacked corresponding environmental data. The physical, macrofauna and meiofauna data were composited by site in to compare with the molecular data sets. The physical, macrofaunal and meiofaunal datasets were also compared against each other using all replicates. For comparison between the meiofauna and the molecular metazoan data the taxonomic resolution of the molecular OTUs was reduced to higher level taxonomic categories to match the level of meiofaunal identifications.

The second stage MDS results (Figure 7.1; Table 7.1) show that the macrofauna are more strongly correlated to the environmental data than either the meiofauna or molecular datasets. The meiofauna had the second highest correlation with the



environmental data, while both the eukaryotic and metazoan molecular communities had relatively weak correlations (Table 7.1). Since the molecular metazoan dataset is a subset of the eukaryotic dataset, they both have similar correlations with the physical data and are also highly correlated to each other (Table 7.1). The meiofauna dataset had a weak correlation with the molecular metazoan data (Table 7.1). Table 7.2 shows the second stage MDS correlations between the physical data, macrofauna and meiofauna using all 50 replicate samples. These results mirror Table 7.1 although the correlation values are lower due to the variability among the replicate samples. Overall, the morphologically based macrofauna and meiofauna appear to be better indicators of environmental changes along the transect than the molecular analysis. The macrofauna were better indicators than the meiofauna which may have been due to the lower level of taxonomic identification of the macrofauna. Conversely, the identification of OTUs in the molecular dataset was dependent on the coverage of a particular taxonomic group in the GENBANK database. Additionally, setting the criteria for assembling OTUs at 99% similarity for the molecular data set may have underestimated the number of species in a sample, as has been shown with soil nematodes and mites (Wu *et al.* 2009).

To further compare the meiofauna and the molecular metazoan data, I looked at the higher level taxonomic composition of both datasets, standardizing them by relative abundance for the meiofauna and relative number of sequences for the molecular metazoans (Figure 7.2). Both datasets were proportionally similar for nematodes and some of the lesser known phyla such as gastrotrichs. The meiofauna data showed a much higher proportion of arthropods. The molecular data had higher proportions of platyhelminthes, annelids, mollusks (probably larvae) and tardigrades. These results

suggest that the molecular methods used show a bias towards softer bodied organisms such as flatworms. The manual picking and counting of meiofauna may underestimate the number of soft bodied taxa due to problems with preservation and their small size.

The difference in sample sizes in the two datasets may also have affected the comparison. The meiofauna were represented by over 17,000 individual specimens compared to fewer than 3,000 18S rDNA sequences in the final eukaryote dataset. The sediment DNA extractions used only a small amount (< 1 g) of the total sediment samples whereas the meiofauna from the entire core sample were counted. Additionally, the meiofaunal analysis was based on five replicate samples from each site while for the molecular samples, replicate sediment cores were pooled into a single sample at each site.

Despite these issues, the molecular dataset revealed a much broader phylogenetic diversity than the macrofauna and meiofauna datasets, and reflected the contribution of the non-metazoan eukaryotes such as fungi, stramenopiles and alveolates to the overall sediment community. These often overlooked levels of biodiversity serve important ecological functions such as the breakdown of organic matter and the recycling of nutrients and primary productivity through photosynthesis by benthic diatoms and dinoflagellates.

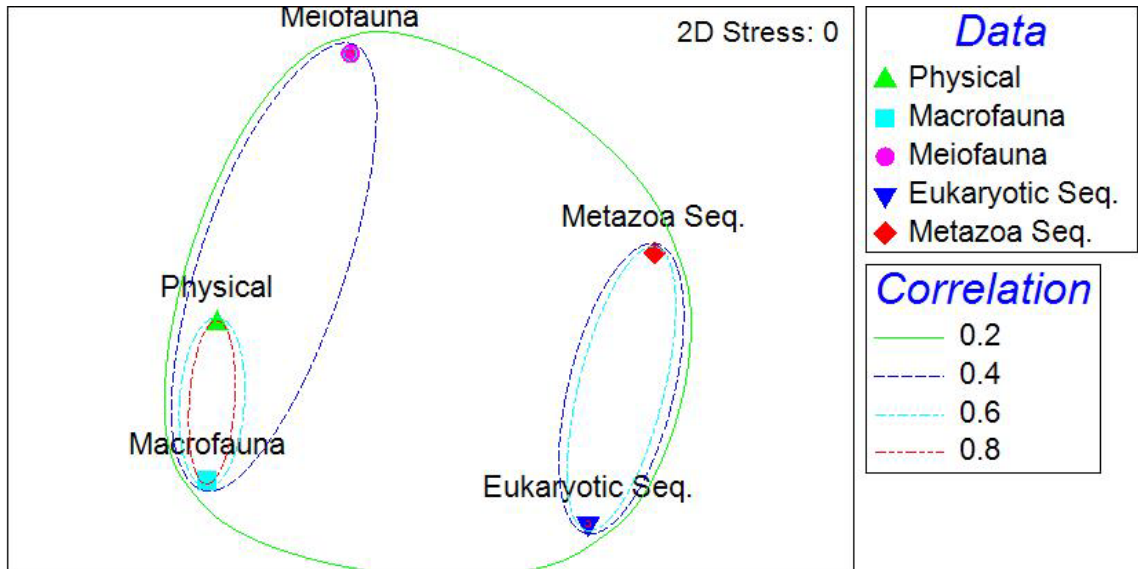


**Figure 7.1 Second Stage Multi-Dimensional Scaling plot showing correlation between the different datasets.**

**Table 7.1 Second Stage MDS Spearman correlations. Physical parameters, macrofauna and meiofauna relative abundance data averaged by site for comparison.**

	Physical parameters	Eukaryotic sequences	Macrofauna	Metazoa sequences
Physical parameters				
Eukaryotic sequences	0.39			
Macrofauna	0.84	0.39		
Metazoa sequences	0.38	0.76	0.31	
Meiofauna	0.53	0.24	0.37	0.40

**Table 7.2 Second Stage MDS Spearman correlations for physical parameters, macrofauna, and meiofauna relative abundance for all replicate samples.**

	Physical (all reps)	Macrofauna (all reps)
Physical (all reps)		
Macrofauna (all reps)	0.65	
Meiofauna (all reps)	0.51	0.22

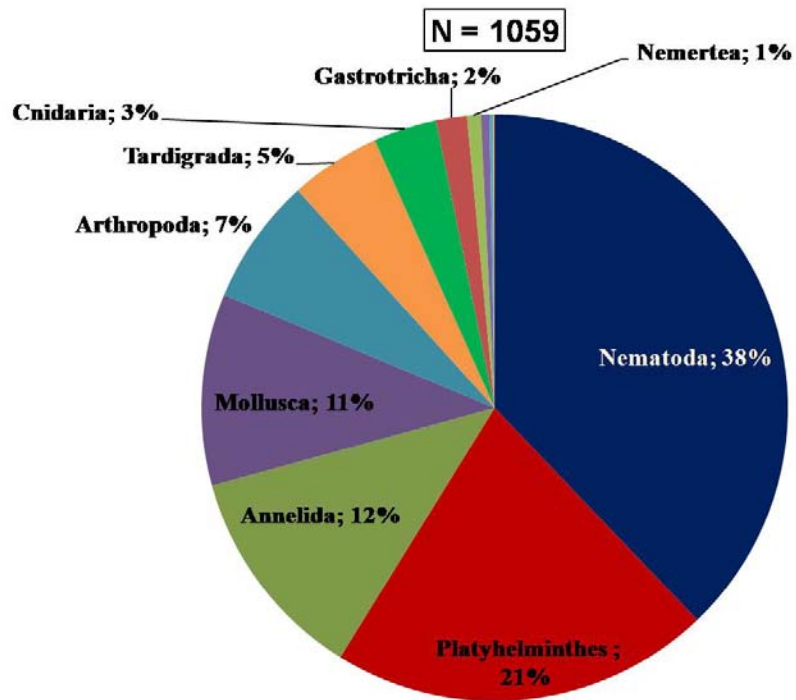
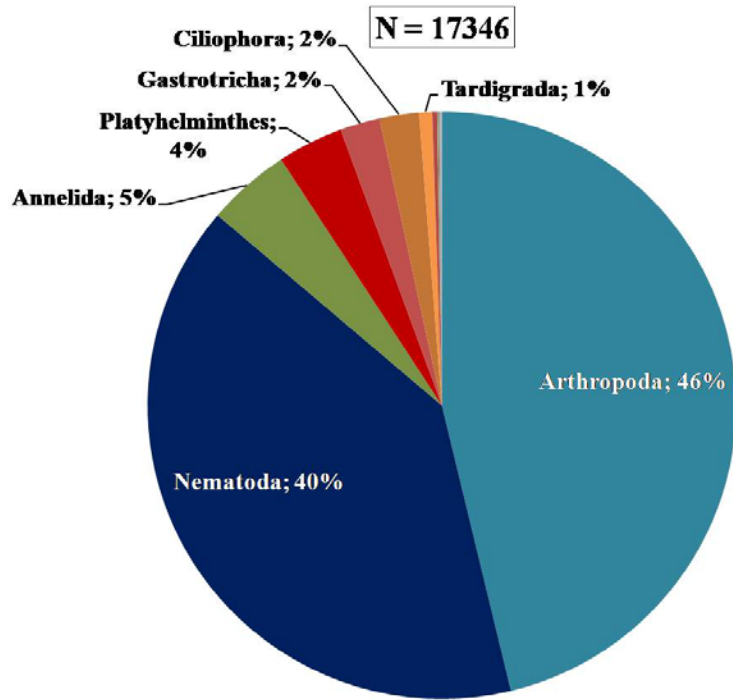


**Figure 7.2** Percentage of meiofaunal abundance (top graph) and metazoan sequences (bottom graph) by phyla.

## **7.2 Summary of findings and conclusions: the biocomplexity of the Tutum Bay hydrothermal system:**

The physical environment and biological communities in Tutum Bay and at the Danlum Bay reference site formed four distinct communities based on their pore water and sediment characteristics and the corresponding macrofaunal, meiofaunal, and molecular eukaryotic and bacterial community structure. These communities are further developed by complex interactions between the biological benthic community and physical environment and among the different levels of the biodiversity.

### **7.2.1 The Vent Community (0 m)**

The focused hydrothermal vent at the 0 m site directly impacts the sediment and pore water characteristics resulting in extreme conditions of high temperature, high arsenic, low salinity and pH in the acidic range. The combination of low pH and physical disturbance caused by the focused venting and possibly the influence of wave action due to the shallow depth at that site further influence the sediment composition, resulting in a coarse-grained, poorly sorted volcanic gravel and an absence of calcareous sediments due to the low pH. The pore water environment and sediment characteristics together have a direct influence on the biotic communities present at the vent site. Both the macrofaunal and meiofaunal communities are represented by a few species that can tolerate the harsh conditions at that site. The macrofaunal community is defined by the polychaete *Capitella cf. capitata*, which were found in very high abundance possibly due to the lack of competition with other macrofauna or a release from predation. The meiofaunal

community also had a low number of taxa present and a low overall abundance. The meiofaunal taxa were apparently less tolerant of the extreme pore water conditions than the macrofauna, and no single taxon reached high abundances as was seen with the macrofaunal community. The meiofauna at the vent site were represented by a high proportion of nematodes, but other taxa were present including harpacticoid copepods and mites. Also present among the meiofaunal community were juvenile *Capitella* cf. *capitata*, which indicates a continued recruitment of the dominant polychaete at the vent site.

The molecular eukaryotic diversity at the vent site was very similar to the macrofaunal and meiofaunal communities. There was a relatively low number of OTUs despite a large number of sequences that were obtained from that site. Metazoans dominated both in the number of OTUs and in the number of sequences, with the dominant OTUs identified as a nematode (*Viscosia viscosa*) and a polychaete (*Capitella capitata*). There were no bacterial samples collected at the 0 m site, but the two closest sites (7.5 m and 12 m) were characterized by a high number of bacterial phyla. Actinobacteria were dominant at the 7.5 m site in both the number of OTUs and sequences, while Chloroflexi were dominant at the 12 m site.

### **7.2.2 The Diffuse Venting Zone Community (30 m – 140 m).**

The samples collected along the transect from 30 m to the 140 m site grouped together based on their physical characteristics. This area was influenced by the diffuse venting of hydrothermal fluids and CO<sub>2</sub> gas through the sediment, which resulted in low pore water pH and elevated arsenic concentrations. The temperature and salinity were

near that of normal seawater in the surface sediments, but there was a noticeable increase in temperature with depth in the sediment profile. This area was also surrounded by higher relief from the surrounding reef, which may have protected these sites from physical disturbance from wave action. The combination of this and the low pH influenced the sediment environment resulting in a well-sorted, fine-grained volcanic sand with low to absent carbonate content. The macrofaunal community at these sites was characterized by low species richness and abundances and was dominated by burrowing crustaceans such as thalassinid shrimp and the amphipod *Platyischnopus* sp.A. The low diversity in this area may have been due to several factors. First, the elevated arsenic and low pH of the pore waters could have affected the survival of infaunal taxa. Secondly, the fine-grained, well-sorted and unconsolidated sand may have provided a poor habitat for benthic infauna. And finally biological influences such as bioturbation by the high density of thalassinid shrimp and predation on settling larvae by *Platyischnopus* sp. A could have significantly reduced the macrofaunal community at these sites.

The meiofaunal community in this zone split into two subgroups. The meiofaunal community at the 30 m and 60 m sites had fewer taxa and lower abundances than the 90 m – 140 m sites, which also had relatively fewer taxa but increased abundances. This trend reflects the sensitivity of the meiofaunal taxa to the pore water conditions. At all sites, nematodes were proportionally most abundant, but there was an increasing number of arthropods with distance along the transect. This may reflect the gradual increase in sediment grain size along the transect. The meiofaunal community in this zone may also have been influenced by the dominant macrofaunal taxa through physical disturbance by burrowing as well as direct predation.

The molecular eukaryotic community in this zone also encompassed the 300 m site and was grouped by the presence of a contig provisionally identified as the fungus *Paecilomyces* sp. and two Metazoan OTUs provisionally identified as the nematode *Chromadorita tentabundum* and the bivalve mollusk *Astarte castanea*, as well as a Stramenopile (Oomycetes) which closely matched *Phytophthora infestans*. The presence of the molluscan sequence in this zone is enigmatic since there were few mollusks found in the corresponding meiofaunal samples. These sequences may represent recently settled larvae, which may not survive to the adult stage in the low pH environment. The 30 m and 60 m sites formed a subgrouping defined by the fungus *Paecilomyces* sp. and several Stramenopile OTUs provisionally identified as the diatoms *Pauliella toeniata*, *Navicula* sp., and unidentified Bacillariophyta.

Sediment samples for bacterial analysis were collected in this zone at sites 20 m, 30 m, 60 m, 90 m and 120 m. The bacterial community in this zone was characterized by a high number of phyla and unique OTUs and was dominated by Actinobacteria and  $\gamma$ -Proteobacteria.

### **7.2.3 The Low-hydrothermal Activity Zone Community (180 m – 300 m)**

The three transect sites farthest from the vent also grouped together based on their physical characteristics. The pore water at these sites had the same temperature and salinity as the ambient seawater. Arsenic concentrations of the pore water were slightly elevated and pH values were slightly depressed from normal seawater than at the other sites. This suggests that there was still a hydrothermal influence at these sites, though to a lesser extent than in the diffuse venting zone. The sediments were predominantly



biogenic carbonate sand and gravel consisting of coral and shell fragments from the surrounding reef environment.

The macrofaunal community had a high species richness and abundance. Dominant macrofauna included the amphipod *Cyrtophium?* sp. A, the bivalve *Codakia* sp. A and several polychaetes; *Typosyllis cornuta*, *Pholoe* sp. A, *Grubeosyllis* sp. B and *Protodorvillea* sp. B. The high diversity at these sites may reflect the coarser sediment type and less variable water quality being more favorable to benthic infauna.

The meiofaunal community in this zone had a higher taxonomic richness than the other transect sites but the abundances were similar to the 90 m – 140 m sites. The offshore transect sites had nearly equal proportion of nematodes and copepods. The higher abundance of copepods and of many typically interstitial phyla was due to the larger median grain size and more poorly sorted sediments, resulting in more interstitial spaces between sediment grains to support meiofaunal diversity.

The molecular eukaryotic community for this zone was represented by the 180 m and 250 m sites. These two sites had the most eukaryotic OTUs and dominant eukaryotes included the fungus *Cladosporium cladosporioides* (Contig[0008]), the Chlorophytes *Polytoma oviforme* (Contig [0218]) and *Cladophora glomerata* (Contig[0074]) and a marine mite, *Thalassarachna basteri* (Contig[0115]).

Bacterial sequences were only obtained from the 180 m site. The bacterial community here had only four phyla represented and a total of 27 OTUs. The phylum Firmicutes was dominant at that site. Unlike with the other biological communities, the less variable physical environment provides fewer niches for bacteria, resulting in lower diversity.

#### **7.2.4 Danlum Bay Reference Site**

The Danlum Bay reference site was located near the mouth of a large stream and as a result was influenced by terrestrial runoff and detritus from the island. The sediment grain size at Danlum Bay was similar to the Tutum Bay transect site, which was the original rationale for choosing this location as a reference site for this study. Also, the sediment carbonate content was similar to the 180 m site and represented a comparable transitional sediment zone of volcanic sands and calcareous sediments. The Danlum Bay site was unique in the high percentage of organic carbon in the sediments which was due to the input of plant detritus washing in from Ambitle Island. This resulted in a reducing sediment environment as seen by the negative ORP measurements at this site.

The high sediment organics were the primary factor structuring the biological communities at this site at all levels of biodiversity. The macrofaunal community at this site was intermediate to the transect sites in terms of its species richness and abundance. The reference site community was characterized by deposit feeding polychaetes which reflects the high organic content of the sediments.

The meiofaunal community had a relatively low number of taxa and abundance and grouped with the 0 m vent site in terms of its species similarity. This site was unique in the strong dominance of copepods, which accounted for 47% of the relative abundance. This was most likely due also to the large amount of plant detritus in the sediment.

The molecular eukaryotic community was dominated by fungi, which are probably associated with the breakdown of detritus found at that site. Among the most abundant OTUs were the fungi *Cladosporium cladosporioides* and *Penicillium chrysogenum*. The eukaryotic community was most similar to the 0 m site due to the presence of common fungal sequences. This is possibly due to the proximity to shore of both of these sites and the input of detrital material from Ambitle Island. Bacterial sequences were not obtained from this site.

The effect of the high sediment organic content and negative ORP values on the benthic communities at the Danlum Bay reference site had a confounding impact on the overall data analysis of this study. Reanalysis of the community similarity and environmental datasets without the reference site resulted in stronger correlations in the BIO-ENV results for the Tutum Bay transect sites. This indicates that Danlum Bay did not serve as a good reference site for this study, despite its apparent similarity in sediment composition to Tutum Bay. The characteristics of the Danlum Bay site suggest that this site should be omitted in future analysis of the Tutum Bay datasets.

### **7.3 Conclusions**

Overall, the physical environment along the hydrothermal gradient at Tutum Bay correlated with the biological community structure, directly or indirectly. Different levels of the biodiversity (macrofaunal, meiofaunal, molecular) correlated with different environmental variables. The macrofaunal and eukaryotic community structure were more strongly influenced by the sediment characteristics while the meiofauna were more closely tied to temperature and salinity.

Despite the high arsenic concentrations in the pore water and sediments, this variable appeared to have a lesser influence on the structure of the biological communities. This may be due to the binding of the bioavailable arsenic in the sediments, the dispersion of the lower density hydrothermal effluent in the surface waters, or quite possibly to the tolerance and physiological adaptations of the benthic fauna.

The results from the 2003 macrofaunal analysis had suggested that pH was a controlling factor in the benthic community structure. The results from the more intensive 2005 sampling however failed to uphold that and instead indicated that the macrofauna community was correlated to sediment characteristics. Most notably, the %CaCO<sub>3</sub> was found to have the highest correlation for a single parameter. This in turn is correlated with pH and suggests that though the macrofaunal community structure is not directly affected by pH, there is an indirect effect where pH influences the sediment composition.

Overall, the influence of the hydrothermal vents increased the biocomplexity at Tutum Bay by creating new habitats which added to the overall habitat complexity of the region. This provided unique niches for certain taxa that might otherwise be outcompeted in regular reef habitats and affecting the entire community assemblage.

Shallow-water hydrothermal vents are unique, local habitats associated with volcanic regions. These systems also tend to be transient in nature; vents can stop flowing when there are changes in the underground flow of the source water of the hydrothermal fluids. The ephemeral nature of these systems also influences the associated benthic community, which is composed primarily of opportunistic species that can quickly colonize these habitats and are pre-adapted to tolerate extreme environmental conditions. The polychaetes in the *Capitella capitata* species complex are well known for their

ability to occupy sites that have been disturbed either by natural events or anthropogenic pollution. The dominance of *Capitella cf. capitata* at the Tutum Bay vent reflects this. Interestingly, the benthic community around this vent is similar to the shallow-water vents found in Milos, Greece in the Aegean Sea, which were also dominated by a sibling species of *Capitella capitata* and had high densities of thalassinid shrimp burrows around the periphery of the hydrothermal area (Thiermann *et al.* 1994, 1997, Gamenick *et al.* 1998).

The constant physical disturbance from the venting and the extreme environmental conditions at the vent additionally keep the biological community at an early stage of succession. This was evident along the transect at Tutum Bay where the benthic communities changed from being dominated by a few opportunistic taxa near the vent to a highly diverse community associated with the calcareous sediments farther away.

The taxa comprising the benthic community around the vent represent a subset of species recruited from the surrounding area. This has also been noted at similar vent systems around the world (Thiermann *et al.* 1997, Tarasov *et al.* 1999, Melwani and Kim 2008). This is in contrast to deep-sea hydrothermal vent systems, where selective pressures for alternative carbon sources (chemosynthesis) and tolerance for highly toxic conditions result in the evolution of endemic vent communities. At Tutum Bay, the shallow-water environment allows for photosynthesis to serve as the primary carbon source, while the potentially toxic concentrations of arsenic are largely bound in the sediments or possibly dispersed in the surface waters.

Perhaps the most interesting finding in this study is the effect of the low pH environment on the sediment carbonates and the interrelationships between the pore water chemistry and biological community in structuring the sediment, and in turn, the influence of the sediment composition on the benthic community structure. In the immediate area around the vent and in the zone of diffuse venting as far away as 140 m from the vent, carbonate sediments were absent. This was farther influenced by the reworking of the sediment by thalassinid shrimp. Farther from the vent, where pore water pH was closer to normal seawater, the sediments were predominantly carbonate sands and gravel derived from biological sources such as foraminiferan and molluscan shell fragments, calcareous algae and coral rubble.

McCloskey (2009) observed increasing abundance and diversity in the foraminiferan assemblages in Tutum Bay with distance along the transect. Foraminiferans were nearly absent in the sediments surrounding the vent and within the area influenced by diffuse venting, presumably due to the reduced pH. These results corroborate the results seen in the macrofauna and meiofauna communities along the transect and further support the hypothesis that pH is an important factor in structuring the benthic communities associated with the hydrothermal system.

There has been much recent attention on the effects of increased atmospheric CO<sub>2</sub> from anthropogenic sources on lowering ocean pH (Caldeira and Wickett 2003, Feely *et al.* 2004, Caldeira and Wickett 2005) and the possible effects this may have on marine organisms (Anthony *et al.* 2008, Fabry *et al.* 2008, Dupont *et al.* 2010, Wood *et al.* 2010). Because of the release of CO<sub>2</sub> from the hydrothermal fluids, shallow-water vent systems offer a unique natural laboratory for looking at these effects on marine organism

(Hall-Spencer *et al.* 2008). Several recent studies have taken advantage of shallow vent systems, including Tutum Bay, to look at the impacts of low pH on calcareous organisms such as bryozoans (Rodolfo-Metalpa *et al.* 2010) and foraminiferans (Engle 2010). These systems offer even greater potential for studying the effects of ocean acidification on the entire marine community and the complex interactions among the different levels of biodiversity and the physical environment – the overall biocomplexity of the system. The results of my study illustrate this potential, showing the link between reduced pH, changes in sediment composition and benthic community structure.

## Literature Cited

Aller, R.C. 1982. Carbonate dissolution in nearshore terrigenous muds: the role of physical and biological reworking. *Journal of Geology* 90: 79-95.

Alongi, D.M. 1986. Population structure and trophic composition of the free-living nematodes inhabiting carbonate sands of Davies Reef, Great Barrier Reef, Australia. *Australian Journal of Marine & Freshwater Research* 37: 609 – 619.

Anand, M. and B.C. Tucker. 2003. Defining biocomplexity: an ecological perspective. *Comments on Theoretical Biology* 8: 497 – 510.

Andreae, M.O. 1979. Arsenic speciation in seawater and interstitial waters: the influence of biological-chemical interactions on the chemistry of a trace element. *Limnology & Oceanography* 24: 440-452.

Anthony, K.R.N., D.I. Kline, G. Diaz-Pulido, S. Dove, and O. Hoegh-Guldberg. 2008. Ocean acidification causes bleaching and productivity loss in coral reef builders. *Proceedings of the National Academy of Sciences* 105: 17442 – 17446.



- Argese, E., C. Bettiol, C. Rigo, S. Bertini, S. Colomban, and P.F. Ghetti. 2005. Distribution of arsenic compounds in *Mytilus galloprovincialis* of the Venice lagoon (Italy). *Science of the Total Environment* 348: 267 – 277.
- Atkins, M.S., A.P. Teske and O.R. Anderson. 2000. A survey of flagellate diversity at four deep-sea hydrothermal vents in the Eastern Pacific Ocean using structural and molecular approaches. *Journal of Eukaryotic Microbiology* 47: 400 – 411.
- Barwick, M., and W. Maher. 2003. Biotransference and biomagnification of selenium, copper, cadmium, zinc, arsenic and lead in a temperate seagrass ecosystem from Lake Macquarie Estuary, NSW, Australia. *Marine Environmental Research* 56: 471 – 502.
- Bass, D. and T. Cavalier-Smith. 2004. Phylum-specific environmental DNA analysis reveals remarkably high global biodiversity of Cercozoa (Protozoa). *International Journal of Systematic and Evolutionary Microbiology* 54: 2393 – 2404.
- Behnke, A., J. Bunge, K. Barger, H-W. Breiner, B. Alla, and T. Stoeck. 2006. Microeukaryote community patterns along an O<sub>2</sub>/H<sub>2</sub>S gradient in a supersulfidic anoxic fjord (Framvaren, Norway). *Applied & Environmental Microbiology* 72: 3626 – 3636.
- Blake, J.A. 2009. Redescription of *Capitella capitata* (Fabricius) from West Greenland and designation of a neotype (Polychaeta, Capitellidae). *Zoosymposia* 2: 55 – 80.

Bhadury, P., M.C. Austen, D.T. Bilton, P.J.D. Lambshead, A.D. Rogers, G.R. Smerdon. 2006. Molecular detection of marine nematodes from environmental samples: overcoming eukaryotic interference. *Aquatic Microbial Ecology* 44: 97 – 103.

Bright, M. C. Arndt, H. Keckeis, and H. Felbeck. 2003. A temperature –tolerant interstitial worm with associated epibiotic bacteria from the shallow water fumaroles of Deception Island, Antarctica. *Deep Sea Research Part II: Topical Studies in Oceanography* 50: 1859 – 1871.

Burdige, D.J., and R.C. Zimmerman. 2002. Impact of sea grass density on carbonate dissolution in Bahamian sediments. *Limnology & Oceanography* 47: 1751-1763.

Byrne, M., N.A. Soars, M.A. Ho, E. Wong, D. McElroy, P. Selvakumaraswamy, S.A. Dworjanyn, and A.R. Davis. 2010. Fertilization in a suite of coastal marine invertebrates from SE Australia is robust to near-future ocean warming and acidification. *Marine Biology* 157: 2061 – 2069.

Cadenasso, M.L., S.T.A. Pickett, and J.M. Grove. 2006. Dimensions of ecosystem complexity: Heterogeneity, connectivity, and history. *Ecological Complexity* 3: 1 – 12.

Caldeira, K. and M.E. Wickett. 2003. Anthropogenic carbon and ocean pH. *Nature* 425: 365.

Caldeira, K. and M.E. Wickett. 2005. Ocean model predictions of chemistry changes from carbon dioxide emissions to the atmosphere and ocean. *Journal of Geophysical Research* 110, C09S04 doi: 10.1029/2004JC002671.

Clarke, K.R., and M. Ainsworth. 1993. A method of linking multivariate community structure to environmental variables. *Marine Ecology Progress Series* 92: 205 – 219.

Clarke, K.R., and R.N. Gorley. 2006. Primer v6: User manual/tutorial. PRIMER-E: Plymouth, U.K.

Cocito, S., C.N. Bianchi, C. Morri, and A. Peirano. 2000. First survey of sessile communities on subtidal rocks in an area with hydrothermal vents: Milos Island, Aegean Sea. *Hydrobiologia* 426: 113-121.

Cutter, G.A., L.S. Cutter, A.M. Featherstone, and S.E. Lohrenz. 2001. Antimony and arsenic biogeochemistry in the western Atlantic Ocean. *Deep Sea Research Part II: Topical Studies in Oceanography* 48: 2895-2915.

Dando, P.R., Stüben, D., Varnavas, S.P. 1999. Hydrothermalism in the Mediterranean Sea. *Progress in Oceanography* 44: 333-367.

Dando, P.R., Aliani, S., Arab, H., Bianchi, C.N., Brehmer, M. Cocito, S. Fowler, S.W., Gundersen, J. Hooper, L.E., Kölbl, R., Kuever, J., Linke, P., Makropoulos, K.C., Meloni,

R. Miwuel, J.-C., Morri, C., Müller, S., Robinson, C., Schlesner, H., Sievert, S. Stöhr, D. Thomm, M., Varnavas, S.P., Ziebis, W. 2000. Hydrothermal Studies in the Aegean Sea. *Physics and Chemistry of the Earth (B)* 25: 1-8.

Das, S., P.S. Lyla, S.A. Khan. 2009. Filamentous fungal population and species diversity from the continental slope of Bay of Bengal, India. *Acta Oecologica* 35: 269 – 279.

Dawson, S.C. and N.R. Pace. 2002. Novel kingdom-level eukaryotic diversity in anoxic environments. *Proceedings of the National Academy of Sciences* 99: 8324 – 8329.

Deheyn, D.D., P. Gendreau, R.J. Baldwin, and M.I. Latz. 2005. Evidence for enhanced bioavailability of trace elements in the marine ecosystem of Deception Island, a volcano in Antarctica. *Marine Environmental Research* 60: 1 – 33.

Dhalgren, C.P., M.H. Posey, and A.W. Hulbert. 1999. The effects of bioturbation on the infaunal community adjacent to an offshore hardbottom reef. *Bulletin of Marine Science* 64: 21-34.

Dupont, S., N. Dorey, and M. Thorndyke. 2010. What meta-analysis can tell us about vulnerability of marine biodiversity to ocean acidification? *Estuarine, Coastal and Shelf Science* 89:182 – 185.

- Edgcomb, V.P., D.T. Kysela, A. Teske, A. de Vera Gomez, and M.L. Sogin. 2002. Benthic eukaryotic diversity in the Guaymas Basin hydrothermal vent environment. *Proceedings of the National Academy of Sciences* 99: 7658 – 7662.
- Engel, B.E. 2010. Effects of a shallow-water hydrothermal vent gradient on benthic calcifiers, Tutum Bay, Ambitle Island, Papua New Guinea. M.S. Thesis. University of South Florida, St. Petersburg, FL.
- Fabry, V.J., B.A. Seibel, R.A. Feely, and J.C. Orr. 2008. Impacts of ocean acidification on marine fauna and ecosystem processes. *ICES Journal of Marine Science* 65: 414 – 432.
- Fauchald, K and P.A. Jumars. The diet of worms: a study of polychaete feeding guilds. *Oceanography and Marine Biology an Annual Review* 17: 193 – 284.
- Feely, R.A., Sabine, C.L., Lee, K., Berelson, W. Kleypas, J., Fabry, V.J., and Millero, F.J. 2004. Impact of anthropogenic CO<sub>2</sub> on the CaCO<sub>3</sub> system in the oceans. *Science* 304: 362- 366.
- Fenchel, T.M. and R.J. Riedl. 1970. The sulfide system: a new biotic community underneath the oxidized layer of marine sand bottoms. *Marine Biology* 7: 255 – 268.

Francesconi, K.A., and D. Kuehnelt. 2002. Arsenic compounds in the environment. Pp. 51-94 in *Environmental Chemistry of Arsenic*, W.T. Frankenberger, Jr., ed. Marcel Dekker, Inc., New York.

Gagliano, M., M.I. McCormick, J.A. Moore, and M. Depczynski. 2010. The basics of acidification: baseline variability of pH on Australian coral reefs. *Marine Biology* 157: 1849 – 1856.

Gamenick, I., M. Abbiati, and O. Giere. 1998a. Field distribution and sulphide tolerance of *Capitella capitata* (Annelida: Polychaeta) around shallow water hydrothermal vents off Milos (Aegean Sea). A new sibling species? *Marine Biology* 130: 447-453.

Gamenick, I., B. Vismann, M.K. Grieshaber, and O. Giere. 1998b. Ecophysiological differentiation of *Capitella capitata* (Polychaeta). Sibling species from different sulfidic habitats. *Marine Ecology Progress Series* 175: 155-166.

Grassle, J.F. and J.P. Grassle. 1974. Opportunistic life histories and genetic systems in marine benthic polychaetes. *Journal of Marine Research* 32: 253 – 284.

Giménez, F. and A. Marín. 1991. Los anélidos poliquetos de una solfatara submarina en el Golfo de Nápoles. *Anales de Biología* 17: 143 – 151.

Grassle, J.P., and J.F. Grassle. 1976. Sibling species in the marine pollution indicator *Capitella* (Polychaeta). *Science* 192: 567-569.

Gray, J.S. and M. Elliott. 2009. Ecology of Marine Sediments: From Science to Management. 2<sup>nd</sup> ed. Oxford University Press. New York.

Green, M.A., R.C. Aller, and J.Y. Aller. 1993. Carbonate dissolution and temporal abundances of Foraminifera in Long Island Sound sediments. *Limnology & Oceanography* 38: 331-345.

Grotti, M. C. Lagomarsino, W. Goessler, and K.A. Francesconi. 2010. Arsenic speciation in marine organisms from Antarctic coastal environments. *Environmental Chemistry* 7: 207 – 214.

Hall-Spencer, J.M., R. Rodolfo-Metalpa, S. Martin, E. Ransome, M. Fine, S.M. Turner, S.J. Rowley, D. Tedesco, and M-C. Buia. 2008. Volcanic carbon dioxide vents show ecosystem effects of ocean acidification. *Nature* 454: 96-99.

Handley, K.M., M. Héry, and J.R. Lloyd. 2009. Redox cycling of arsenic by the hydrothermal marine bacterium *Marinobacter santoriniensis*. *Environmental Microbiology* 11: 1601 – 1611.

Heiri, O., A.F. Lotter, and G. Lemcke. 2001. Loss on ignition as a method for estimating organic and carbonate content in sediments: reproducibility and comparability of results.

*Journal of Paleolimnology* 25: 101-110.

Hendriks, I.E., C.M. Duarte, M. Álvarez. 2010. Vulnerability of marine biodiversity to ocean acidification: A meta-analysis. *Estuarine, Coastal, and Shelf Science* 86: 157 –

164.

Hendriks, I.E. and C.M. Duarte. 2010. Ocean acidification: Separating evidence from judgment – A reply to Dupont *et al.* *Estuarine, Coastal and Shelf Science* 89: 186 – 190.

Hicks, G.R.F. and B.C. Coull. 1983. The ecology of marine meiobenthic harpacticoid copepods. *Oceanography and Marine Biology an Annual Review* 21: 67 – 175.

Higgins, R.P. and H. Thiel (eds.). 1988. Introduction to the study of meiofauna.

Smithsonian Institution Press, Washington, D.C.

Inskip, W.P., T.R. McDermott, and S. Fendorf. 2002. Arsenic (V)/(III) cycling in soils and natural waters: chemical and microbiological processes. Pp. 183-215 in

Environmental Chemistry of Arsenic, W.T. Frankenberger, Jr., ed. Marcel Dekker, Inc.,

New York.



Jordan, M.A., D.T. Welsh, R.J.K. Dunn, and P.R. Teasdale. 2009. Influence of *Trypaea australiensis* density on benthic metabolism and nitrogen dynamics in sandy estuarine sediment: A mesocosm simulation. *Journal of Sea Research* 61: 144 – 152.

Kamenev, G.M., V.I. Fadeev, N.I. Selin, V.G. Tarasov, and V.V. Malakhov. 1993. Composition and distribution of macro- and meiobenthos around sublittoral hydrothermal vents in the Bay of Plenty, New Zealand. *New Zealand Journal of Marine & Freshwater Research* 27: 407-418.

Kamenev, G.M., V. Ya. Kavun, V.G. Tarasov, and V.I. Fadeev. 2004. Distribution of bivalve mollusks *Macoma golikovi* Scarlato and Kafanov, 1998 and *Macoma calcarea* (Gmelin, 1791) in the shallow-water hydrothermal ecosystem of Kraternaya Bight (Yankich Island, Kuril Islands): connection with feeding type and hydrothermal activity of Ushishir Volcano. *Continental Shelf Research* 24: 75-95.

Karlen, D.J. R.E. Price, T. Pichler, and J.R. Garey. 2010. Changes in benthic macrofauna associated with a shallow-water hydrothermal vent gradient in Papua New Guinea. *Pacific Science* 64: 391 – 404.

Kirby, J. and W. Maher. 2002. Tissue accumulation and distribution of arsenic compounds in three marine fish species: relationship to trophic position. *Applied Organometallic Chemistry* 16: 108 – 115.

Kitts, H.J., G.E. Millward, A.W. Morris, and L. Ebdon. 1994. Arsenic biogeochemistry in the Humber Estuary, U.K. *Estuarine, Coastal and Shelf Science* 39: 157-172.

Langdon, C.J., T.G. Pearce, A.A. Meharg, and K.T. Semple. 2003. Interactions between earthworms and arsenic in the soil environment: a review. *Environmental Pollution* 124: 361 – 373.

Le Calvez, T. G. Burgaud, S. Mahé, G. Barbier, and P. Vandenkoornhuysen. 2009. Fungal diversity in deep-sea hydrothermal ecosystems. *Applied and Environmental Microbiology* 75: 6415 – 6421.

Lohrer, A.M., S.F. Thrush, and M.M. Gibbs. 2004. Bioturbators enhance ecosystem function through complex biogeochemical interactions. *Nature* 431: 1092 – 1095.

López-García, P. F. Rodríguez-Balera, C. Pedrós-Alló, and D. Morelra. 2001. Unexpected diversity of small eukaryotes in deep-sea Antarctic plankton. *Nature* 409: 603 – 607.

López-García, P., H. Philippe, F. Gail, and D. Moreira. 2003. Autochthonous eukaryotic diversity in hydrothermal sediment and experimental microcolonizers at the Mid-Atlantic Ridge. *Proceedings of the National Academy of Sciences* 100: 697 – 702.

López-García, P., A. Vereshchaka, and D. Moreira. 2007. Eukaryotic diversity associated with carbonates and fluid-seawater interface in Lost City hydrothermal field.

*Environmental Microbiology* 9: 546 – 554.

Mancinelli, G., S. Fazi, and L. Rossi. 1998. Sediment structural properties mediating dominant feeding types patterns in soft-bottom macrobenthos of the Northern Adriatic

Sea. *Hydrobiologia* 367: 211 – 222.

Mannini, E., G.M. Luna, C. Corinaldesi, D. Zeppilli, G. Bortoluzzi, G. Caramanna, F. Raffa, and R. Danovaro. 2008. Prokaryote diversity and virus abundance in shallow hydrothermal vents of the Mediterranean Sea (Panarea Island) and the Pacific Ocean (North Sulawesi-Indonesia). *Microbial Ecology* 55: 626 – 639.

McCloskey, B.J. 2009. Foraminiferal responses to arsenic in a shallow-water hydrothermal system in Papua New Guinea and in the laboratory. Ph.D. Dissertation. University of South Florida, St. Petersburg, FL.

Melwani, A.R. and S.L. Kim. 2008. Benthic infaunal distributions in shallow hydrothermal vent sediments. *Acta Oecologia* 33: 162-175.

Mermillod-Blondin, F. and R. Rosenberg. 2006. Ecosystem engineering: the impact of bioturbation on biogeochemical processes in marine and freshwater benthic habitats.

*Aquatic Sciences* 68: 434 – 442.

Michener, W.K., T.J. Baerwald, P. Firth, M.A. Palmer, J.L. Rosenberger, E.A. Sandlin, and H. Zimmerman. 2001. Defining and unraveling biocomplexity. *BioScience* 51: 1018 – 1023.

Milliman. J.D., 1974. Marine Carbonates. SpringerVerlag, Berlin Heidelberg New York.

Moon-van der Staay, S.Y., R. De Wachter, and D. Vaultot. 2001. Oceanic 18S rDNA sequences from picoplankton reveal unsuspected eukaryotic diversity. *Nature* 409: 607 – 610.

Morri, C., C.N. Bianchi, S. Cocito, A. Peirano, A.M. De Biase, S. Aliani, M. Pansini, M. Boyer, F. Ferdeghini, M. Pestarino, P. Dando. 1999. Biodiversity of marine sessile epifauna at an Aegean island subject to hydrothermal activity: Milos, eastern Mediterranean Sea. *Marine Biology* 135: 729-739.

Oremland, R.S., and J.F. Stolz. 2003. The ecology of arsenic. *Science* 300: 939-944.

Oremland, R.S., T.R. Kulp, J. Switzer Blum, S.E. Hoefft , S. Baesman, L.G. Miller, and J.F. Stolz. 2005. A microbial arsenic cycle in a salt-saturated extreme environment. *Science* 308: 1305-1308.

Paarlberg, A.J., M.A.F. Knaapen, M.B. de Vries, S.J.M.H. Hulscher and Z.B. Wang. 2005. Biological influences on morphology and bed composition of an intertidal flat. *Estuarine, Coastal and Shelf Science* 64: 577 – 590.

Pelejero, C., E. Calvo, M.T. McCulloch, J.F. Marshall, M.K. Gagan, J.M. Lough, and B.N. Opdyke. 2005. Preindustrial to modern interdecadal variability in coral reef pH. *Science* 309: 2204 – 2207.

Percival, J.B., and P.J. Lindsay. 1997. Measurement of physical properties of sediments. Pp.7-45 in *Manual of Physico-Chemical Analysis of Aquatic Sediments*, A. Mudroch, J.M. Azcue, and P. Mudroch, eds, CRC Press, Boca Raton.

Pichler, T., and G.R. Dix. 1996. Hydrothermal venting within a coral reef ecosystem, Ambitle Island, Papua New Guinea. *Geology* 20: 435-438.

Pichler, T., and J. Veizer. 1999. Precipitation of Fe(III) oxyhydroxide deposits from shallow-water hydrothermal fluids in Tutum Bay, Ambitle Island, Papua New Guinea. *Chemical Geology* 162: 15-31.

Pichler, T., J. Veizer, and G.E.M. Hall. 1999a. Natural input of arsenic into a coral-reef ecosystem by hydrothermal fluids and its removal by Fe(III) oxyhydroxides. *Environmental Science & Technology* 33: 1373-1378.

Pichler, T., J. Veizer, and G.E.M. Hall. 1999b. The chemical composition of shallow-water hydrothermal fluids in Tutum Bay, Ambitle Island, Papua New Guinea and their effect on ambient seawater. *Marine Chemistry* 64: 229-252.

Pichler, T., J. P. Amend, J. Garey, P. Hallock, N. P. Hsia, D. J. Karlen, D. R. Meyer-Dombard, B. J. McCloskey, and R. E. Price (2006), A Natural Laboratory to Study Arsenic Geobiocomplexity, *Eos Transactions, AGU*, 87(23), doi:10.1029/2006EO230002.

Powell, E.N. and T.J. Bright. 1981. A thiobios does exist – Gnathostomulid domination of the canyon community at the East Flower Garden brine seep. *Internationale Revue der gesamten Hydrobiologie und Hydrographie* 66: 675 – 683.

Powell, E.N., T.J. Bright, A. Woods, and S. Gittings. 1983. Meiofauna and the thiobios in the East Flower Garden brine seep. *Marine Biology*. 73: 269 – 283.

Price, R.E. 2008. Biogeochemical cycling of arsenic in the marine shallow-water hydrothermal system of Tutum Bay, Ambitle Island, Papua New Guinea. Ph.D. Dissertation. University of South Florida, Tampa, FL.

Price, R.E., and T. Pichler. 2005. Distribution, speciation and bioavailability of arsenic in a shallow-water submarine hydrothermal system, Tutum Bay, Ambitle Island, PNG. *Chemical Geology* 224: 122-135.

Price, R.E., Amend, J.P. and Pichler, T. 2007. Enhanced geochemical gradients in a marine shallow-water hydrothermal system: unusual arsenic speciation in horizontal and vertical pore water profiles. *Applied Geochemistry*. 22: 2595-2605.

Potvin, M. and C. Lovejoy. 2009. PCR-based diversity estimates of artificial and environmental 18S rRNA gene libraries. *Journal of Eukaryotic Microbiology* 56: 174 – 181.

Raffaelli, D.G. and C.F. Mason. 1981. Pollution monitoring with meiofauna, using the ratio of nematodes to copepods. *Marine Pollution Bulletin* 12: 158 – 163.

Riemann, F. 1988. Nematoda. Chapter 23 pp. 293 – 299 in Introduction to the Study of Meiofauna, Higgins, R.P. and H. Thiel (eds). Smithsonian Institution Press, Washington, D.C.

Rodolfo-Metalpa, R., C. Lombardi, S. Cocito, J.M. Hall-Spencer, and M.C. Gambi. 2010. Effects of ocean acidification and high temperatures on the bryozoans *Myriapora truncate* at natural CO<sub>2</sub> vents. *Marine Ecology* 31: 447 – 456.

Rolf, F.J., and R.R.Sokal. 1981. Statistical Tables. Freeman and Company, New York.

Samson, R.A. 1974. *Paecilomyces* and some allied *Hyphomycetes*. *Studies in Mycology* 6: 1 - 119

Sanders, H.L., 1958. Benthic studies in Buzzards Bay. I. Animal-sediment relationships. *Limnology & Oceanography* 3: 245-258.

Shirayama, Y. and H. Thornton. 2005. Effect of increased atmospheric CO<sub>2</sub> on shallow water marine benthos. *Journal of Geophysical Research* 110 C09S08, doi: 10.1029/2004JC002618.

Sievert, S.M., T. Brinkhoff, G. Muyzer, W. Ziebis, and J. Kuever. 1999. Spatial heterogeneity of bacterial populations along an environmental gradient at a shallow submarine hydrothermal vent near Milos Island (Greece). *Applied and Environmental Microbiology* 65: 3834 – 3842.

Sievert, S.M., W. Ziebis, J. Kuever, and K. Sahm. 2000. Relative abundance of Archaea and Bacteria along a thermal gradient of a shallow-water hydrothermal vent quantified by rRNA slot-blot hybridization. *Microbiology* 146: 1287 – 1293.

Snelgrove, P.V.R., and C.A. Butman. 1994. Animal sediment relationships revisited – cause versus effect. *Oceanography & Marine Biology* 32: 111-177.



- Snelgrove, P.V.R., H.T. Blackburn, P.A. Hutchings, D.M. Alongi, J.F. Grassle, H. Hummel, G. King, I. Koike, P.J.D. Lamshead, N.B. Ramsing, and V. Solis-Weiss. 1997. The importance of marine sediment biodiversity in ecosystem processes. *Ambio* 26: 578 – 583.
- Sorokin, Yu.I., P. Yu. Sorokin, and O. Yu. Zakouskina. 2003. Microplankton and its function in a zone of shallow hydrothermal activity: the Craternaya Bay, Kurile Islands. *Journal of Plankton Research* 25: 495-506.
- Stoeck, T. and S. Epstein. 2003. Novel eukaryotic lineages inferred from small-subunit rRNA analyses of oxygen-depleted marine environments. *Applied and Environmental Microbiology* 69: 2657 – 2663.
- Takishita, K., H. Miyake, M. Kawato, and T. Maruyama. 2005. Genetic diversity of microbial eukaryotes in anoxic sediment around fumaroles on a submarine caldera floor based on the small-subunit rDNA phylogeny. *Extremophiles* 9: 185 – 196.
- Takishita K., M. Tsuchiya, M. Kawato, K. Oguri, H. Kitazato, and T. Maruyama. 2007a. Genetic diversity of microbial eukaryotes in anoxic sediment of the saline meromictic lake Namako-ike (Japan): on the detection of anaerobic or anoxic-tolerant lineages of eukaryotes. *Protist* 158: 51 -64.

Takishita, K., N. Yubuki, N. Kakizoe, Y. Inagaki, and T. Maruyama. 2007b. Diversity of microbial eukaryotes in sediment at a deep-sea methane cold seep: surveys of ribosomal DNA libraries from raw sediment samples and two enrichment cultures. *Extremophiles* 11: 563 – 576.

Takishita, K., N. Kakizoe, T. Yoshida, and T. Maruyama. 2010. Molecular evidence that phylogenetically diverged ciliates are active in microbial mats of deep-sea cold-seep sediments. *Journal of Eukaryotic Microbiology* 57: 76 – 86.

Tarasov, V.G. 2006. Effects of shallow-water hydrothermal venting on biological communities of coastal marine ecosystems of the western Pacific. *Advances in Marine Biology* 50: 267 – 421.

Tarasov, V.G., M.V. Propp, L.N. Propp, A.V. Zhirmunsky, B.B. Namsaraev, V.M. Gorlenko, and D.A. Starynin. 1990. Shallow-water gasohydrothermal vents of Ushishir volcano and the ecosystem of Kraternaya Bight (the Kurile Islands). *Marine Ecology* 11: 1-23.

Tarasov, V.G., A.V. Gebruk, V.M. Shulkin, G.M. Kamenev, V.I. Fadeev, V.N. Kosmynin, V.V. Malakhov, D.A. Starynin, and A.I. Obxhirov. 1999. Effect of shallow-water hydrothermal venting on the biota of Matupi Harbour (Rabaul Caldera, New Britain Island, Papua New Guinea). *Continental Shelf Research* 19: 79-116.

Thiermann, F., R. Windoffer, O. Giere. 1994. Selected meiofauna around shallow water hydrothermal vents off Milos (Greece): ecological and ultrastructural aspects. *Vie Milieu* 44: 215 – 226.

Thiermann, F., I. Akoumianaki, J.A. Hughes, and O. Giere. 1997. Benthic fauna of a shallow-water gaseohydrothermal vent area in the Aegean Sea (Milos, Greece). *Marine Biology* 128: 149-159.

Thiermann, F., B. Vismann, O. Giere. 2000. Sulphide tolerance of the marine nematode *Oncholaimus campylocercoides* a result of internal sulphur formation? *Marine Ecology Progress Series* 193: 251 – 259.

Vanreusel, A., I. Van den Bossche, F. Thiermann. 1997. Free-living marine nematodes from hydrothermal sediments: similarities with communities from diverse reduced habitats. *Marine Ecology Progress Series* 157: 207 – 219.

Varnavas, S.P. and D.S. Cronan. 1988. Arsenic, antimony and bismuth in sediments and waters from the Santorini hydrothermal field, Greece. *Chemical Geology* 67: 295 – 305.

Watt, C., and X.E. Le. 2003. Arsenic speciation in natural waters. Pp. 11-32 in *Biogeochemistry of Environmentally Important Trace Elements: ACS symposium series* 835. Y. Cai, and O.C. Brails, eds. American Chemical Society, Washington D.C.

Wenzhöfer, F. O. Holby, R.N. Glud, H.K. Nielsen, and J.K. Gundersen. 2000. In situ microsensor studies of a shallow water hydrothermal vent at Milos, Greece. *Marine Chemistry* 69: 43 – 54.

Widdicombe, S., M.C. Austen, M.A. Kendall, R.M. Warwick, and M.B. Jones. 2000. Bioturbation as a mechanism for setting and maintaining levels of diversity in subtidal macrobenthic communities. *Hydrobiologia* 440: 369 - 377.

Wood, H.L., J.I. Spicer, D.M. Lowe, and S. Widdicombe. 2010. Interaction of ocean acidification and temperature; the high cost of survival in the brittlestar *Ophiura ophiura*. *Marine Biology* 157: 2001 – 2013.

Wu, T. E. Ayres, G. Li, R.D. Bardgett, D.H. Wall, and J.R. Garey. 2009. *Soil Biology and Biochemistry* 41: 849 – 857.

Zeppilli, D. and R. Danovaro. 2009. Meiofaunal diversity and assemblage structure in a shallow-water hydrothermal vent in the Pacific Ocean. *Aquatic Biology* 5: 75 – 84.

### **About the Author**

David Karlen was born on September 11, 1968 in Wausau, Wisconsin and grew up in Ohio. He graduated from Lancaster High School in Lancaster, Ohio in 1987 and moved to Melbourne, Florida that fall to attend the Florida Institute of Technology. David completed his B.S. in Biological Oceanography in the spring of 1991 and continued on as a graduate student at F.I.T. studying benthic ecology under Dr. Walter G. Nelson. David completed his M.S. in Biological Oceanography in the fall of 1993.

David worked for the Caribbean Marine Research Center during the winter of 1994, working at the CMRC field research facility on Lee Stocking Island, Bahamas and at the CMRC lab in Vero Beach, Florida. He later took a job at Mote Marine Lab in the spring of 1994, working in the MML Benthic Ecology department as an invertebrate taxonomist.

David accepted a position with the Environmental Protection Commission of Hillsborough County in Tampa Florida in October 1994, where he is currently employed as a Manager in the Water Management Division, overseeing the benthic monitoring program for Tampa Bay.